

1993

Application of piezo film for active dampening of a cantilever beam

Steven Chow

San Jose State University

Follow this and additional works at: https://scholarworks.sjsu.edu/etd_theses

Recommended Citation

Chow, Steven, "Application of piezo film for active dampening of a cantilever beam" (1993). *Master's Theses*. 616.

DOI: <https://doi.org/10.31979/etd.yj9n-9fjs>

https://scholarworks.sjsu.edu/etd_theses/616

This Thesis is brought to you for free and open access by the Master's Theses and Graduate Research at SJSU ScholarWorks. It has been accepted for inclusion in Master's Theses by an authorized administrator of SJSU ScholarWorks. For more information, please contact scholarworks@sjsu.edu.

INFORMATION TO USERS

This manuscript has been reproduced from the microfilm master. UMI films the text directly from the original or copy submitted. Thus, some thesis and dissertation copies are in typewriter face, while others may be from any type of computer printer.

The quality of this reproduction is dependent upon the quality of the copy submitted. Broken or indistinct print, colored or poor quality illustrations and photographs, print bleedthrough, substandard margins, and improper alignment can adversely affect reproduction.

In the unlikely event that the author did not send UMI a complete manuscript and there are missing pages, these will be noted. Also, if unauthorized copyright material had to be removed, a note will indicate the deletion.

Oversize materials (e.g., maps, drawings, charts) are reproduced by sectioning the original, beginning at the upper left-hand corner and continuing from left to right in equal sections with small overlaps. Each original is also photographed in one exposure and is included in reduced form at the back of the book.

Photographs included in the original manuscript have been reproduced xerographically in this copy. Higher quality 6" x 9" black and white photographic prints are available for any photographs or illustrations appearing in this copy for an additional charge. Contact UMI directly to order.

U·M·I

University Microfilms International
A Bell & Howell Information Company
300 North Zeeb Road, Ann Arbor, MI 48106-1346 USA
313/761-4700 800/521-0600

Order Number 1354131

**Application of piezo film for active dampening of a cantilever
beam**

Chow, Steven Edmund, M.S.

San Jose State University, 1993

U·M·I

300 N. Zeeb Rd.
Ann Arbor, MI 48106

Application of Piezo Film for Active Dampening of a Cantilever Beam

A Thesis

Presented To

The Faculty of the Department of Mechanical Engineering
San Jose State University

In Partial Fulfillment

of the Requirements For the Degree

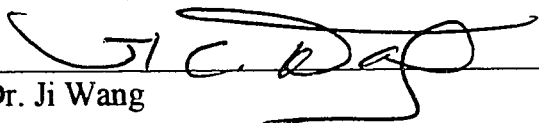
Master of Science

by

Steven Chow

August, 1993

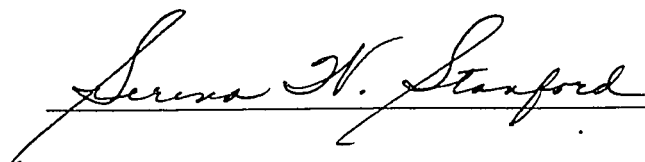
APPROVED FOR THE DEPARTMENT OF
MECHANICAL ENGINEERING


Dr. Ji Wang


Dr. Fred Barez


Dr. Imin Kao

APPROVED FOR THE UNIVERSITY


Serena W. Stanford

Abstract

Application of Piezo Film for Active Dampening of a Cantilever Beam by Steven Chow

The application of piezo film for use in the control of vibration of a cantilever beam is studied in this thesis. The dimensions of the beam were chosen so that it would exhibit a low natural frequency. A low natural frequency was necessary due to the limitation of the available equipment. Two control systems were employed in simulation to dampen the beam. The two systems were the bang bang type of control system and optimal full state feedback with estimator control system. Independent modal space control analysis was also implemented for the full state feedback with estimator. The finite element approach with the state space concept was the approach used in this study.

It was found that the bang bang type of control system dampened the beam more effectively but at the cost of more energy. The optimal control system was slower but used less energy.

Table of Contents

Introduction	1
Modeling of Beam	2
I-DEAS Finite Element Model	5
Experimental Model	9
Experimental And Theoretical Comparison of Open Loop System	10
State Space Representation	12
Piezo Film Modeling	13
Introduction of Piezo Film Into The Finite Element Model	15
MATLAB Modeling	17
Controllability and Observability	19
Applied Control Systems (Bang Bang)	20
Full State Feedback	24
Full State Feedback with Estimator	31
Independent Modal Space Control Analysis	38
Conclusion and Recommendations	46
Bibliography	48
Appendix A: Parametric Study of Beam	A1
Appendix B: Natural Frequency Vs. Length	A5
Appendix C: I-DEAS Finite Element Analysis	A9
Appendix D: Matlab Variables	A19
Appendix E: Bang Bang Control	A20
Appendix F: Observability and Controllability	A23
Appendix G: Optimal Control Simulations	A26

List of Figures

<u>Figure</u>	<u>Title</u>	<u>Page</u>
1	Cantilever Beam Model	1
2	Mode Shape of First Natural Frequency	6
3	Mode Shape of Second Natural Frequency	7
4	Mode Shape of Third Natural Frequency	8
5	Experimental Setup	9
6	Measured Open Loop Response of Cantilever Beam	9a
7	Open Loop Response of Cantilever Beam	11
8	Beam and Piezo Film Model	13
9	Visual Representation of Applied Voltages to Applied Moments	15
10	Simulink Model of Bang Bang Control System	21
11	Response of Bang Bang Control System	
	Using 100 Volts For Feedback	22
12	Response of Bang Bang Control System	
	Using 400 Volts For Feedback	22
13	Response of Bang Bang Control System	
	Using 800 Volts For Feedback	23
14	Full State Feedback model	24
15	Response of Displacement at the Beam Tip	
	Using Full State Feedback	27
16	Voltage 1 Input for Full State Feedback System	27
17	Voltage 2 Input for Full State Feedback System	28
18	Voltage 3 Input for Full State Feedback System	28

19	Response of Displacement at the Beam Tip	
	Using Full State Feedback and Increased Input	29
20	Increased Voltage 1 Input for Full State	
	Feedback System	29
21	Increased Voltage 2 Input for Full State Feedback System	30
22	Increased Voltage 3 Input for Full State Feedback System	30
23	Full State Feedback With Estimator	31
24	Response at Beam Tip using Full State	
	Feedback With Estimator	34
25	Input Voltage 1 Using Full State Feedback With Estimator	34
26	Input Voltage 2 Using Full State Feedback With Estimator	35
27	Input Voltage 3 Using Full State Feedback With Estimator	35
28	Response at Beam Tip using Full State Feedback With	
	Estimator and Increase Voltage	36
29	Increased Input Voltage 1 Using Full State Feedback	
	With Estimator	36
30	Increased Input Voltage 2 Using Full State Feedback	
	With Estimator	37
31	Increased Input Voltage 3 Using Full State Feedback	
	With Estimator	37
32	Open Loop Response Of The First Mode	40
33	Closed Loop Response Of The Second Mode	40
34	Open Loop Response Of The Second Mode	41
35	Closed Loop Response Of The Second Mode	41
36	Open Loop Response Of The Third Mode	42

37	Closed Loop Response Of The Third Mode	42
38	Input Voltage 1 For Closed Loop System	43
39	Input Voltage 2 For Closed Loop System	43
40	Input Voltage 3 For Closed Loop System	44
41	Displacement At Tip For The Open Loop Response	45
42	Displacement At Tip For The Closed Loop Response	45

Introduction

The application of piezo film to actively dampen vibration is an interest of study which touches the idea of intelligent materials. Intelligent materials are presently being used in such applications as the space station. In space, light weight materials are more susceptible to vibration due to the vacuum. A control system can be designed to minimize the vibration caused by any disturbances using these intelligent materials.

The damping method used in this report is similar to the approach of Newman, Perlas, and Quan [1990]. A layer of piezo-electric polymer is placed on both sides of a cantilever beam. For this study, the layer of piezo-electric film is divided into three sections along the length of the beam. Each section has a separate control voltage. With three separate control voltages, modern control theory such as Independent Modal Space Control could be implemented.

Finite element analysis method was also implemented to develop a method to analyze complex systems. With the use of finite element analysis method, the dynamic equation for modal space analysis could be obtained with greater ease. The finite element solution could then be adapted to fit into modern state space control theory.

Modeling of the Beam

The selection of the beam length was chosen such that the natural frequencies of the first and second mode were approximately 1 and 8 Hz, respectively. Low natural frequencies were necessary so that sampling of the accelerometer output signal could be done effectively due to the nature of the available equipment. The fastest sampling rate of the computer and A/D converter was approximately 50 Hz.

The natural frequencies of a beam could be determined by using the theoretical formulas for the calculations of a cantilever beam (See Figure 1).

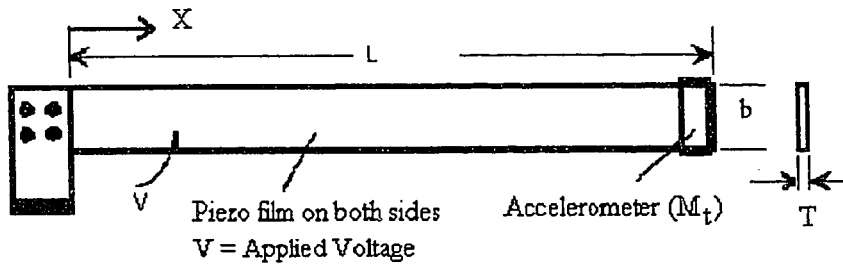


Figure 1: Cantilever Beam Model

The governing differential equation for a beam is given by equation (1)

$$EI \frac{\partial^4 y}{\partial x^4} + m \frac{\partial^2 y}{\partial t^2} = 0 \quad (1)$$

E = Young's Modulus

I = Moment of inertia = $Tb^3/12$

t = time

y = deflection in beam

ρ = density of material

m = mass per unit length of beam

M_t = Mass at tip of beam

ω_n = Natural frequency of beam

The properties of steel used for the experimental beam are:

$$\rho = 283 \frac{\text{lb}}{\text{in}^3}, m = 8.214 \times 10^4 \frac{\text{slug}}{\text{in}}, E = 30 \times 10^6 \frac{\text{lb}}{\text{in}^2}$$

The boundary conditions associated with the displacement of the beam at the fixed end are given by equations (2) and (3).

$$y(0) = 0 \quad (2)$$

$$\frac{\partial y(0)}{\partial x} = 0 \quad (3)$$

The boundary conditions related to the beam displacement at the free end, assuming a mass is at the tip, are given by equations (4) and (5).

$$EI \frac{\partial^3 y(L)}{\partial x^3} = -M_t \frac{\partial^2 y(L)}{\partial t^2} \quad (4)$$

$$EI \frac{\partial^2 y(L)}{\partial x^2} = 0 \quad (5)$$

Solving equation (1) using the boundary conditions specified by equations (2), (3), (4), and (5) gives the following frequency equation.

$$\frac{M_t}{mL} B(\sin(B) \cosh(B) - \cos(B) \sinh(B)) = 1 + \cos(B) \cosh(B) \quad (6)$$

Solving equation (6) for the roots gives

$$B_1 = -1.397, B_2 = -4.098, B_3 = -7.181$$

The natural frequencies for the first three modes can now be calculated using B_n in equation (7).

$$\omega_n = B_n^2 \sqrt{\frac{12EI}{\rho L^4}} \quad n = 1, 2, 3 \quad (7)$$

The first step in determining a beam configuration was to do a parametric study of a beam to see the effect on natural frequency by varying the parameters. The parameters

considered were the length, height, base, Young's Modulus, and density. The mass at the tip was considered constant. The natural frequency vs. percent change for each parameter was plotted for the first three modes (see Appendix A). It can be seen that beam length and thickness has the most effect on natural frequency.

Taking advantage of material currently available, C-1095 spring steel with a cross section of .05" x 1", the problem was then narrowed to determining the length of the beam. The analysis was done first by theoretical method. The frequency was calculated for the first three modes while varying the length of the beam (see Appendix B). It should be noted that this analysis is for a simple cantilever beam without the tip mass. This is because an accelerometer has not been chosen as of this time. Knowing that adding a mass at the tip of the beam will lower the natural frequency, the beam length was chosen such that the second mode natural frequency was approximately 8 Hz. From the graphs of frequency vs. length, it can be seen that a length of 35" will give a natural frequency of the second mode of approximately 8 Hz.

For this study, however, the application of finite element method was mainly used so that the mass, stiffness and damping matrix could be obtained. The matrix would later be used in conjunction with state space control theory to obtain a model of the active dampening system.

I-DEAS Finite Element Model

The software package I-DEAS was used to implement the finite element model. Beam elements were used with a cross section of .05 inch by 1 inch. The beam was modeled to have 35 elements of one inch long each. This model resulted in a total of 35 elements with 36 nodes. The first node was constrained in all direction to model the cantilever beam. The beam was found to have natural frequencies of 1.34 Hz, 8.37 Hz, and 23.4 Hz for modes 1, 2, and 3, respectively. After adding a small accelerometer at the end of the beam, the natural frequency should drop slightly. Adding the piezo film should raise the natural frequency slightly. This can be seen from the results of the parametric study in Appendix A.

Figures 2 to 4 are the mode shapes of the beam. The first mode (Figure 2) is the fundamental mode which is the easiest to excite. The second mode (Figure 3) can be distinguished by crossing the X axis twice. The third mode (Figure 4) can be distinguished by crossing the X axis three times.

The mass, damping and stiffness matrix was also obtained and will be used in the equation (8) listed below.

$$\ddot{M}\delta + \dot{D}\delta + K\delta = \Psi^T F \quad (8)$$

M	Modal Mass Matrix [3 x 3]
D	Damping Matrix [3 x 3]
K	Modal Stiffness Matrix [3 x 3]
δ	Modal degree of freedom
Ψ	Mode Shapes [216 x 3]
F	Applied force and moment at nodes
T	Transpose of matrix

The data for the above matrixes are found in Appendix C.

SDRC I-DEAS VI: System_Dynamics_Analysis
02-OCT-92 11:46:38
Units: IN
Display: No stored Option
Model Bim: 1-MAIN

Database: Vibrating beam
View: No stored View
Last: System Solution
System: 2-SYSTEM2

MODE: 1 FREQ: 1.34 (HZ)



Y X
Z

Figure 2: Mode Shape of First Natural Frequency

SDRC I-DEAS VI: System_Dynamics_Analysis

02-OCT-92 11:37:08

Database: Vibrating Beas
View: No stored View
Last: System Solution
Subject: 2-SYS.CAT

Units: 1
Display: No stored Optic
Model Bin: 1-HALN

MODE: 2 FREQ: 8.37 (HZ)



Y X
Z

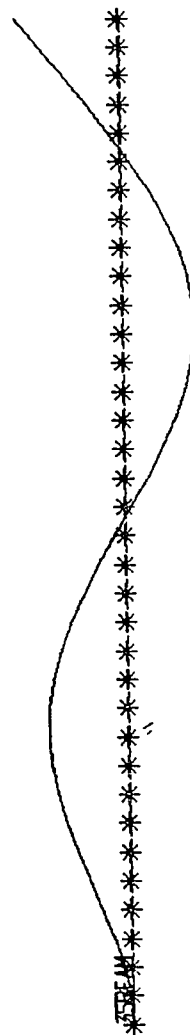
Figure 3: Mode Shape of Second Natural Frequency

02-OCT-92 10:59:36
Units : IN
Display : No stored Option
Model Bin: 1-MIN

SDRC I-DEAS VI: System_Dynamics_Analysis

Database: Vibrating beam
View: No stored View
Last: System Solution
System: 2-315.DGE

MODE: 3 FREQ: 23.4 (HZ)



Y X
Z

Figure: Mode Shape of Third Natural Frequency

Experimental Model

The beam used in this experiment was constructed by Gordan Liang and his senior project group (SJSU). The test setup for the open loop system is shown in Figure 5. The natural frequencies were determined using a HP 3852A Spectrum Analyzer. The open loop test was plotted and can be seen in Figure 6.

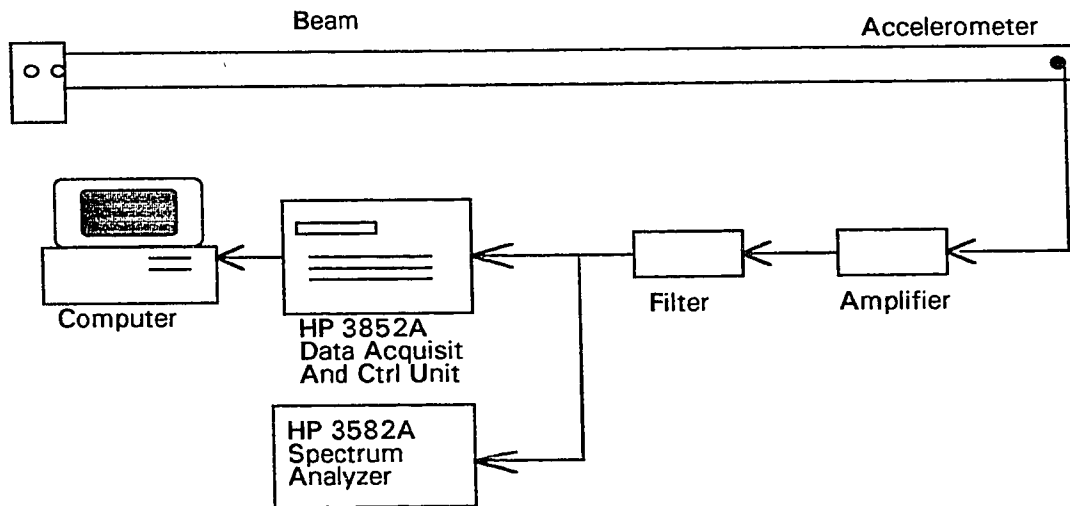


Figure 5: Experimental Setup

RANGE: -20 dBV STATUS: PAUSED

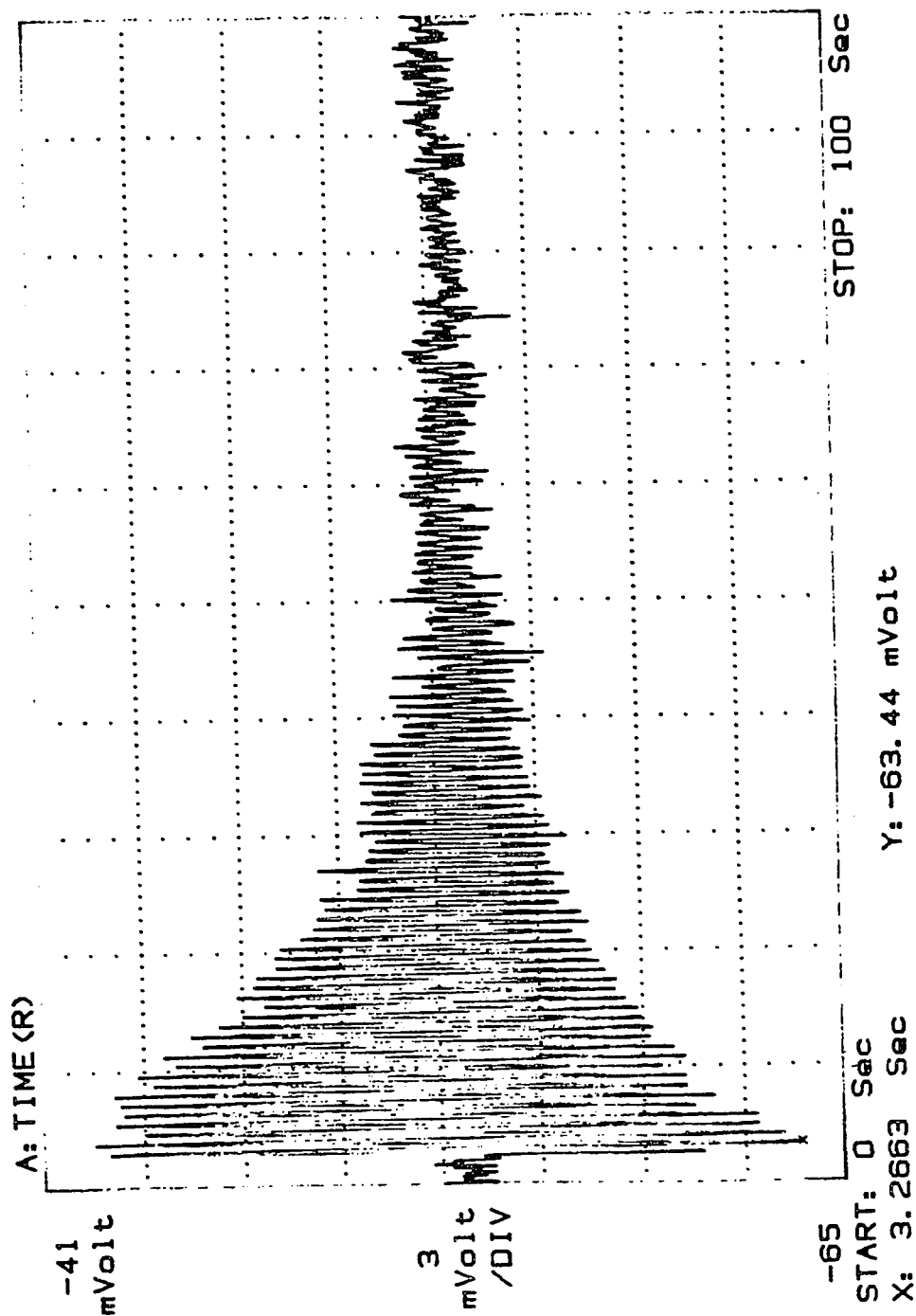


Figure 6: Measured Open Loop Response of Cantilever Beam

Experimental And Theoretical Comparison of Open Loop System

Figure 7 displays the simulated open loop response of the analytical system using the INITIAL command in MATLAB (refer to MATLAB Modeling) where the first three modal displacements were assigned the initial values of [1 0 0]. Note that since 1 was chosen for the initial state for the first mode, the corresponding initial displacement of 24 inches seems very high, but for simulation purpose of obtaining damping characteristics is irrelevant. Comparing Figures 6 with Figure 7, it can also be seen that the results of the system response are relatively close.

Calculations of natural frequency of the 35" beam were then compared with a finite element analysis (FEA). The FEA was using beam elements in I-DEAS (see Appendix C). The results are compared and listed in table 1. It could be seen that the open loop testing was very close to the predicted natural frequencies by the theoretical and the finite element analysis.

Table 1: Results of Theoretical Analysis and Finite Element Analysis

Natural Frequency	Mode 1 (Hz)	Mode 2 (Hz)	Mode 3 (Hz)
Theoretical Calculations	1.335	8.366	23.405
Finite Element Method	1.334	8.362	23.416
Measurement	1.3	8.1	22.5

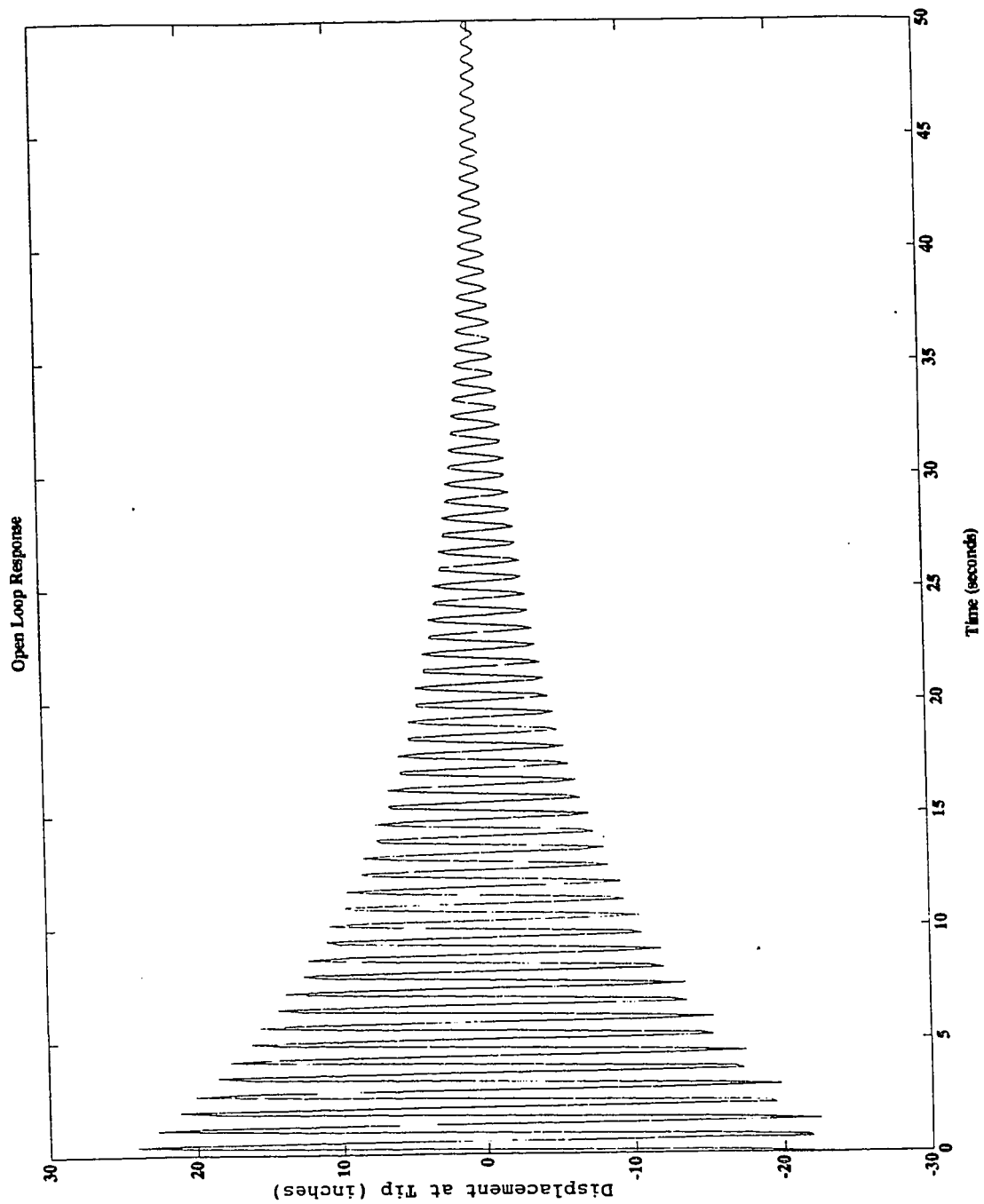


Figure 7: Open Loop Response of Cantilever Beam

State Space Representation

The mass, damping, stiffness, and mode shape matrices from I-DEAS finite element analysis package must be represented in a useful form for control analysis. The second order equation from I-DEAS is now transformed into first order terms using the state space representation. The state space equations are derived from the dynamic equation by the following analysis.

Referring to equation (8), let us define the state variables to be $X_1 = \delta$ and $X_2 = \dot{\delta}$.

Substituting the defined state variables in equation (8) gives equations (9) and (10).

$$\dot{X}_1 = \dot{\delta} = X_2 \quad (9)$$

$$\dot{X}_2 = -M^{-1}DX_2 - M^{-1}KX_1 + M^{-1}\Psi^T F \quad (10)$$

Equation (11) is the state space form of equations (9) and (10).

$$\begin{bmatrix} \dot{X}_1 \\ \dot{X}_2 \end{bmatrix} = \begin{bmatrix} 0 & I \\ -M^{-1}K & -M^{-1}D \end{bmatrix} \begin{bmatrix} X_1 \\ X_2 \end{bmatrix} + \begin{bmatrix} 0 \\ M^{-1}\Psi^T \end{bmatrix} F \quad (11)$$

The output of displacement at the nodal points is in the form:

$$Y = \begin{bmatrix} \Psi & 0 \end{bmatrix} \begin{bmatrix} X_1 \\ X_2 \end{bmatrix} \quad (12)$$

where Ψ , the mode shape, is selected by the user from the Finite Element Analysis (FEA) package.

The force term F above is the input to the system. The input in this case would be the moment from the piezo film acting on the nodes of the beam. Derivation of the applied moment due to voltage is done in the following section.

Piezo Film Modeling

The piezo film used in this study is a thin layer of uniaxially polarized polyvinylidene flouride or PVF₂. When voltage is applied to the piezo film, it will strain in the longitudinal direction. This causes a resultant moment which can be used to dampen the vibration of the beam. This material can be modeled as shown in Figure 8. A detailed analysis can be found in Newman, Perlas, and Quan [1990].

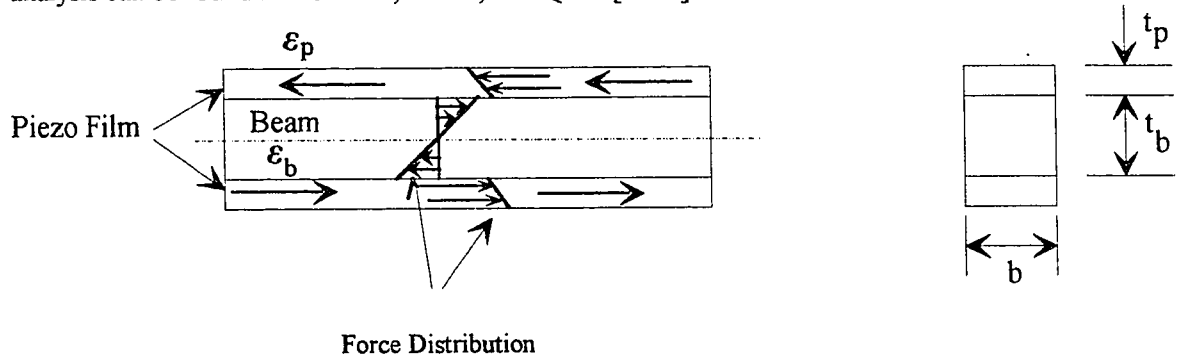


Figure 8: Beam and Piezo Film Model

When a voltage is applied to a piezoelectric film, it introduces a strain ϵ_p .

$$\epsilon_p = d_{31} \left(\frac{V}{t_p} \right) \quad (13)$$

This strain in the film also causes a longitudinal strain ϵ_b in the axial x direction in the beam to insure a force equilibrium which is given by equation (14).

$$\epsilon_b = \frac{-E_p t_p \epsilon_p}{E_b t_b + E_p t_p} \quad (14)$$

Substituting equation (13) into equation (14) gives:

$$\epsilon_b = \frac{-E_p t_p d_{31} V}{(E_b t_b + E_p t_p) t_p} \quad (15)$$

Both strains in the layers act through the moment arm from the mid plane of each layer to the neutral axis of the beam, which in this case is the centroid of force distribution (refer to Figure 8). From summing the moment about the neutral axis, equation (16) is obtained.

$$M = 2E_p A_p (\varepsilon_p + \varepsilon_b)(t_p + t_b)/2 \quad (16)$$

$$\text{where } A_p = t_p b \quad (17)$$

Substituting equations (14) and (15) and (17) into equation (16) gives the wanted relationship of voltage to applied moment (equation 18).

$$M = \frac{E_p t_p b d_{31} V E_b t_b (t_b + t_p)}{(E_b t_b + E_p t_p) t_p} = \frac{d_{31} V E_p b E_b t_b (t_b + t_p)}{(E_b t_b + E_p t_p)} \quad (18)$$

The variables are defined as:

V = Applied Voltage (Volts)

M = Applied Moment (lb-in)

E_b = Beam Young's Modulus = 30×10^6 psi

t_b = Beam Thickness = 0.05 inch

E_p = Piezo Film Young's Modulus = 0.29×10^6 psi

t_p = Piezo Film Thickness = 0.001102 inch

ε_p = strain of piezo film (inch/inch)

ε_b = strain of beam (inch/inch)

A = cross sectional area (inch²)

b = beam height = 1 inch

d_{31} = piezo film constant = 9.055×10^{10} in-Volts

To simplify the equation, c is defined such that $M = c V$ (c was calculated from the following equations to be $1.3417\text{e-}005$ in-lb/volt)

Introduction of Piezo Film Into The Finite Element Model

The moment created by each strip of piezo film due to the three voltages were modeled by creating a moment at the end nodes of the piezo film. Referring to equation (8), it can be seen that Ψ^T is a large matrix of 216×3 . The dimension of 216 comes from the fact that there are 36 nodes with 6 degrees of freedom each. The size of the matrix can be reduced by taking into consideration that the applied moment due to the input voltage only acts on the moment about the y axis. This simplification makes Ψ^T a 36×3 matrix. Ψ^T is renamed Ψ_m^T since only the moments about y axis are considered. Ψ_m^T can be further simplified since it is assumed that three control voltages will be used.

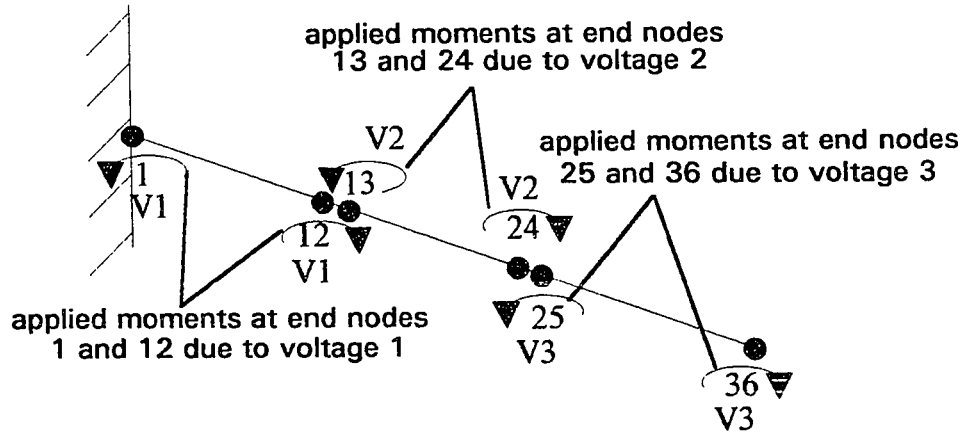


Figure 9: Visual Representation of Applied Voltages to Applied Moments

The voltage 3 strip of piezo film, for example, acts on the range of nodes from 25 to 36. The moments about each node from 25 to 36 were summed together and placed on the end nodes 25 and 36 with equal but opposite magnitudes. The same method was applied for the voltage 2 which ranged from node 13 to 24 and voltage 1 which ranged

from 1 to 12. The resultant moment between the strips of piezo film is small but does not cancel out. The resultant moment of the whole beam basically will act at the tip of the beam if $V_1 = V_2 = V_3$. A visual representation in Figure 9 is given to illustrate the effective moment acting at the selected end nodes. Ψ_m^T now becomes a 3 x 3 matrix.

Equation (8) can now be modified to incorporate equation (18) and the mode shape of moments acting on the nodes to obtain equation (19). Equation (19) describes how the voltage can affect the motion of the beam.

$$M\ddot{\delta} + D\dot{\delta} + K\delta = \Psi_m^T c V \quad (19)$$

V Vector of input voltages.(3 X 1)

c Constant from voltage to moment = 1.3417e-005 in-lb/volt

Ψ_m^T Mode shape of moments acting on nodes 1-12, 13-24, 25-36 (3 X 3)

δ Modal degree of freedom (3 X 1)

MATLAB Modeling

From the application of piezo film model to the finite element model, the dynamic equation can be written in state space form for use in MATLAB. MATLAB is a program that can manipulate matrices, simulate control systems and build and solve systems through block diagrams.

Equation 11 is then modified to incorporate the voltage to applied moment relationship of equation (19) to obtain the state space model of the system (equations 20 and 21).

$$\begin{bmatrix} \dot{X}_1 \\ \dot{X}_2 \end{bmatrix} = \begin{bmatrix} 0 & I \\ -M^{-1}K & -M^{-1}D \end{bmatrix} \begin{bmatrix} X_1 \\ X_2 \end{bmatrix} + \begin{bmatrix} 0 \\ M^{-1}\Psi_m^T c \end{bmatrix} V \quad (20)$$

$$Y = \begin{bmatrix} \Psi & 0 \end{bmatrix} \begin{bmatrix} X_1 \\ X_2 \end{bmatrix} \quad (21)$$

where Ψ , modal degree of freedom, is specified for the desired output

Comparing with the general form

$$\dot{X} = AX + BU$$

$$Y = CX + DU$$

$$A = \begin{bmatrix} 0 & I \\ -M^{-1}K & -M^{-1}D \end{bmatrix}$$

$$B = \begin{bmatrix} 0 \\ M^{-1}Y_m^T c \end{bmatrix}$$

$$C = \begin{bmatrix} \Psi & 0 \end{bmatrix}$$

$$D = \begin{bmatrix} 0 \end{bmatrix}$$

Matlab variables

am	A
bm	B
cm	C

Matlab variables are found in Appendix D.

Controllability and Observability

The analysis of controllability and observability must be considered to insure that the current system can be controlled with given inputs and given measuring devices. The controllability matrix $[m]$ (equation 22) was created for the system and can be found in Appendix F. From the controllability matrix it can be seen that the rank is six. This means that the system is totally controllable.

The output controllability and observability were done for two cases. One was when one accelerometer was placed at the end of the beam (node 36). The other was when two accelerometers were used. One accelerometer was placed at the end and one was placed mid span (node 16) of the beam. From the analysis it could be seen that output controllability matrix $[o]$ (equation 23) was totally controllable for both cases.

Observability was the crucial question, since it was important to know if the second mode could be observed with just one accelerometer or whether two accelerometers were necessary. The observability matrix $[L]$ was created (equation 24) and the rank of the matrix was found to be 6. This shows that either case would give a totally observable system.

The Controllability Matrix (Appendix F) for our system is given by equation (22)

$$[m] = [B \quad AB \quad A^2B \quad A^3B \quad A^4B \quad A^5B] \quad (22)$$

The rank of the controllability matrix was found to be 6. Therefore, the system is totally controllable.

Output Controllability Matrix for our system is given by equation (23)

$$[o] = [CB \quad CAB \quad CA^2B \quad CA^3B \quad CA^4B \quad CA^5B] \quad (23)$$

RANK(o) = 2 For two accelerometers

RANK(o) = 1 For one accelerometer

were the output controllability matrix for 1 or 2 accelerometer were found to be output controllable

Observability Matrix for our system is given by

$$[L] = \begin{bmatrix} C \\ CA \\ CA^2 \\ CA^3 \\ CA^4 \\ CA^5 \end{bmatrix} \quad (24)$$

RANK(L) = 6 For two accelerometers

RANK(L) = 6 For one accelerometer

Applied Control Systems

Two control systems were employed in the simulation of beam vibration control: (1) the basic bang bang control system with a single voltage and (2) the optimal control state feedback with state estimator. The bang bang control system (Figure 10) used the velocity as feedback which was calculated from the accelerometer. Depending upon the direction of the velocity at the beam tip (positive or negative) opposite constant voltage was returned to all pieces of piezo film. This simulation was done with the aid of Simulink. Simulink is a subset of MATLAB in which control block could be modeled graphically then simulated.

The State Space block contain the state matrixes A, B, C, D which describe the beam. The demux is a one to many output module. The mux is a many to one input module. The switch activates the first pin when the input to the second pin is positive and activates the third pin when the input to the second pin is negative. When the first or third pin was activated, a constant unit step multiplied by the voltage gain gave the return voltage to the piezo film. This voltage in turn caused an opposing moment which caused the beam to dampen.

The voltages used in the simulation were 800, 400, and 100 volts. V1, V2, and V3 were assumed equal. All simulations were done with the same initial conditions as the open loop simulation, $[1 \ 0 \ 0 \ 0 \ 0 \ 0]$. Note that since 1 was chosen for the initial state for the first mode, the corresponding initial displacement of 24 inches seems very high, but for simulation purpose of obtaining damping characteristics is irrelevant. The plots of displacement at the beam tip for all voltages are displayed in Figures 11 - 13. Plots for velocity and acceleration at the beam tip can be found in Appendix E.

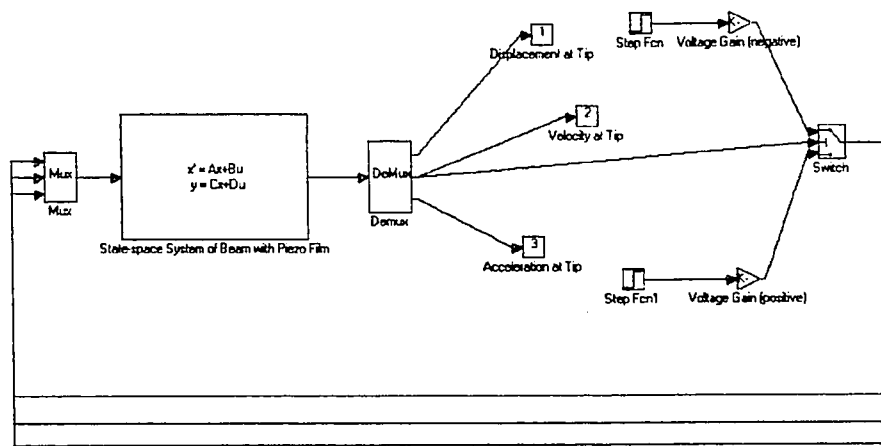


Figure 10: Simulink Model of Bang Bang Control System

Comparing the outputs of various applied voltages with the open loop response (Figure 6), it can be seen that the system works relatively well with all the single voltage feedback. As the voltage increases, the system settles faster. The question now comes is the available power to keep this applied voltage readily available? What if the amount of voltage was limited? The solution would be to try full state feed back with optimal control.

Note: All displacements on following graphs are at the tip of the beam and in inches.

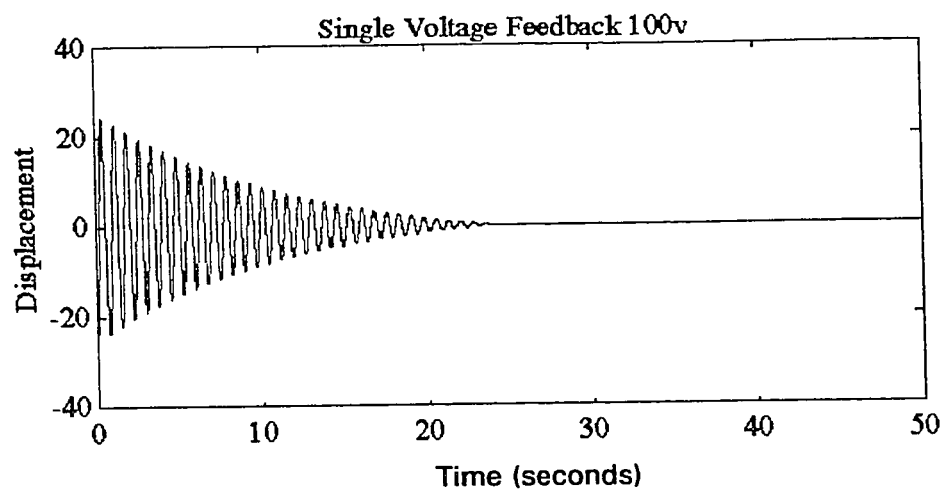


Figure 11: Response of Bang Bang Control System Using 100 Volts For Feedback

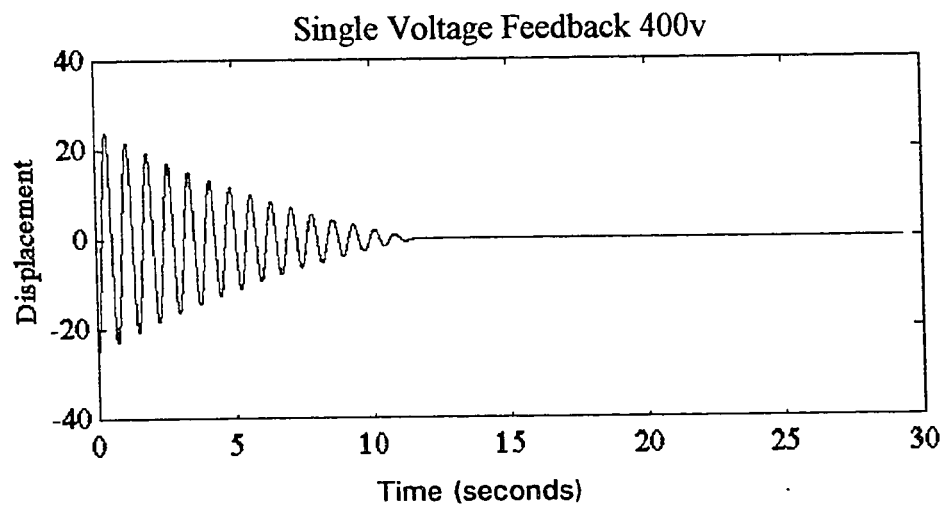


Figure 12: Response of Bang Bang Control System Using 400 Volts For Feedback

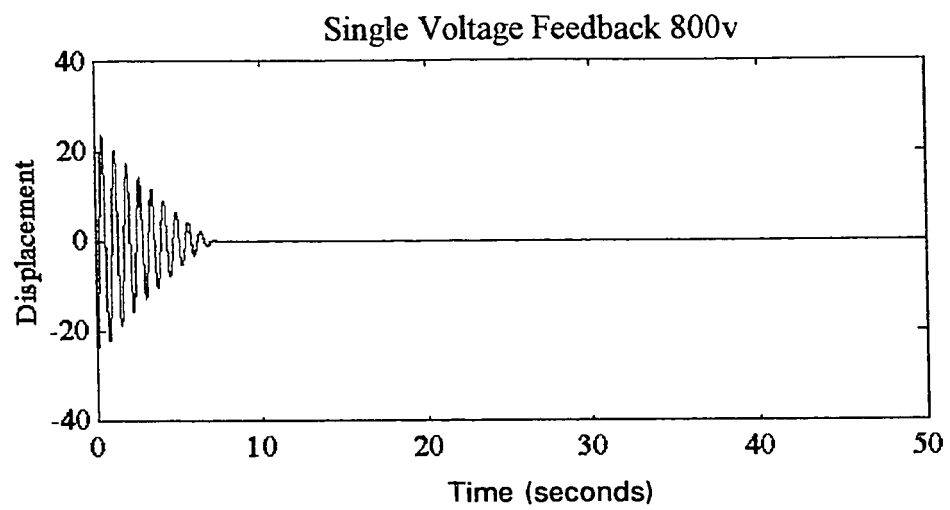


Figure 13: Response of Bang Bang Control System Using 800 Volts For Feedback

Full State Feedback

Referring to Figure 14, it can be seen that the feedback is now coming from all states of the system (displacement and velocity of each mode) as oppose to the velocity feedback in the single voltage feedback system. It can also be seen that since the system has multiple inputs and multiple outputs, the proportional gain constant must be obtained from optimal control theory. The steady state version of optimal control or Linear Quadratic Regulator (LQR) will be used. LQR implies the cost function (equation 25) is quadratic and it applies to regulator case.

The weighting functions Q and R were arbitrarily chosen with the weight mainly on velocity. The velocity term is more important in this analysis since it is directly associated with damping. Equation (29) shows that the displacement for the first three modes were normalized to one and the velocity terms were heavily weighted to 80000. Q was varied and R kept constant until the desired system response was obtained. Then R was varied and Q was kept constant until the input to the system was approximately what was desired. The weighting matrices chosen for this study were equations (29), (30), and (31).

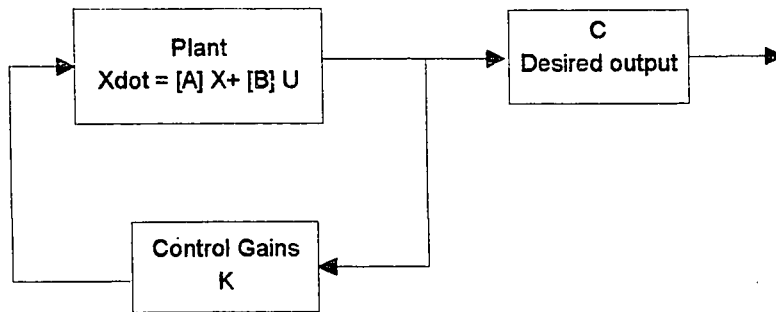


Figure 14: Full State Feedback model

Linear Quadratic Regulator

$$\text{Cost Function } j = \frac{1}{2} \sum_{k=0}^N [X_k^T Q + U_k^T R U_k] \quad (25)$$

$$S_{\infty} = A^T [S_{\infty} - S_{\infty} B P^{-1} B^T S_{\infty}] A + Q \quad (26)$$

$$P = R + B^T S_{\infty} B \quad (27)$$

$$K_{\infty} = [R + B^T S_{\infty} B]^{-1} B^T S_{\infty} A \quad (28)$$

The steady state LQR can be obtained using equations (26), (27), and (28). S_{∞} must first be obtained by iterating equations (26) and (27) until S_{∞} makes the equality true. K_{∞} can then be calculated from equation (29) knowing S_{∞} . For this study, equation (32) shows the calculated K_{∞} . The closed loop system can now be described using equation (33).

The Q and R chosen for this simulation are

$$Q = \begin{bmatrix} 1 & 0 & 0 & 0 & 0 & 0 \\ 0 & 1 & 0 & 0 & 0 & 0 \\ 0 & 0 & 1 & 0 & 0 & 0 \\ 0 & 0 & 0 & 80000 & 0 & 0 \\ 0 & 0 & 0 & 0 & 80000 & 0 \\ 0 & 0 & 0 & 0 & 0 & 80000 \end{bmatrix} \quad (29)$$

- R chosen for approximately 400 volt input

$$R_{400} = \begin{bmatrix} 1 & 0 & 0 \\ 0 & 2 & 0 \\ 0 & 0 & 3 \end{bmatrix} \quad (30)$$

- R chosen for approximately 800 volt input

$$R_{800} = \begin{bmatrix} 0.5 & 0 & 0 \\ 0 & 1.0000 & 0 \\ 0 & 0 & 1.5000 \end{bmatrix} \quad (31)$$

- The controller constants were calculated to be

$$k = \begin{bmatrix} 0.4494 & 1.9036 & 9.0885 & 49.9216 & -146.5945 & 67.5547 \\ 0.0341 & -0.0118 & 0.5151 & 60.7886 & 10.9384 & -64.2015 \\ -0.2867 & 1.6697 & -2.5856 & 48.2292 & 62.4385 & 54.6163 \end{bmatrix} \quad (32)$$

- The closed loop system now becomes

$$\dot{X} = [A-Bk] [X] \quad (33)$$

Assuming that 400 volts was the maximum peak voltage, the best results are displayed in the following graphs. Appendix G contains the other attempts. Figure 15 shows the system without the estimator. The beam dampens to a minimum in approximately 35 seconds while Figures 16 -18 show the input for all three voltages which start off at approximately 400 volts and then decay. The response isn't as fast as the bang bang type of control but the voltage doesn't have to remain constant, therefore saving energy.

If the maximum peak voltage is increased, the response of the system does improve. Figure 19 shows the response due to maximum input voltages of approximately 800 volts (Figure 20 - 22). The decay is more noticeable than that of the 400 volt case. The system dampens to a minimum in approximately 25 seconds.

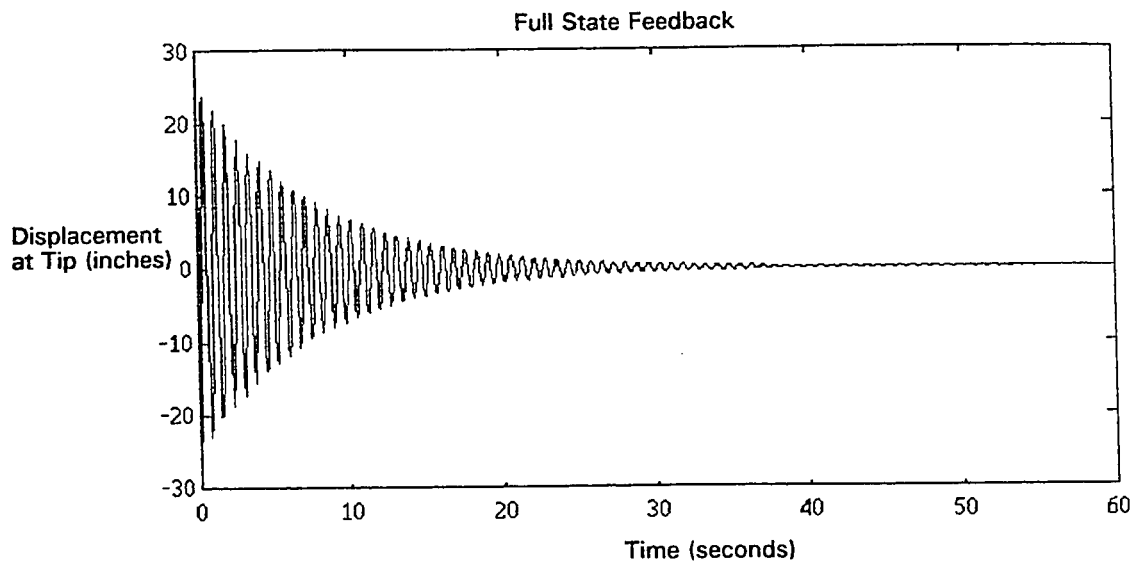


Figure 15: Response of Displacement at the Beam Tip Using Full State Feedback

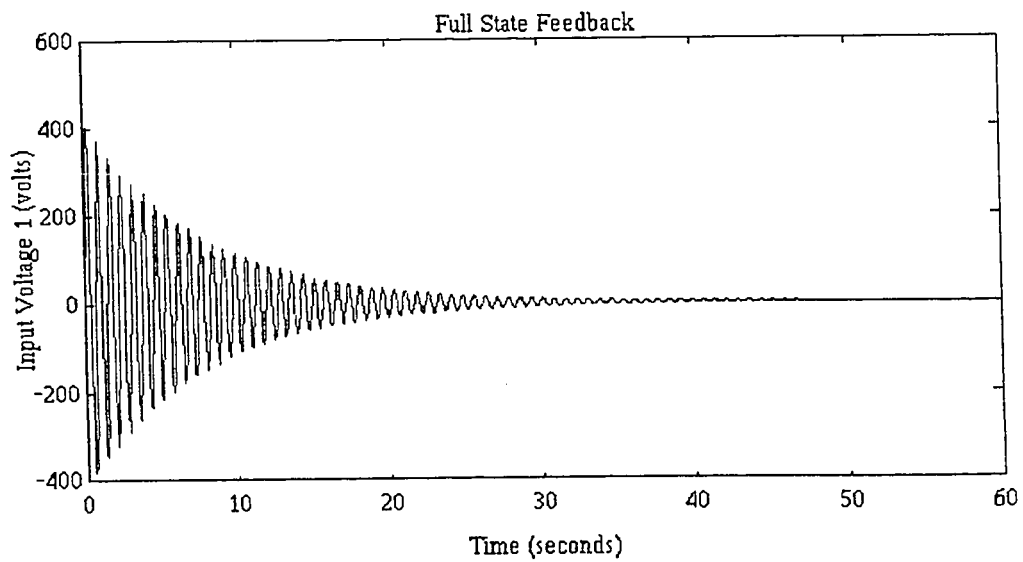


Figure 16: Voltage 1 Input for Full State Feedback System

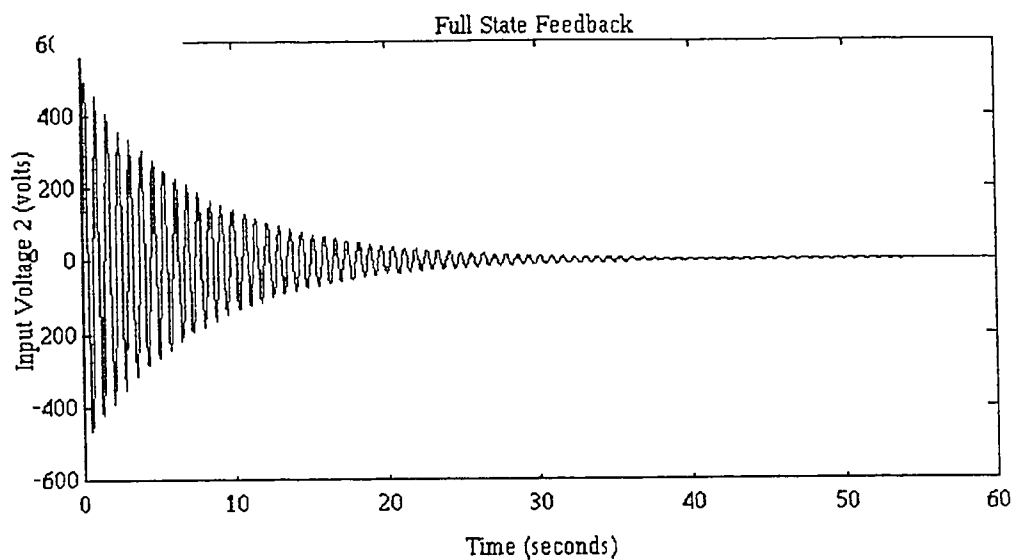


Figure 17: Voltage 2 Input for Full State Feedback System

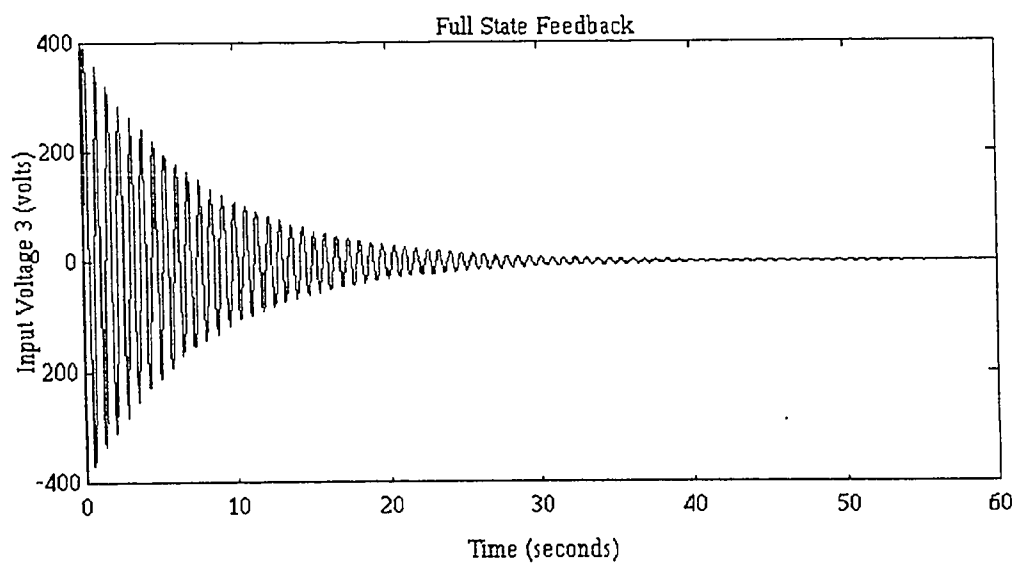


Figure 18: Voltage 3 Input for Full State Feedback System

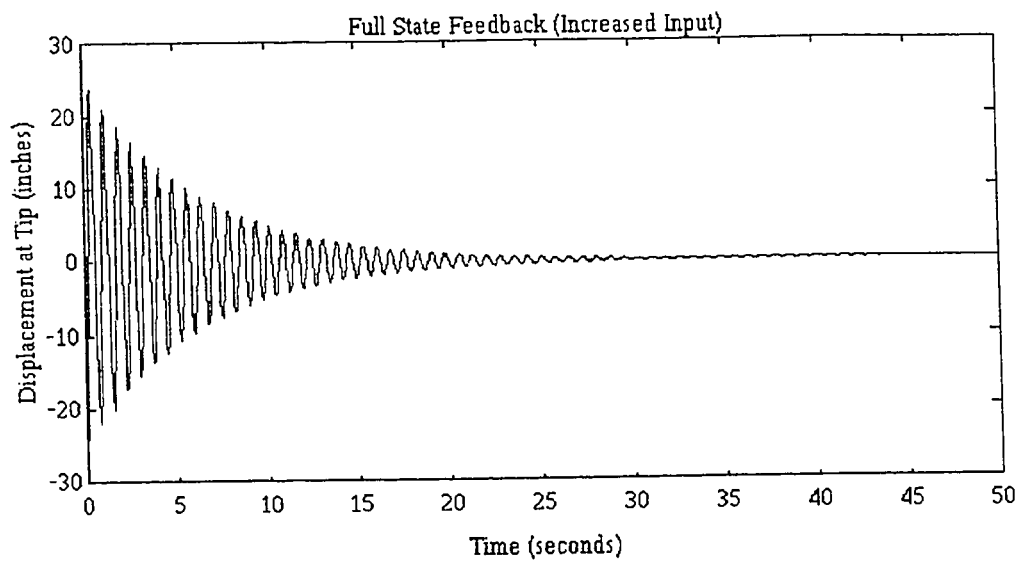


Figure 19: Response of Displacement at the Beam Tip Using Full State Feedback and Increased Input

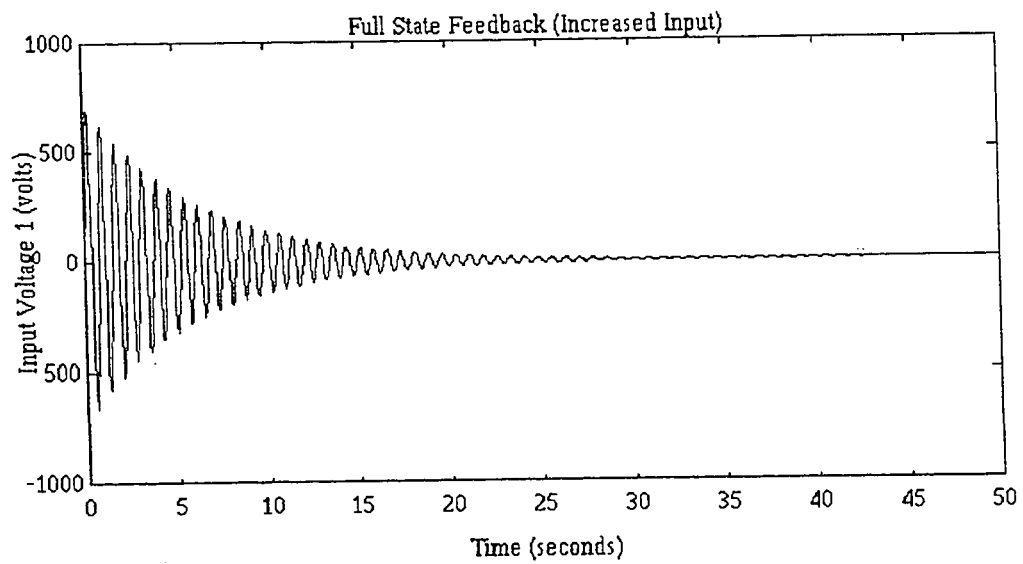


Figure 20: Increased Voltage 1 Input for Full State Feedback System

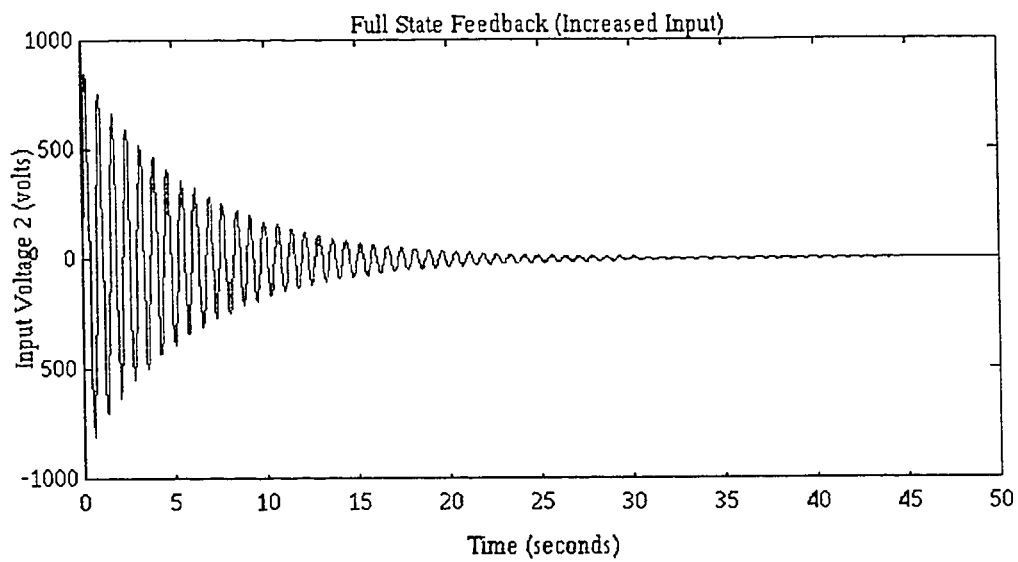


Figure 21: Increased Voltage 2 Input for Full State Feedback System

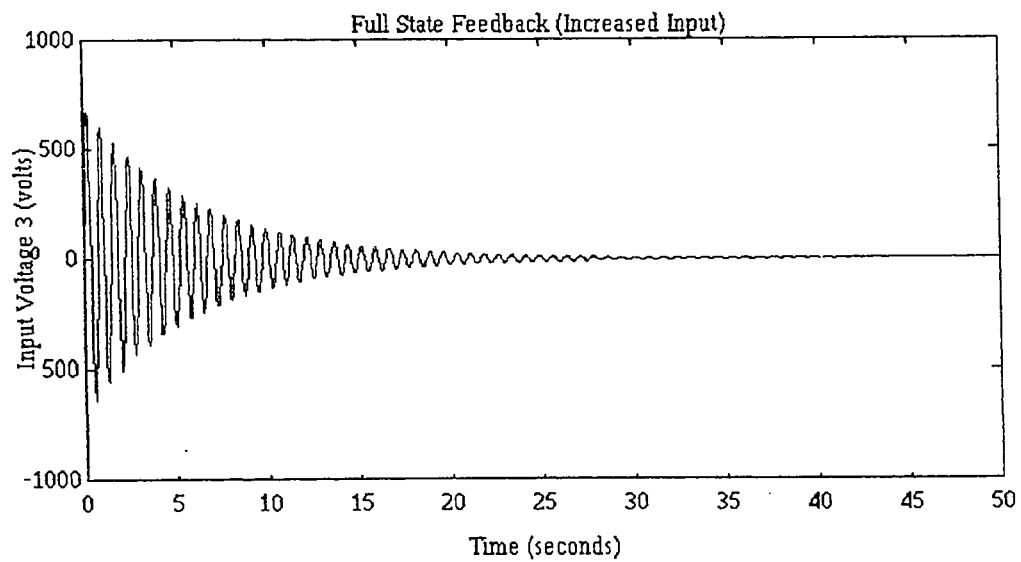


Figure 22: Increased Voltage 3 Input for Full State Feedback System

Full State Feedback with Estimator

Since an accelerometer was the only feedback signal that was being received in our system, an estimator was also required. Referring to Figure 23, the output matrix $[C]$ now become the mode shape for acceleration (\ddot{X}_2). The estimator takes the information from the input and the available output to predict the states of the system. A full state estimator was used to help filter out some of the noise that might appear from the reading of the accelerometer. The output of the estimator is then subject to the control gains. Finally, the outputs of the control gains block are the control voltages to the piezo film and the feedback to the estimator.

From the analysis on observability in Appendix E, we know that the system is observable; therefore, the estimator could be designed. Using the same poles as that given by the LQR for the chosen controller constants ($\text{roots}(A-Bk)$), the observer constants were calculated by using pole placement. Ackermann's Formula (equation 34) was used to calculate the pole placement. The calculated estimator gains are shown in equation (35). The state matrix is then reorganized and put in a different form for simulation of the real system with the state estimator (equation 36).

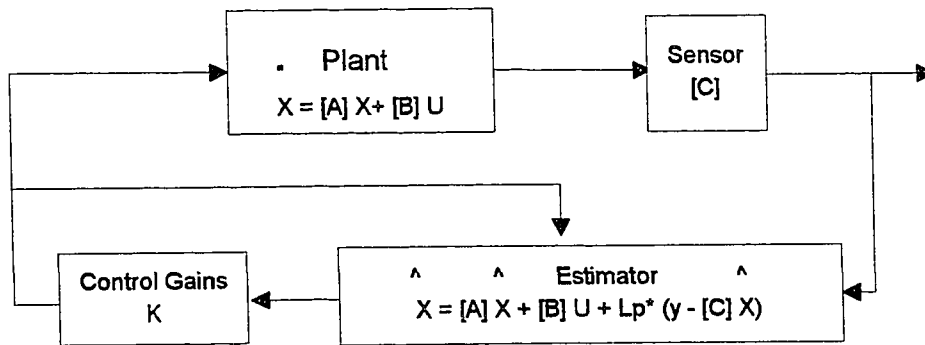


Figure 23: Full State Feedback With Estimator

Ackermann's Formula

$$L_p = J(A) \begin{bmatrix} C \\ CA \\ CA^2 \\ CA^3 \\ CA^4 \\ CA^5 \end{bmatrix} \begin{bmatrix} 0 \\ 0 \\ 0 \\ 0 \\ 0 \\ 1 \end{bmatrix} \quad (34)$$

where $J(A) = Z^6 + C_1*Z^5 + C_2*Z^4 + C_3*Z^3 + C_4*Z^2 + C_5*Z + C_6 I$ is the desired characteristic equation

The estimator gains were calculated to be

$$L_p = 1.0e-004 * \begin{bmatrix} 0.5008 \\ 0.7459 \\ 0.2276 \\ -0.0233 \\ -0.1713 \\ 0.4142 \end{bmatrix} \quad (35)$$

The system with estimator then becomes

$$\begin{bmatrix} \dot{X} \\ \dot{X}_E \end{bmatrix} = \begin{bmatrix} A & -BK \\ L_p C & A-BK-L_p C \end{bmatrix} \begin{bmatrix} X \\ X_E \end{bmatrix} \quad (36)$$

where X_E is the estimated states

Figure 24 shows the response of the system with the estimator (assuming peak voltage is approximately 400 volts). The estimator does cause the system response to slow down as compared with the full state feedback without the estimator. The estimator also causes a slight difference in the required input voltage (Figures 25 - 27) as compared to Figure 16 to Figure 18. The form of the input voltage is not as smooth as the case without the estimator because the initial conditions of the estimator was assumed to be $[0 \ 0 \ 0 \ 0 \ 0]^T$, and the fact that the states are estimated and not the actual. The beam vibration still settles to a minimum in approximately 40 seconds.

Increasing the maximum input voltage to approximately 800 volts was attempted. Figure 27 shows the displacement response of the beam tip. The response shows a slight improvement over the 400 volt case. The input voltages are displayed in Figures 29 - 31. The maximum input voltages are very close to the actual states case. However, it is obvious that the full state feedback without the estimator has a more significant effect on the system than the cases with the estimator.

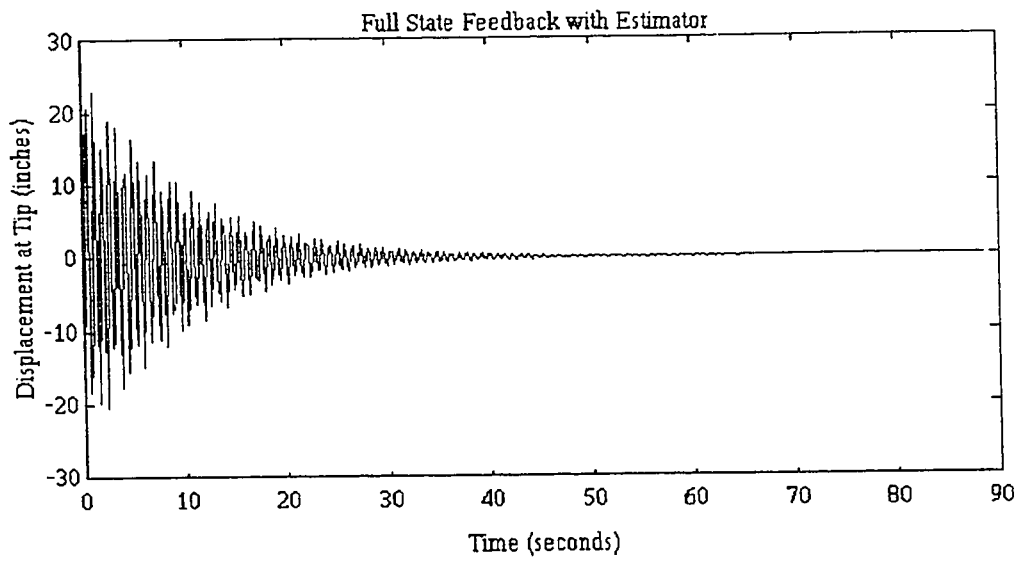


Figure 24: Response at Beam Tip using Full State Feedback With Estimator

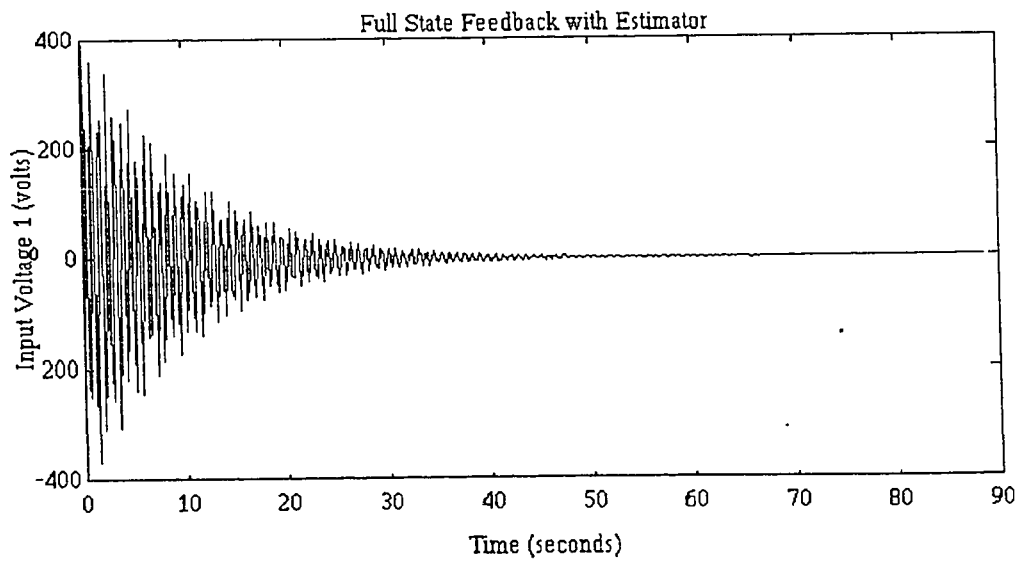


Figure 25: Input Voltage 1 Using Full State Feedback With Estimator

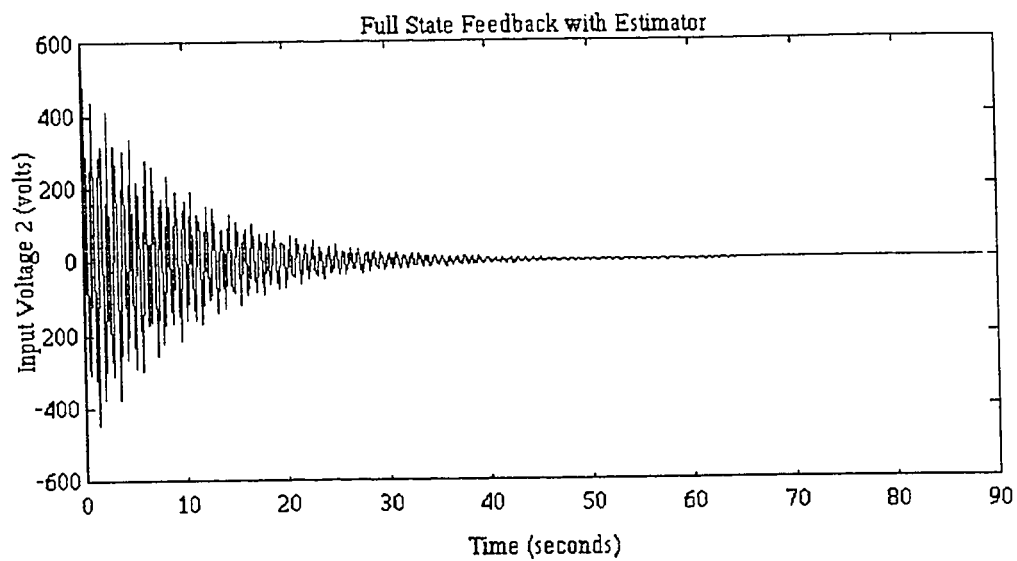


Figure 26: : Input Voltage 2 Using Full State Feedback With Estimator

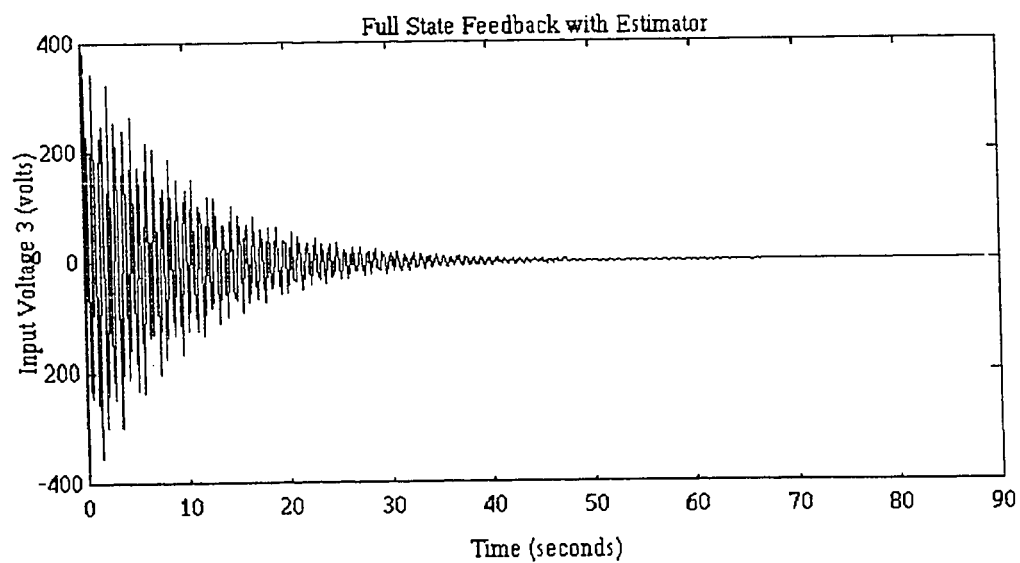


Figure 27: Input Voltage 3 Using Full State Feedback With Estimator

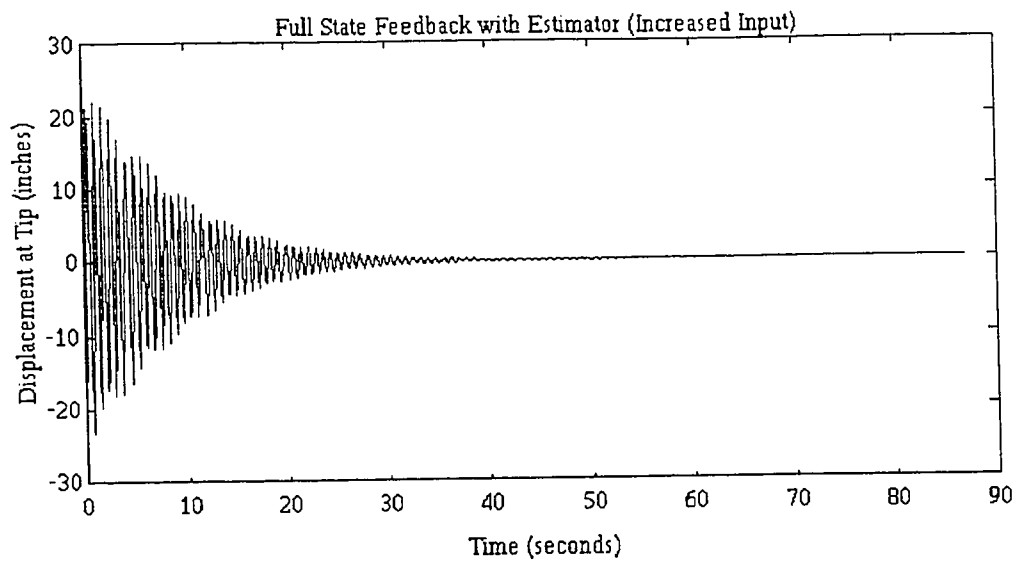


Figure 28: Response at Beam Tip using Full State Feedback With Estimator and Increase Voltage

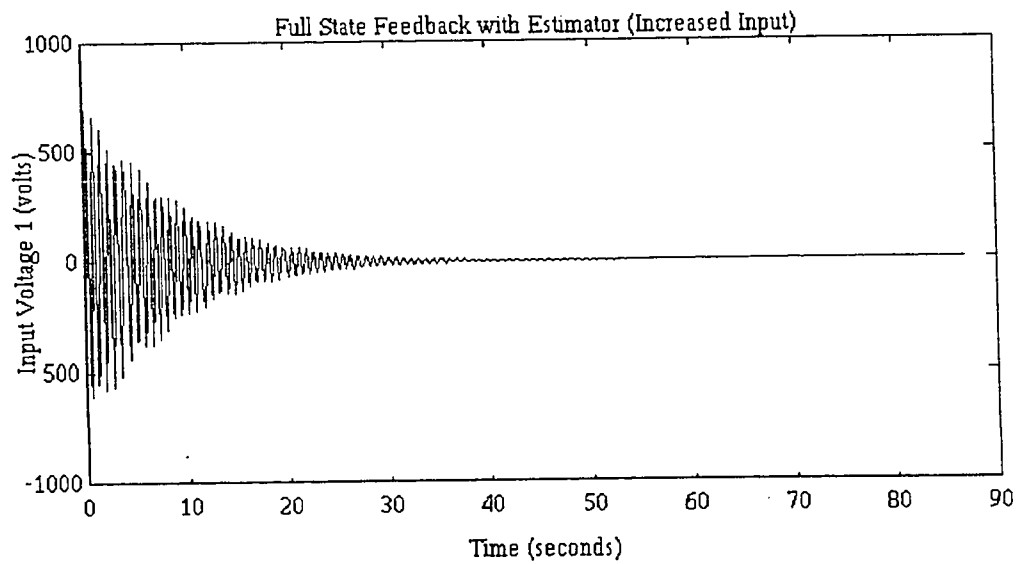


Figure 29: Increased Input Voltage 1 Using Full State Feedback With Estimator

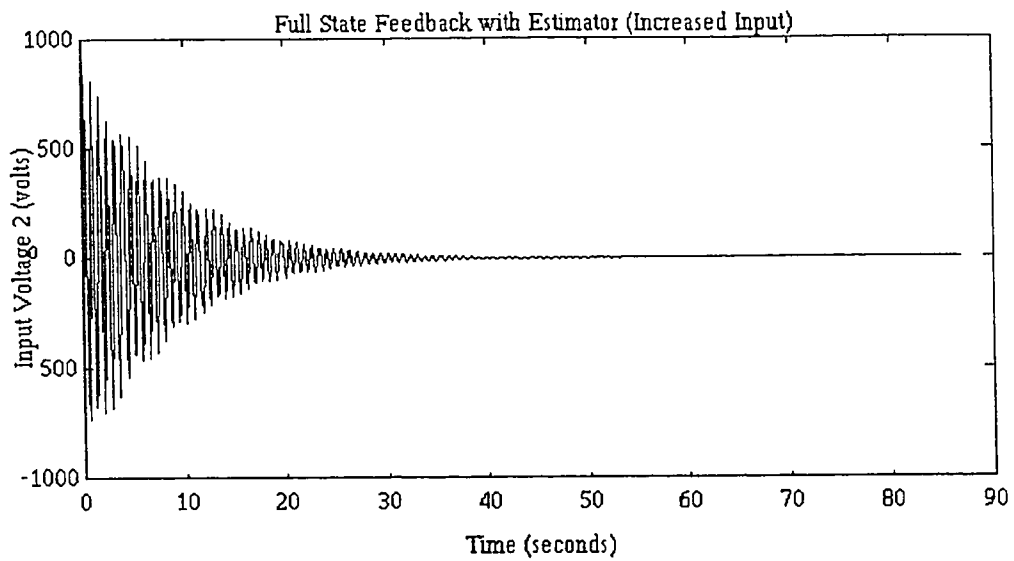


Figure 30: Increased Input Voltage 2 Using Full State Feedback With Estimator

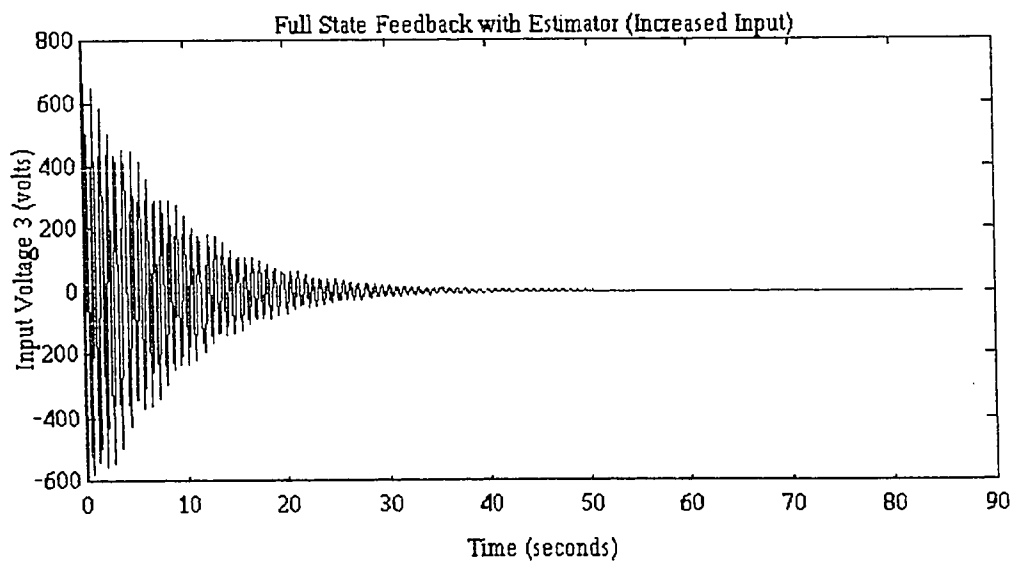


Figure 31: Increased Input Voltage 3 Using Full State Feedback With Estimator

Independent Modal Space Control Analysis

By referring back to the system model of the beam and the finite element model, it can be seen that the systems of equations are independent of each other. Basically the eigenvectors were actually the three modes of vibrations and the eigenvalues were the natural frequencies. This type of analysis becomes an integral part in the study of Independent Modal Space Control (IMSC). In the case of the beam, the IMSC would attempt to control the different modes of the beam. The control gains are calculated using pole placement or optimal control as previously done.

Using the model of the full state feedback with estimator (increased voltage), the system was tested to see the modal responses. The initial displacement of the modes were assigned as $[.2 \ .05 \ .02 \ 0 \ 0 \ 0 \ 0 \ 0 \ 0 \ 0 \ 0]$. This means that the first mode was initial displaced .2 inch, the second mode was initial displaced .05 inch, the third mode was initially displaced .02 inch, the derivatives of the modes were set to zero, and all the estimator states were set to zero. The first mode can now be compared in Figures 32 and 33. The second mode can be compared in Figures 34 and 35. The third mode can be compared in Figures 36 and 37.

From the comparison, it can be seen that the first mode dampening isn't that noticeable as compared with the second and third mode. The dampening can definitely be seen in the higher modes. Since the first mode is most dominant and naturally takes longer to die down, higher input voltages are required to dampen this mode faster. From the input voltage graphs in Figures 38 to 40, it can be seen the initial voltage input is high as compared the rest of the input as time passes. The highest peak voltage for this case is approximately 600 volts. This peak voltage is most likely due to the estimator error in keeping up with the actual system. If the voltage of the overall system was increased and

a limiter put on the peak voltages the performance of the system may improve dramatically. The limiter would cause the system to act like a bang bang control system during the time the input voltage is greater the voltage limit. As could be seen in the bang bang control , this would cause the system to dampen quickly. When the voltage dropped below the voltage limit, the system would behave like the full state feedback with estimator case.

Looking at the actual system response in Figure 42 and comparing it with the open loop response (Figure 41), it could be seen that the first mode is dominating and does dampen with the current system. Improvement can be made by increasing the input voltage and adding a limiter as discussed above, or by adjusting the poles of the closed loop system as well as the estimator so that the control of the first mode can be done more effectively. This is the advantage of using independent modal space control.

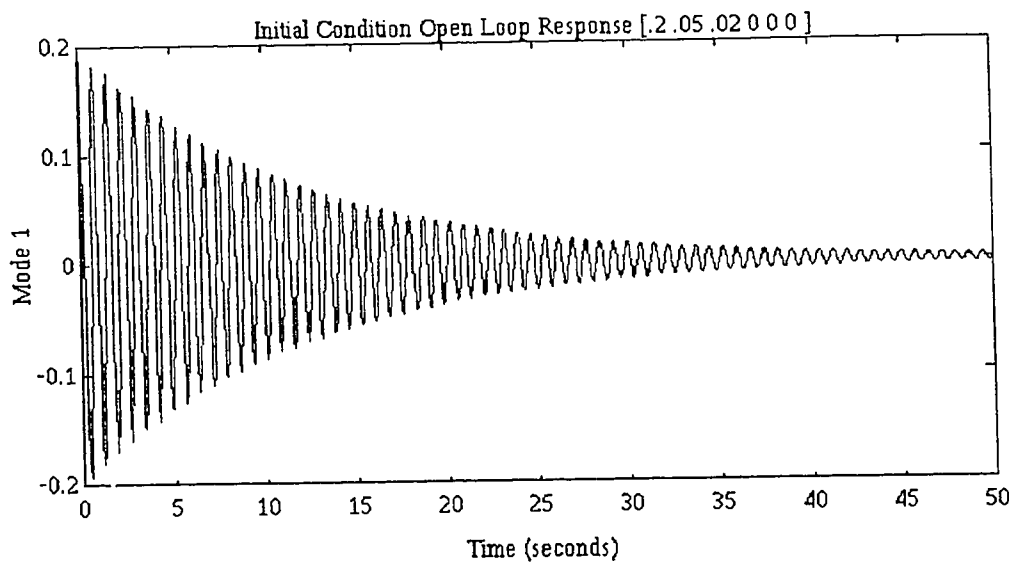


Figure 32: Open Loop Response Of The First Mode

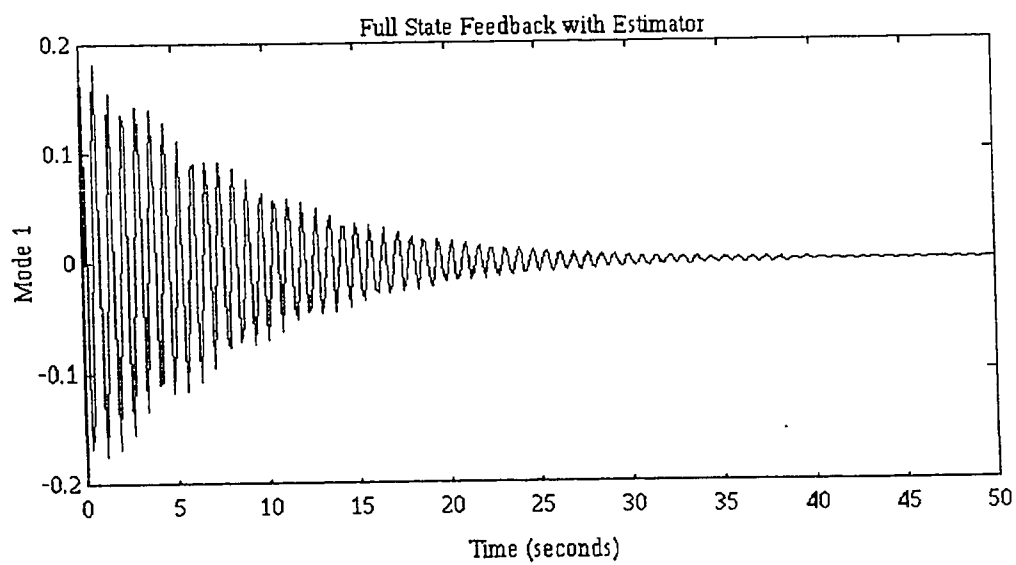


Figure 33: Closed Loop Response Of The Second Mode

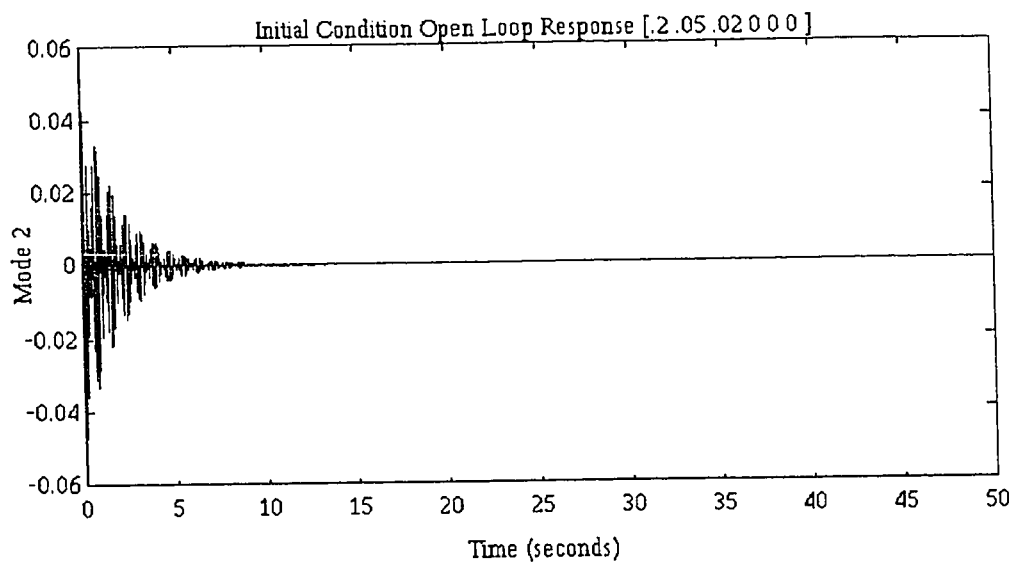


Figure 34: Open Loop Response Of The Second Mode

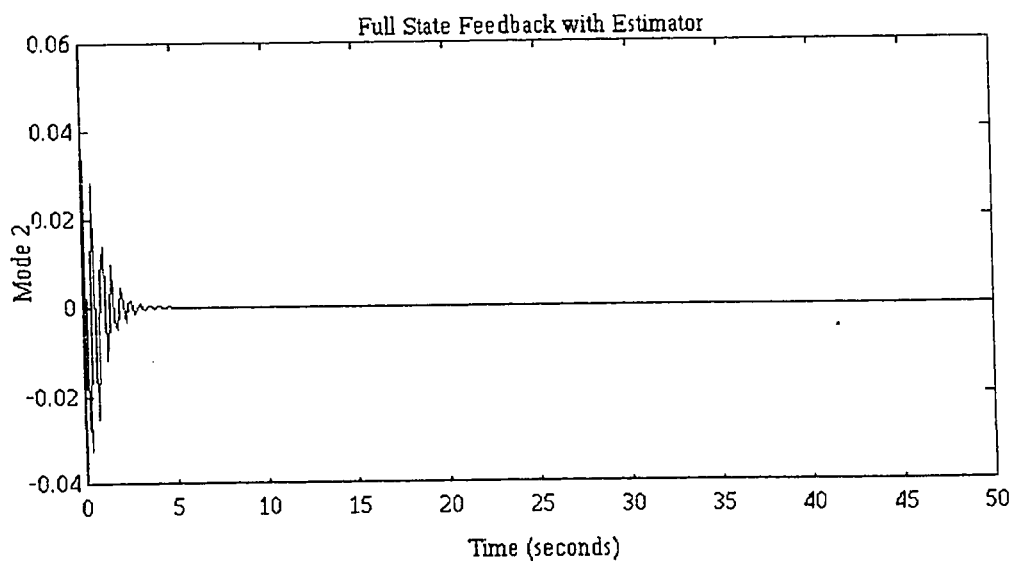


Figure 35: Closed Loop Response Of The Second Mode

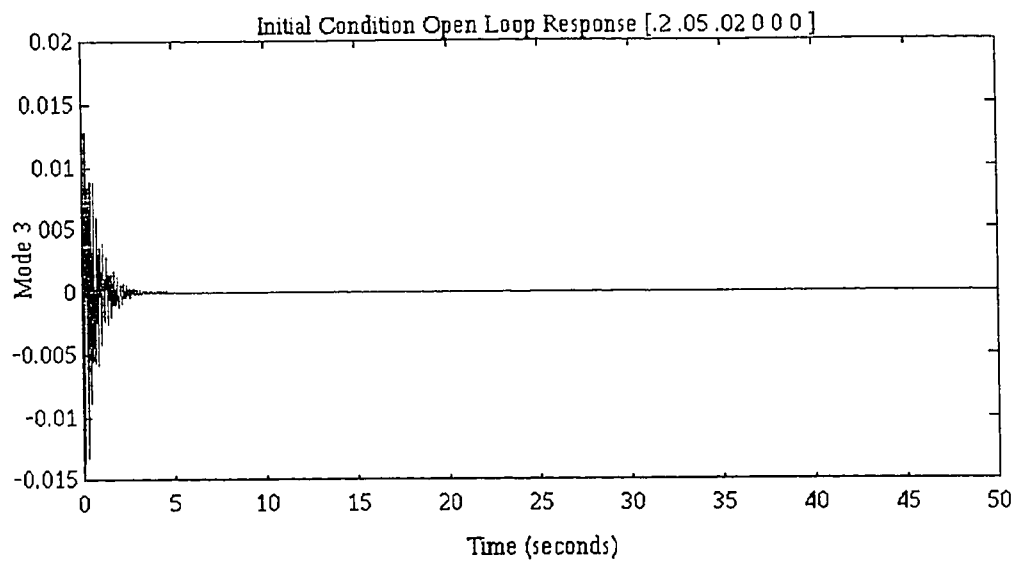


Figure 36: Open Loop Response Of The Third Mode

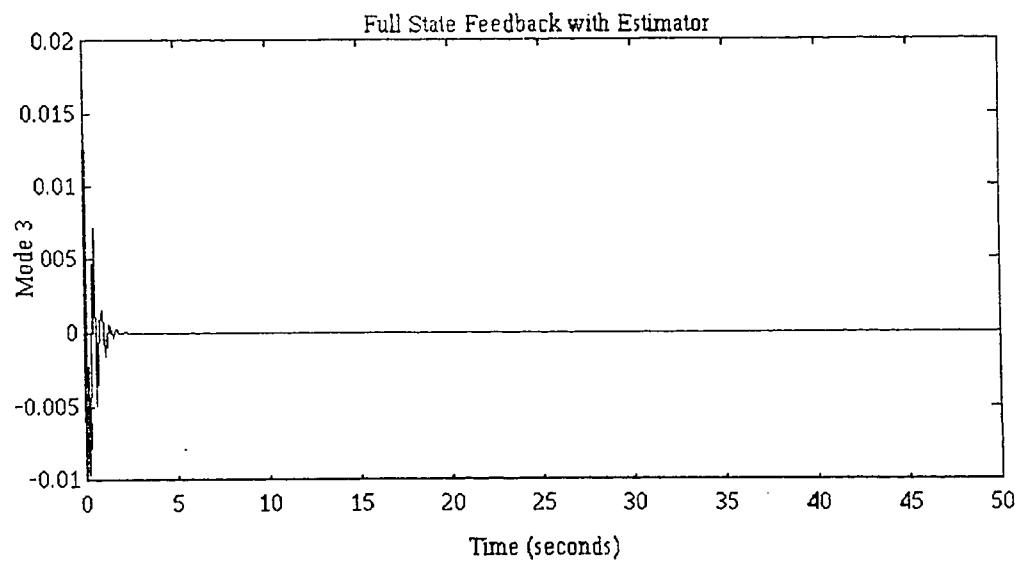


Figure 37: Closed Loop Response Of The Third Mode

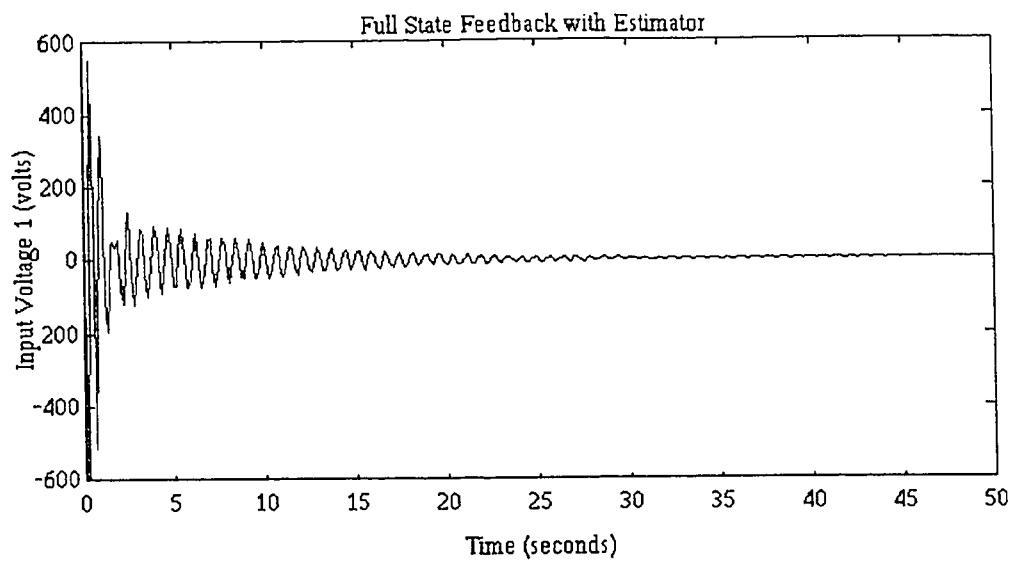


Figure 38: Input Voltage 1 For Closed Loop System

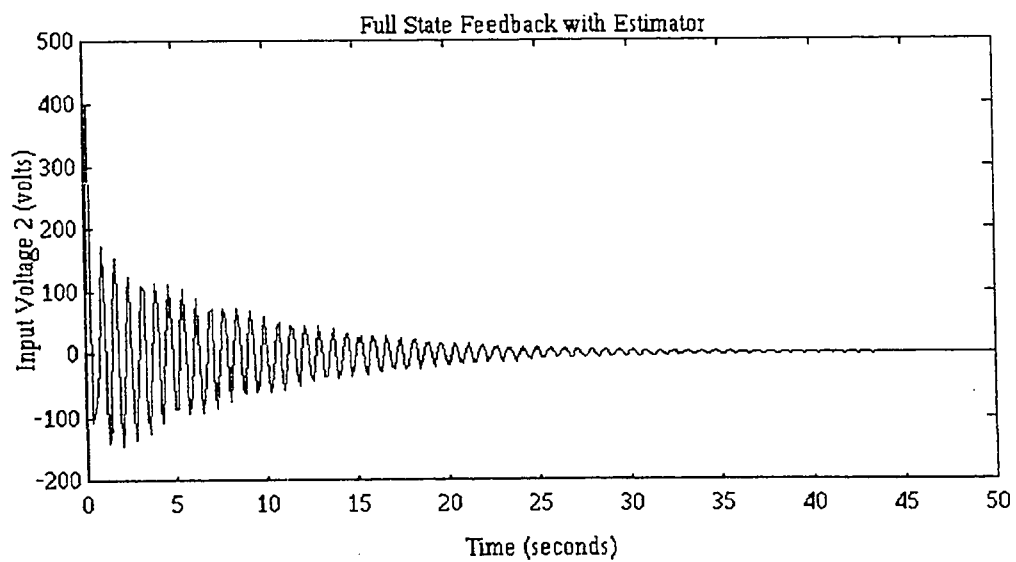


Figure 39: Input Voltage 2 For Closed Loop System

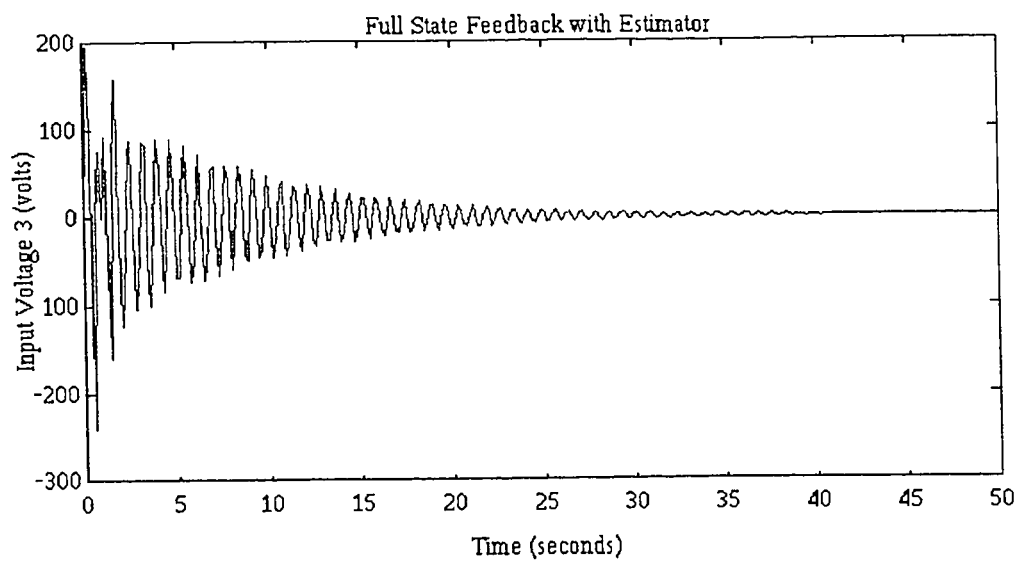


Figure 40: Input Voltage 3 For Closed Loop System

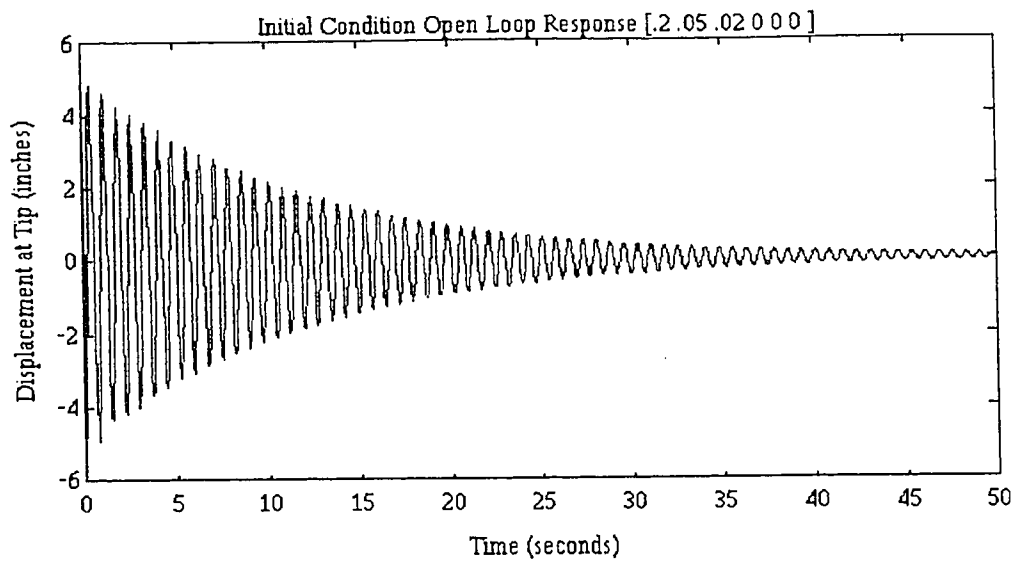


Figure 41: Displacement At Tip For The Open Loop Response

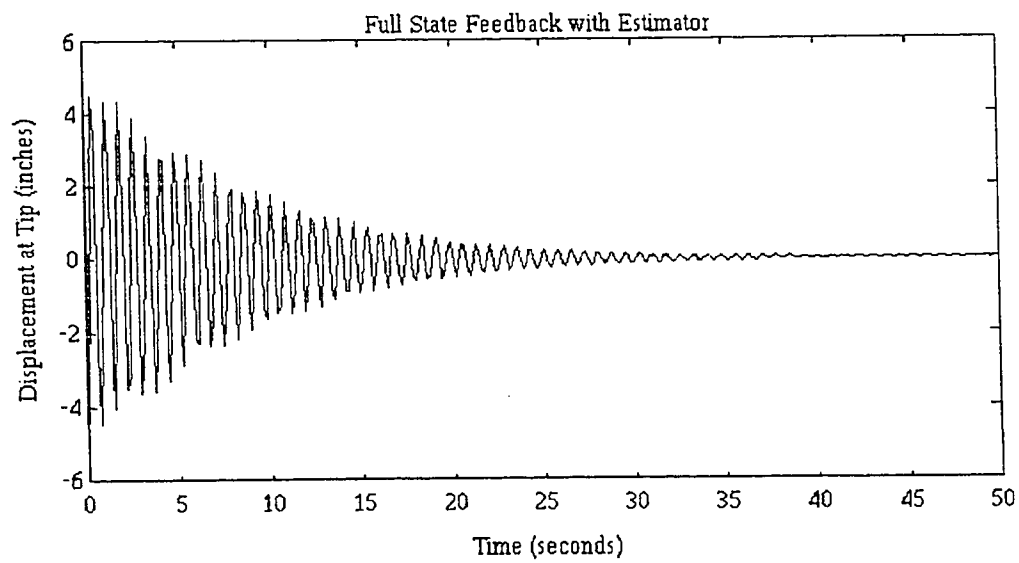


Figure 42: Displacement At Tip For The Closed Loop Response

Conclusion and Recommendations

We have shown that a simple bang bang control system works well in controlling vibration of a beam with a low natural frequency. The more sophisticated full state feedback with estimator does not improve the response in dampening the vibration if equal maximum input voltages are used. However, dampening does work well and the energy saved from the optimal control system may be significant to a designer. Increasing the voltage in either case will give improved responses.

As suggested previously, the response of the system could be improved by using a combination of the two control strategies. The gain matrix must be increased in the full state feedback case to get a higher return voltage. Then by combining the higher return voltage with a voltage limiter, a bang bang effect is obtained. This is not as difficult to implement and more efficient than to just increase the peak voltage. Also additional pole placement analysis could be done to try to get a better response in the case of independent modal space control. Attempting to better control the first mode in this case would be the most relevant.

This study has not been verified in terms of actual implementation. It is recommended that this study be used in conjunction with the completion of the actual implementation of the two types of control systems that have been analyzed in this study. The bang bang control has been implemented in previous studies such as [Newman, Perlas, and Quan, 1990] and [Bailey Thomas and Hubbard, 1985]. Therefore, this type of control should be easily implemented for this configuration of the cantilever beam. The optimal control system will require more software control, thus making it more difficult to implement. The system should be used and tested to the maximum voltage input that the

available equipment can achieve. The higher the input voltage is, the better responses that can be expected from the system.

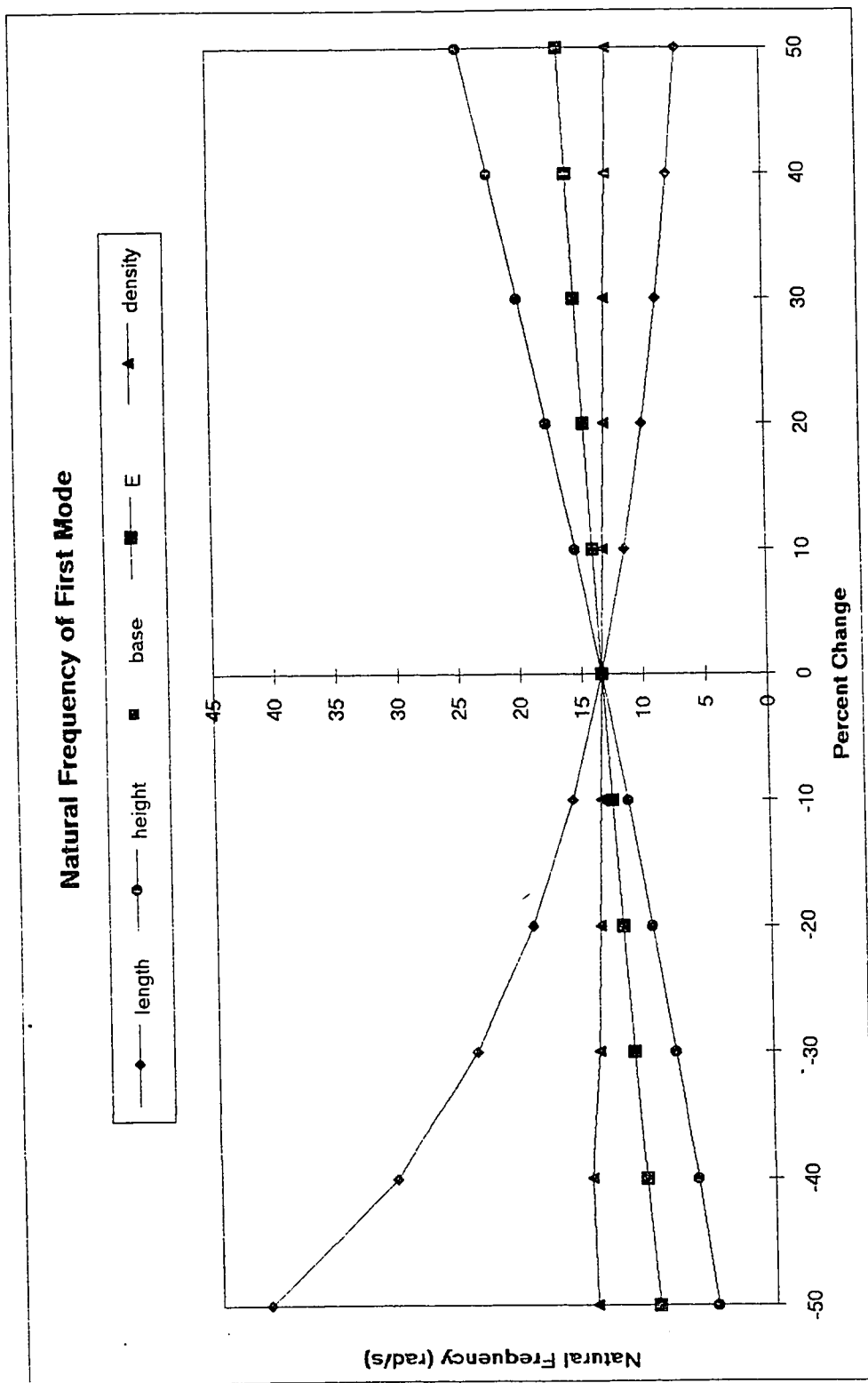
Finally, the approach of using FEA and state space control theory gives more flexibility and ease to analyze complex problems. Additional analyses that can be done using the information obtained from this study include: reaction of the system to external forces in addition to initial displacements, application of piezo film to structure as oppose to just one beam, and practical applications such as using piezo film to actively dampen an airplane wing or even reduce the development of ice build up on an airplane wing through applied vibration.

Bibliography

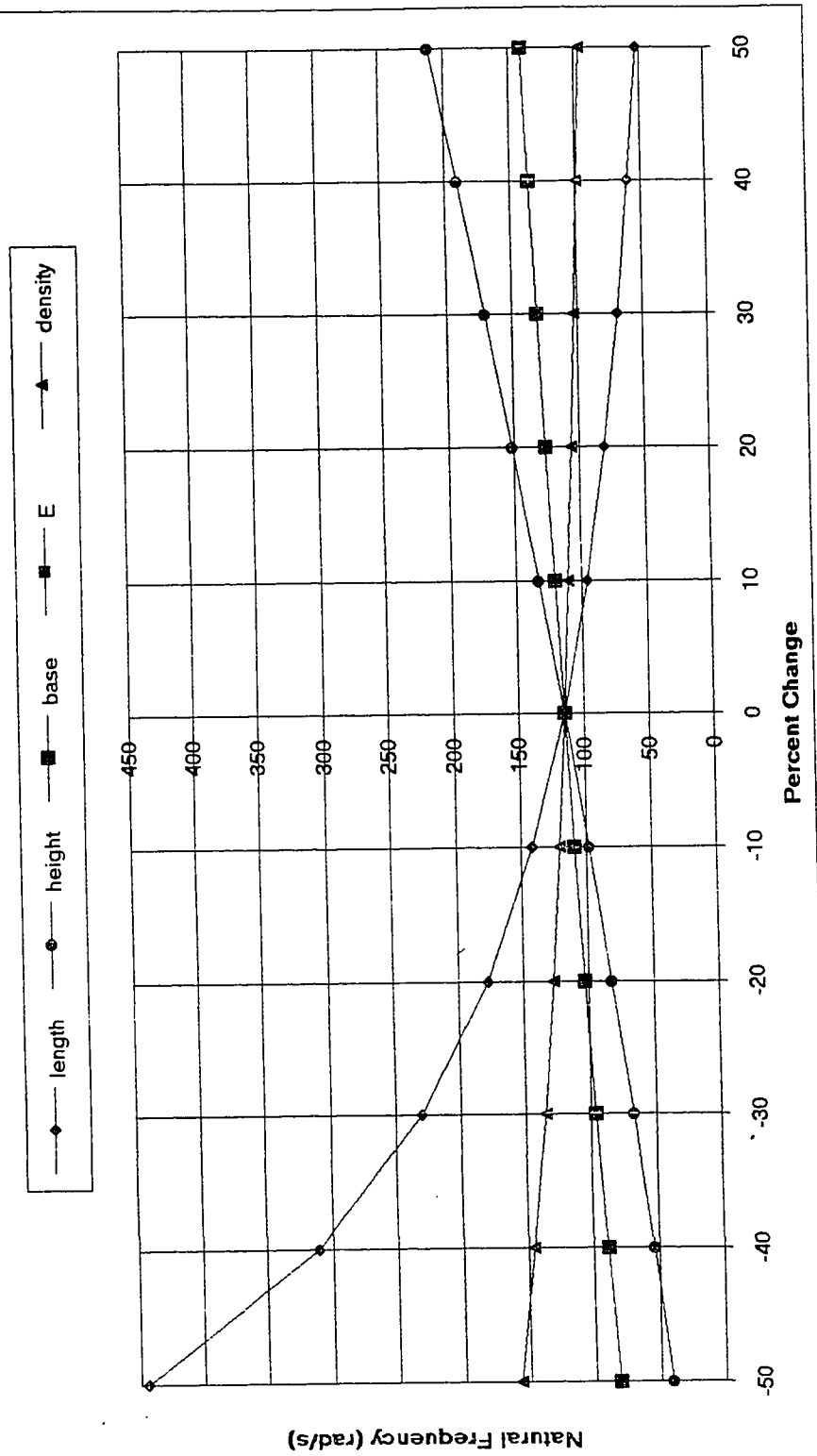
- Bailey, Thomas and Hubbard, James E. Jr.; Distributed Piezoelectric-Polymer Active Vibration Control of a Cantilever Beam, American Institute of Aeronautics and Astronautics, Vol. 8, NO. 5, Oct. 1985.
- Franklin, Powell, and Workman, Digital Control of Dynamic Systems, Second Edition, Addison-Wesley publishing Company, New York, 1990.
- Lawry, Mark H., I-Deas Student Guide, Structural Dynamics Research Corporation, Ohio, 1991
- Meirovitch, Leonard, Dynamics and Control of Structures, Wiley-Interscience Publication, New York, 1990.
- Newman, Perlas, and Quan, Active Damping of a Cantilever Beam Using Piezo-Active Film, San Jose State University, May 20, 1990.
- Thomson, William T., Theory of Vibration With Applications, Third Edition, Prentice Hall, New Jersey, 1988.

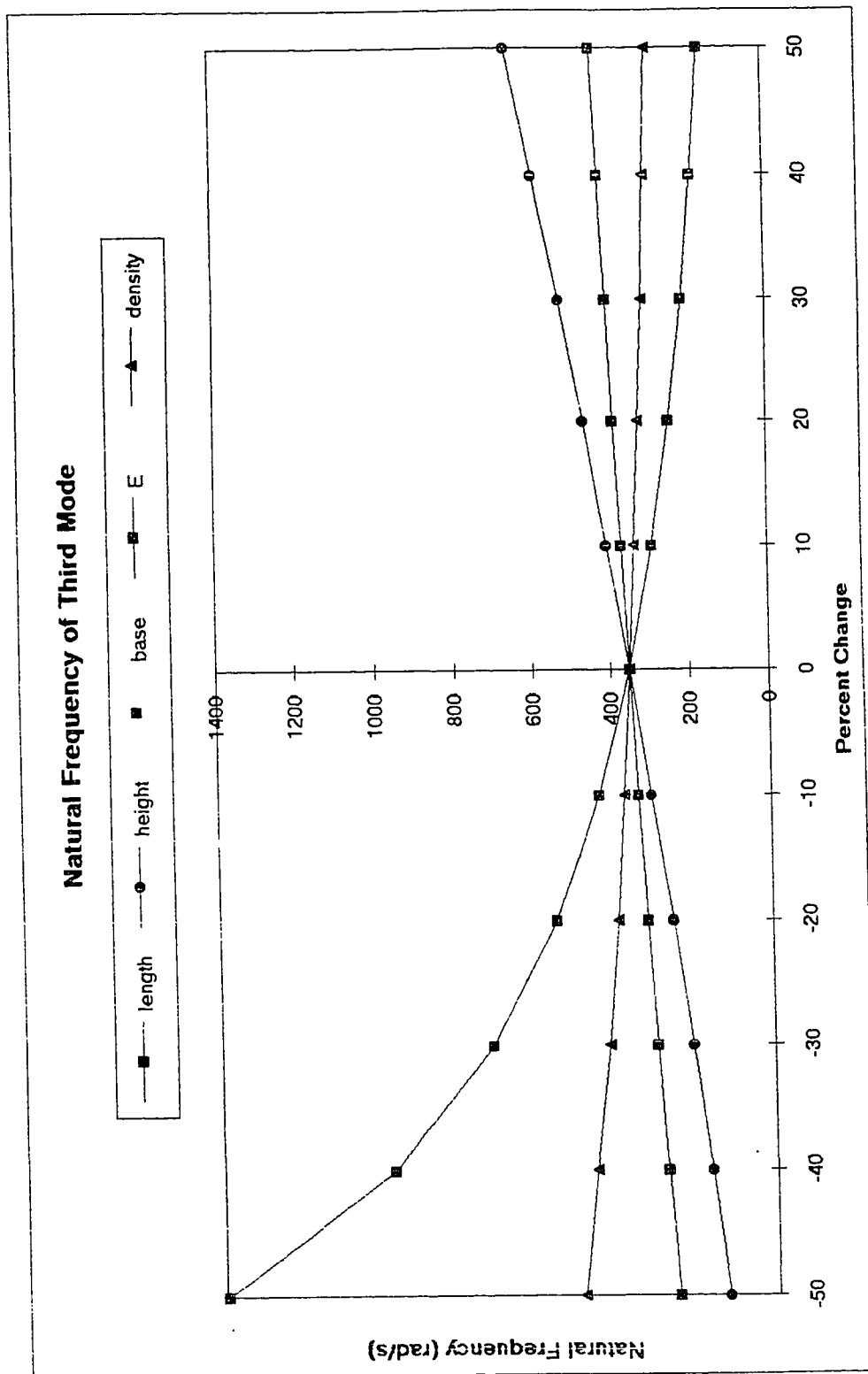
Appendix A

Parametric Study of Beam



Natural Frequency of Second Mode

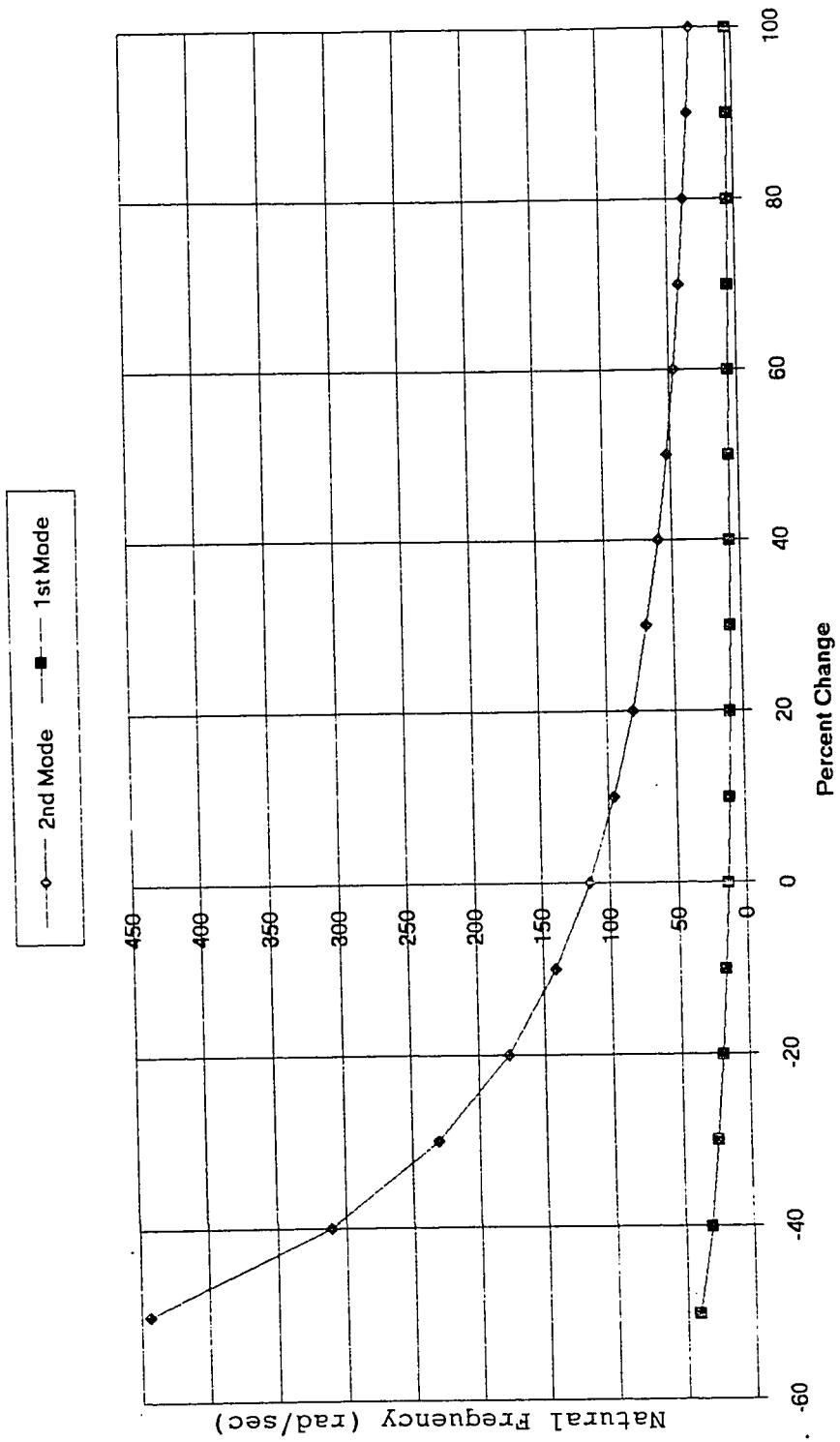




Appendix B

Natural Frequency VS Length

Natural Frequency Due to Change in Length



Project: Cantilever Beam

Mode 1

$$g := 386 \cdot \frac{\text{in}}{\text{sec}^2}$$

$$E := 30000000 \cdot \frac{\text{lb}}{\text{in}^2}$$

$$t := .05 \cdot \text{in}$$

$$h := 1 \cdot \text{in}$$

$$I := \frac{h \cdot t^3}{12}$$

$$\rho := .283 \cdot \frac{\text{lb}}{\text{in}^3}$$

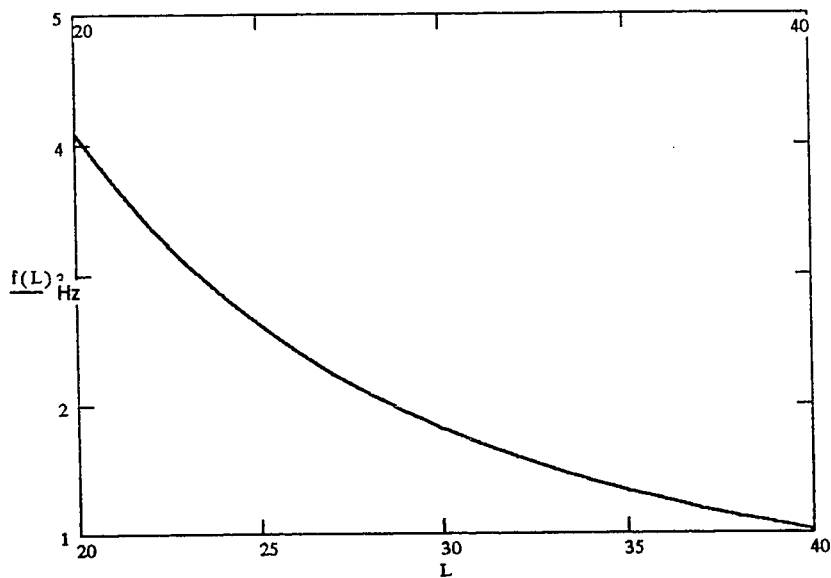
$$w := t \cdot h \cdot \rho$$

$$C := .560$$

$$L := 20..40$$

$$f(L) := C \cdot \sqrt{\frac{g \cdot E \cdot I}{w \cdot (L \cdot \text{in})^4}}$$

Mode 1



$$L := 35$$

$$f(L) = 1.335 \cdot \text{sec}^{-1}$$

Project: Cantilever Beam

Mode 2

$$g := 386 \cdot \frac{\text{in}}{\text{sec}^2}$$

$$E := 30000000 \cdot \frac{\text{lb}}{\text{in}^2}$$

$$t := .05 \cdot \text{in}$$

$$h := 1 \cdot \text{in}$$

$$I := \frac{h \cdot t^3}{12}$$

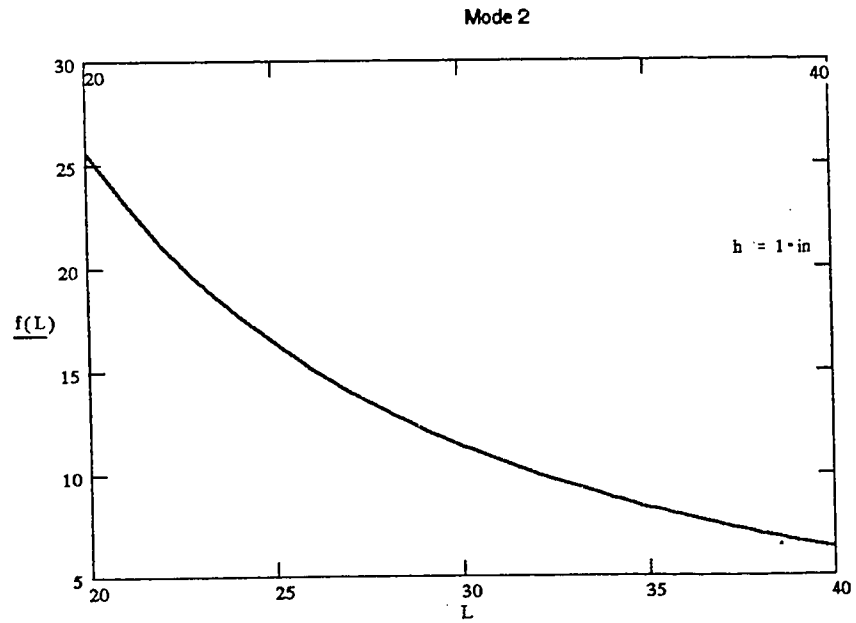
$$\rho := .283 \cdot \frac{\text{lb}}{\text{in}^3}$$

$$w := t \cdot h \cdot \rho$$

$$C := 3.51$$

$$L := 20..40$$

$$f(L) := C \cdot \sqrt{\frac{g \cdot E \cdot I}{w \cdot (L \cdot \text{in})^4}}$$



$$L := 35$$

$$f(L) = 8.366 \cdot \text{sec}^{-1}$$

Project: Cantilever Beam

Mode 3

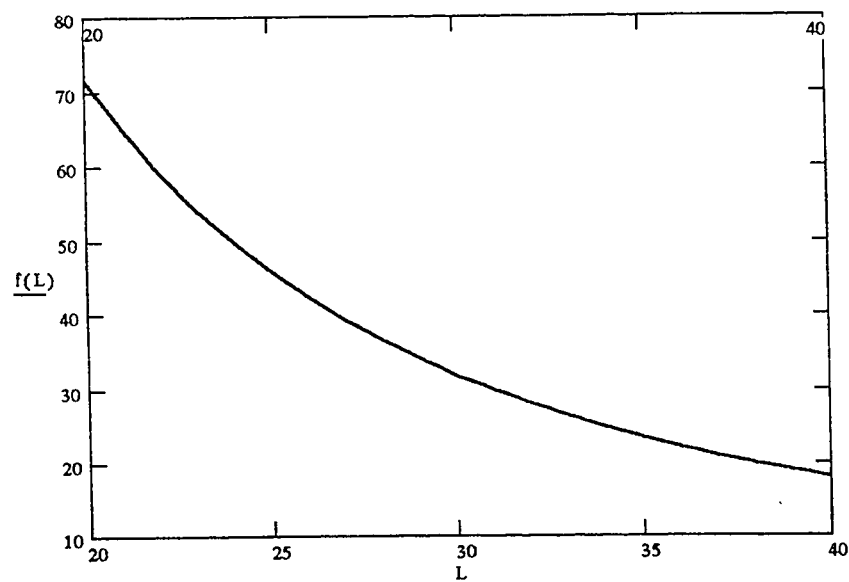
$$g := 386 \cdot \frac{\text{in}}{\text{sec}^2} \quad E := 30000000 \cdot \frac{\text{lb}}{\text{in}^2} \quad t := .05 \cdot \text{in} \quad h := 1 \cdot \text{in}$$

$$I := \frac{h \cdot t^3}{12} \quad \rho := .283 \cdot \frac{\text{lb}}{\text{in}^3} \quad w := t \cdot h \cdot \rho$$

$$C := 9.82 \quad L := 20 \dots 40$$

$$f(L) := C \cdot \sqrt{\frac{g \cdot E \cdot I}{w \cdot (L \cdot \text{in})^4}}$$

Mode 3



$$L := 35$$

$$f(L) = 23.405 \cdot \text{sec}^{-1}$$

Appendix C

Ideas Finite Element Analysis

SDRC I-DEAS VI: System Dynamics_Analysis
 02-OCT-92 11:49:27
 Bin 1-MAIN; System 2-SYSTEM2

Page 1

```

*****
***                                     *
***   Bin 1-MAIN                       *
***   System 2-SYSTEM2                 *
***                                     *
*****

```

Active units = IN

This system is composed of the following entities:

Entity/Kind

Bin 1-MAIN; Component 1-35BEAM
 Finite element

SDRC I-DEAS VI: System Dynamics_Analysis
 02-OCT-92 11:51:34
 Bin 1-MAIN; System 2-SYSTEM2

Page 2

```

*****
Bin 1-MAIN; System 2-SYSTEM2
*****

```

----- Eigensolution summary -----

		Damping Ratio	Damped Frequency	Description
Mode	1	0.00E+00	1.34E+00 Hz	
Mode	2	0.00E+00	8.37E+00 Hz	
Mode	3	0.00E+00	2.34E+01 Hz	

		Modal Mass	Modal Stiffness
Mode	1	2.0697E-01	1.4564E+01
Mode	2	1.7159E-02	4.7417E+01
Mode	3	6.3665E-03	1.3793E+02

----- Mode shapes -----


```

Mode number           = 1
Eigenvalue            = 7.0364E+01
Damped frequency (rad/sec) = 8.3884E+00
Damped frequency (Hertz)  = 1.3350E+00
Viscous damping ratio    = 0.0000E+00
Modal Mass             = 2.0697E-01
Modal Stiffness         = 1.4564E+01

```

Bin 1-MAIN; Component 1-35BEAM

```

1-X Y Z = 0.0000E+00 0.0000E+00 0.0000E+00
1-RXRYRZ= 0.0000E+00 0.0000E+00 0.0000E+00
2-X Y Z = -6.7896E-14 -1.1853E-11 -3.6014E-02
2-RXRYRZ= -6.8642E-11 7.1545E-02 -2.3060E-11
3-X Y Z = -1.2889E-13 -4.6271E-11 -1.4214E-01
3-RXRYRZ= -1.3727E-10 1.4022E-01 -4.5167E-11
4-X Y Z = -2.0733E-13 -1.0238E-10 -3.1550E-01
4-RXRYRZ= -2.0585E-10 2.0603E-01 -6.6412E-11
5-X Y Z = -2.8782E-13 -1.7928E-10 -5.5324E-01
5-RXRYRZ= -2.7437E-10 2.6896E-01 -8.6634E-11
6-X Y Z = -3.5551E-13 -2.7582E-10 -8.5248E-01
6-RXRYRZ= -3.4296E-10 3.2904E-01 -1.0580E-10
7-X Y Z = -4.2151E-13 -3.9102E-10 -1.2104E+00
7-RXRYRZ= -4.1149E-10 3.8625E-01 -1.2428E-10
8-X Y Z = -4.7666E-13 -5.2453E-10 -1.6240E+00
8-RXRYRZ= -4.8007E-10 4.4062E-01 -1.4233E-10
9-X Y Z = -5.3311E-13 -6.7581E-10 -2.0907E+00

```

1

SDRC I-DEAS VI: System Dynamics Analysis
02-OCT-92 11:51:34
Bin 1-MAIN; System 2-SYSTEM2

Page 3

Mode shapes (cont.)

```

9-RXRYRZ= -5.4874E-10 4.9215E-01 -1.5995E-10
10-X Y Z = -6.0212E-13 -8.4446E-10 -2.6074E+00
10-RXRYRZ= -6.1730E-10 5.4086E-01 -1.7705E-10
11-X Y Z = -6.8185E-13 -1.0300E-09 -3.1714E+00
11-RXRYRZ= -6.8578E-10 5.8676E-01 -1.9364E-10
12-X Y Z = -7.5209E-13 -1.2319E-09 -3.7800E+00
12-RXRYRZ= -7.5428E-10 6.2988E-01 -2.0963E-10
13-X Y Z = -8.1068E-13 -1.4494E-09 -4.4303E+00
13-RXRYRZ= -8.2265E-10 6.7025E-01 -2.2490E-10
14-X Y Z = -8.5933E-13 -1.6818E-09 -5.1196E+00
14-RXRYRZ= -8.9094E-10 7.0791E-01 -2.3923E-10
15-X Y Z = -8.8122E-13 -1.9280E-09 -5.8452E+00
15-RXRYRZ= -9.5923E-10 7.4289E-01 -2.5257E-10
16-X Y Z = -8.8016E-13 -2.1871E-09 -6.6045E+00
16-RXRYRZ= -1.0278E-09 7.7523E-01 -2.6504E-10
17-X Y Z = -8.7914E-13 -2.4583E-09 -7.3948E+00
17-RXRYRZ= -1.0966E-09 8.0500E-01 -2.7654E-10
18-X Y Z = -8.8763E-13 -2.7404E-09 -8.2137E+00
18-RXRYRZ= -1.1651E-09 8.3224E-01 -2.8715E-10
19-X Y Z = -8.9727E-13 -3.0327E-09 -9.0585E+00
19-RXRYRZ= -1.2324E-09 8.5702E-01 -2.9678E-10
20-X Y Z = -9.3590E-13 -3.3342E-09 -9.9269E+00
20-RXRYRZ= -1.3002E-09 8.7941E-01 -3.0515E-10
21-X Y Z = -9.7858E-13 -3.6432E-09 -1.0817E+01
21-RXRYRZ= -1.3679E-09 8.9950E-01 -3.1231E-10
22-X Y Z = -1.0482E-12 -3.9590E-09 -1.1725E+01
22-RXRYRZ= -1.4361E-09 9.1736E-01 -3.1878E-10
23-X Y Z = -1.1156E-12 -4.2809E-09 -1.2651E+01
23-RXRYRZ= -1.5164E-09 9.3308E-01 -3.2482E-10
24-X Y Z = -1.1792E-12 -4.6086E-09 -1.3591E+01

```

A10

```

24-RXRYRZ= -1.5992E-09  9.4678E-01 -3.3047E-10
25-X Y Z = -1.2225E-12 -4.9419E-09 -1.4543E+01
25-RXRYRZ= -1.6752E-09  9.5855E-01 -3.3572E-10
26-X Y Z = -1.2620E-12 -5.2801E-09 -1.5507E+01
26-RXRYRZ= -1.7493E-09  9.6852E-01 -3.4060E-10
27-X Y Z = -1.2840E-12 -5.6232E-09 -1.6480E+01
27-RXRYRZ= -1.8214E-09  9.7680E-01 -3.4515E-10
28-X Y Z = -1.3128E-12 -5.9705E-09 -1.7460E+01
28-RXRYRZ= -1.8866E-09  9.9353E-01 -3.4904E-10
29-X Y Z = -1.3234E-12 -6.3215E-09 -1.8447E+01
29-RXRYRZ= -1.9492E-09  9.8885E-01 -3.5224E-10
30-X Y Z = -1.3318E-12 -6.6751E-09 -1.9438E+01
30-RXRYRZ= -2.0182E-09  9.9290E-01 -3.5450E-10
31-X Y Z = -1.3735E-12 -7.0306E-09 -2.0432E+01
31-RXRYRZ= -2.0932E-09  9.9585E-01 -3.5587E-10
32-X Y Z = -1.3891E-12 -7.3870E-09 -2.1429E+01

```

1

SDRC I-DEAS VI: System Dynamics Analysis
02-OCT-92 11:51:35
Bin 1-MAIN; System 2-SYSTEM2

Page

4

Mode shapes (cont.)

```

32-RXRYRZ= -2.1653E-09  9.9785E-01 -3.5662E-10
33-X Y Z = -1.3621E-12 -7.7439E-09 -2.2427E+01
33-RXRYRZ= -2.2292E-09  9.9909E-01 -3.5686E-10
34-X Y Z = -1.3266E-12 -8.1008E-09 -2.3427E+01
34-RXRYRZ= -2.2855E-09  9.9973E-01 -3.5696E-10
35-X Y Z = -1.3261E-12 -8.4578E-09 -2.4427E+01
35-RXRYRZ= -2.3389E-09  9.9997E-01 -3.5697E-10
36-X Y Z = -1.3285E-12 -8.8148E-09 -2.5427E+01
36-RXRYRZ= -2.3655E-09  0.0000E+00 -3.5699E-10

```

```

Mode number      = 2
Eigenvalue       = 2.7634E+03
Damped frequency (rad/sec) = 5.2568E+01
Damped frequency (Hertz)  = 8.3665E+00
Viscous damping ratio    = 0.0000E+00
Modal Mass         = 1.7159E-02
Modal Stiffness     = 4.7417E+01

```

Bin 1-MAIN; Component 1-35BEAM

```

1-X Y Z = 0.0000E+00  0.0000E+00  0.0000E+00
1-RXRYRZ= 0.0000E+00  0.0000E+00  0.0000E+00
2-X Y Z = -2.9071E-14 -4.8117E-12  6.2856E-02
2-RXRYRZ= -1.0835E-11 -1.2269E-01 -9.4881E-12
3-X Y Z = -5.6125E-14 -1.9007E-11  2.3941E-01
3-RXRYRZ= -2.1662E-11 -2.2740E-01 -1.8762E-11
4-X Y Z = -7.5481E-14 -4.2380E-11  5.1171E-01
4-RXRYRZ= -3.2479E-11 -3.1419E-01 -2.7824E-11
5-X Y Z = -9.3103E-14 -7.4706E-11  8.6188E-01
5-RXRYRZ= -4.3295E-11 -3.8317E-01 -3.6644E-11
6-X Y Z = -1.1425E-13 -1.1571E-10  1.2722E+00
6-RXRYRZ= -5.4112E-11 -4.3456E-01 -4.5204E-11
7-X Y Z = -1.3355E-13 -1.6516E-10  1.7253E+00
7-RXRYRZ= -6.4910E-11 -4.6872E-01 -5.3558E-11
8-X Y Z = -1.5642E-13 -2.2287E-10  2.2041E+00
8-RXRYRZ= -7.5675E-11 -4.8612E-01 -6.1717E-11
9-X Y Z = -1.7423E-13 -2.8863E-10  2.6922E+00
9-RXRYRZ= -8.6440E-11 -4.8740E-01 -6.9657E-11
10-X Y Z = -1.8884E-13 -3.6223E-10  3.1738E+00
10-RXRYRZ= -9.7228E-11 -4.7335E-01 -7.7368E-11
11-X Y Z = -2.0569E-13 -4.4341E-10  3.6341E+00

```

A11

```

11-RXRYRZ= -1.0803E-10 -4.4493E-01 -8.4803E-11
12-X Y Z = -2.1596E-13 -5.3190E-10 4.0592E+00
12-RXRYRZ= -1.1880E-10 -4.0323E-01 -9.1918E-11
13-X Y Z = -2.2922E-13 -6.2732E-10 4.4365E+00
13-RXRYRZ= -1.2955E-10 -3.4950E-01 -9.8688E-11

```

1

SDRC I-DEAS VI: System Dynamics Analysis
02-OCT-92 11:51:35
Bin 1-MAIN; System 2-SYSTEM2

Page 5

Mode shapes (cont.)

```

14-X Y Z = -2.4055E-13 -7.2933E-10 4.7547E+00
14-RXRYRZ= -1.4031E-10 -2.8511E-01 -1.0507E-10
15-X Y Z = -2.4691E-13 -8.3752E-10 5.0037E+00
15-RXRYRZ= -1.5103E-10 -2.1155E-01 -1.1109E-10
16-X Y Z = -2.5458E-13 -9.5157E-10 5.1753E+00
16-RXRYRZ= -1.6177E-10 -1.3040E-01 -1.1676E-10
17-X Y Z = -2.6294E-13 -1.0711E-09 5.2626E+00
17-RXRYRZ= -1.7253E-10 -4.3305E-02 -1.2201E-10
18-X Y Z = -2.7283E-13 -1.1957E-09 5.2605E+00
18-RXRYRZ= -1.8329E-10 4.8049E-02 -1.2684E-10
19-X Y Z = -2.8306E-13 -1.3249E-09 5.1656E+00
19-RXRYRZ= -1.9389E-10 1.4196E-01 -1.3125E-10
20-X Y Z = -2.8992E-13 -1.4582E-09 4.9763E+00
20-RXRYRZ= -2.0401E-10 2.3673E-01 -1.3524E-10
21-X Y Z = -2.9884E-13 -1.5954E-09 4.6924E+00
21-RXRYRZ= -2.1421E-10 3.3074E-01 -1.3885E-10
22-X Y Z = -3.0574E-13 -1.7360E-09 4.3156E+00
22-RXRYRZ= -2.2881E-10 4.2240E-01 -1.4217E-10
23-X Y Z = -3.1062E-13 -1.8798E-09 3.8489E+00
23-RXRYRZ= -2.4180E-10 5.1028E-01 -1.4524E-10
24-X Y Z = -3.2088E-13 -2.0265E-09 3.2967E+00
24-RXRYRZ= -2.5313E-10 5.9303E-01 -1.4805E-10
25-X Y Z = -3.3040E-13 -2.1759E-09 2.6649E+00
25-RXRYRZ= -2.6607E-10 6.6952E-01 -1.5058E-10
26-X Y Z = -3.3649E-13 -2.3277E-09 1.9601E+00
26-RXRYRZ= -2.8037E-10 7.3877E-01 -1.5283E-10
27-X Y Z = -3.4589E-13 -2.4816E-09 1.1900E+00
27-RXRYRZ= -2.9455E-10 8.0004E-01 -1.5479E-10
28-X Y Z = -3.4671E-13 -2.6374E-09 3.6282E-01
28-RXRYRZ= -3.0518E-10 8.5282E-01 -1.5642E-10
29-X Y Z = -3.5014E-13 -2.7946E-09 -5.1275E-01
29-RXRYRZ= -3.1451E-10 8.9685E-01 -1.5773E-10
30-X Y Z = -3.5452E-13 -2.9529E-09 -1.4280E+00
30-RXRYRZ= -3.2417E-10 9.3216E-01 -1.5869E-10
31-X Y Z = -3.5590E-13 -3.1120E-09 -2.3743E+00
31-RXRYRZ= -3.3424E-10 9.5907E-01 -1.5933E-10
32-X Y Z = -3.5870E-13 -3.2716E-09 -3.3435E+00
32-RXRYRZ= -3.4597E-10 9.7818E-01 -1.5971E-10
33-X Y Z = -3.5360E-13 -3.4314E-09 -4.3284E+00
33-RXRYRZ= -3.5785E-10 9.9043E-01 -1.5989E-10
34-X Y Z = -3.4222E-13 -3.5914E-09 -5.3225E+00
34-RXRYRZ= -3.6976E-10 9.9706E-01 -1.5997E-10
35-X Y Z = -3.4172E-13 -3.7514E-09 -6.3211E+00
35-RXRYRZ= -3.8047E-10 9.9962E-01 -1.5999E-10
36-X Y Z = -3.3829E-13 -3.9114E-09 -7.3210E+00
36-RXRYRZ= -3.8524E-10 1.0000E+00 -1.6000E-10

```

1

SDRC I-DEAS VI: System Dynamics Analysis
02-OCT-92 11:51:36
Bin 1-MAIN; System 2-SYSTEM2

Page 6

A12

Mode shapes (cont.)

Mode number = 3
 Eigenvalue = 2.1665E+04
 Damped frequency (rad/sec) = 1.4719E+02
 Damped frequency (Hertz) = 2.3426E+01
 Viscous damping ratio = 0.0000E+00
 Modal Mass = 6.3665E-03
 Modal Stiffness = 1.3793E+02

Bin 1-MAIN; Component 1-35BEAM

1-X Y Z =	0.0000E+00	0.0000E+00	0.0000E+00
1-RXRYRZ=	0.0000E+00	0.0000E+00	0.0000E+00
2-X Y Z =	-1.6781E-14	-9.9787E-12	-1.0393E-01
2-RXRYRZ=	-1.4102E-12	1.9941E-01	-1.9540E-11
3-X Y Z =	-2.9424E-14	-3.9191E-11	-3.8214E-01
3-RXRYRZ=	-2.8349E-12	3.4859E-01	-3.8458E-11
4-X Y Z =	-4.0761E-14	-8.7013E-11	-7.8464E-01
4-RXRYRZ=	-4.2501E-12	4.4816E-01	-5.6752E-11
5-X Y Z =	-5.0130E-14	-1.5281E-10	-1.2625E+00
5-RXRYRZ=	-5.6551E-12	4.9958E-01	-7.4399E-11
6-X Y Z =	-6.3776E-14	-2.3593E-10	-1.7687E+00
6-RXRYRZ=	-7.0698E-12	5.0547E-01	-9.1400E-11
7-X Y Z =	-7.8755E-14	-3.3573E-10	-2.2595E+00
7-RXRYRZ=	-8.4809E-12	4.6966E-01	-1.0776E-10
8-X Y Z =	-9.3138E-14	-4.5158E-10	-2.6958E+00
8-RXRYRZ=	-9.8661E-12	3.9726E-01	-1.2347E-10
9-X Y Z =	-1.0667E-13	-5.8279E-10	-3.0440E+00
9-RXRYRZ=	-1.1268E-11	2.9456E-01	-1.3850E-10
10-X Y Z =	-1.2209E-13	-7.2871E-10	-3.2773E+00
10-RXRYRZ=	-1.2683E-11	1.6884E-01	-1.5286E-10
11-X Y Z =	-1.3234E-13	-8.8864E-10	-3.3767E+00
11-RXRYRZ=	-1.4084E-11	2.8108E-02	-1.6650E-10
12-X Y Z =	-1.4278E-13	-1.0619E-09	-3.3313E+00
12-RXRYRZ=	-1.5495E-11	-1.1919E-01	-1.7941E-10
13-X Y Z =	-1.4984E-13	-1.2476E-09	-3.1389E+00
13-RXRYRZ=	-1.6896E-11	-2.6454E-01	-1.9156E-10
14-X Y Z =	-1.5825E-13	-1.4451E-09	-2.8056E+00
14-RXRYRZ=	-1.8297E-11	-3.9975E-01	-2.0297E-10
15-X Y Z =	-1.6758E-13	-1.6537E-09	-2.3453E+00
15-RXRYRZ=	-1.9718E-11	-5.1728E-01	-2.1363E-10
16-X Y Z =	-1.7827E-13	-1.8725E-09	-1.7791E+00
16-RXRYRZ=	-2.1138E-11	-6.1058E-01	-2.2358E-10
17-X Y Z =	-1.8796E-13	-2.1010E-09	-1.1340E+00
17-RXRYRZ=	-2.2616E-11	-6.7443E-01	-2.3278E-10
18-X Y Z =	-1.9930E-13	-2.3382E-09	-4.4127E-01

1

SDRC I-DEAS VI: System Dynamics Analysis
 02-OCT-92 11:51:36
 Bin 1-MAIN; System 2-SYSTEM2

Page 7

Mode shapes (cont.)

18-RXRYRZ=	-2.4074E-11	-7.0514E-01	-2.4122E-10
19-X Y Z =	-2.0673E-13	-2.5835E-09	2.6464E-01
19-RXRYRZ=	-2.5500E-11	-7.0071E-01	-2.4893E-10
20-X Y Z =	-2.1458E-13	-2.8362E-09	9.4838E-01
20-RXRYRZ=	-2.6769E-11	-6.6091E-01	-2.5595E-10
21-X Y Z =	-2.1933E-13	-3.0955E-09	1.5752E+00
21-RXRYRZ=	-2.8230E-11	-5.8728E-01	-2.6231E-10
22-X Y Z =	-2.2417E-13	-3.3609E-09	2.1128E+00

```

22-RXRYRZ= -3.2553E-11 -4.8303E-01 -2.6808E-10
23-X Y Z = -2.2815E-13 -3.6318E-09 2.5326E+00
23-RXRYRZ= -3.5725E-11 -3.5282E-01 -2.7325E-10
24-X Y Z = -2.3311E-13 -3.9076E-09 2.8117E+00
24-RXRYRZ= -3.7588E-11 -2.0256E-01 -2.7785E-10
25-X Y Z = -2.3698E-13 -4.1876E-09 2.9333E+00
25-RXRYRZ= -4.0546E-11 -3.9015E-02 -2.8187E-10
26-X Y Z = -2.4271E-13 -4.4714E-09 2.8878E+00
26-RXRYRZ= -4.4188E-11 1.3052E-01 -2.8532E-10
27-X Y Z = -2.4677E-13 -4.7583E-09 2.6727E+00
27-RXRYRZ= -4.7583E-11 2.9867E-01 -2.8821E-10
28-X Y Z = -2.4897E-13 -5.0479E-09 2.2932E+00
28-RXRYRZ= -4.8928E-11 4.5838E-01 -2.9058E-10
29-X Y Z = -2.5098E-13 -5.3396E-09 1.7609E+00
29-RXRYRZ= -4.9089E-11 6.0334E-01 -2.9247E-10
30-X Y Z = -2.5325E-13 -5.6329E-09 1.0932E+00
30-RXRYRZ= -4.9405E-11 7.2843E-01 -2.9389E-10
31-X Y Z = -2.5372E-13 -5.9274E-09 3.1187E-01
31-RXRYRZ= -4.9652E-11 8.3001E-01 -2.9489E-10
32-X Y Z = -2.5522E-13 -6.2228E-09 -5.5844E-01
32-RXRYRZ= -5.1501E-11 9.0632E-01 -2.9554E-10
33-X Y Z = -2.5319E-13 -6.5186E-09 -1.4924E+00
33-RXRYRZ= -5.4132E-11 9.5765E-01 -2.9592E-10
34-X Y Z = -2.4728E-13 -6.8146E-09 -2.4663E+00
34-RXRYRZ= -5.8622E-11 9.8661E-01 -2.9610E-10
35-X Y Z = -2.4402E-13 -7.1108E-09 -3.4599E+00
35-RXRYRZ= -6.2508E-11 9.9822E-01 -2.9617E-10
36-X Y Z = -2.4294E-13 -7.4070E-09 -4.4594E+00
36-RXRYRZ= -6.3850E-11 1.0000E+00 -2.9618E-10

```

1

SDRC I-DEAS VI: System Dynamics Analysis
02-OCT-92 11:51:37
Bin 1-MAIN; System 2-SYSTEM2

Page 8

----- Matrices -----

Modal Displacement Matrix

Col	1	2	3
Row			
1	0.0000D+00	0.0000D+00	0.0000D+00
2	0.0000D+00	0.0000D+00	0.0000D+00
3	0.0000D+00	0.0000D+00	0.0000D+00
4	0.0000D+00	0.0000D+00	0.0000D+00
5	0.0000D+00	0.0000D+00	0.0000D+00
6	0.0000D+00	0.0000D+00	0.0000D+00
7	-6.7896D-14	-2.9071D-14	-1.6781D-14
8	-1.1853D-11	-4.8117D-12	-9.9787D-12
9	-3.6014D-02	6.2856D-02	-1.0393D-01
10	-6.8642D-11	-1.0835D-11	-1.4102D-12
11	7.1545D-02	-1.2269D-01	1.9941D-01
12	-2.3060D-11	-9.4881D-12	-1.9540D-11
13	-1.2889D-13	-5.6125D-14	-2.9424D-14
14	-4.6271D-11	-1.9007D-11	-3.9191D-11
15	-1.4214D-01	2.3941D-01	-3.8214D-01
16	-1.3727D-10	-2.1662D-11	-2.8349D-12
17	1.4022D-01	-2.2740D-01	3.4859D-01
18	-4.5167D-11	-1.8762D-11	-3.8458D-11
19	-2.0733D-13	-7.5481D-14	-4.0761D-14
20	-1.0238D-10	-4.2380D-11	-8.7013D-11

A14

```

-21 -3.1550D-01 5.1171D-01 -7.8464D-01
22 -2.0585D-10 -3.2479D-11 -4.2501D-12
-23 2.0603D-01 -3.1419D-01 4.4816D-01
24 -6.6412D-11 -2.7824D-11 -5.6752D-11
25 -2.8782D-13 -9.3103D-14 -5.0130D-14
26 -1.7928D-10 -7.4706D-11 -1.5281D-10
-27 -5.5324D-01 8.6188D-01 -1.2625D+00
28 -2.7437D-10 -4.3295D-11 -5.6551D-12
-29 2.6896D-01 -3.8317D-01 4.9958D-01
30 -8.6634D-11 -3.6644D-11 -7.4399D-11
31 -3.5551D-13 -1.1425D-13 -6.3776D-14
32 -2.7582D-10 -1.1571D-10 -2.3593D-10
-33 -8.5248D-01 1.2722D+00 -1.7687D+00
34 -3.4296D-10 -5.4112D-11 -7.0698D-12
-35 3.2904D-01 -4.3456D-01 5.0547D-01
36 -1.0580D-10 -4.5204D-11 -9.1400D-11
37 -4.2151D-13 -1.3355D-13 -7.8755D-14
38 -3.9102D-10 -1.6516D-10 -3.3573D-10

```

1

SDRC I-DEAS VI: System Dynamics Analysis
02-OCT-92 11:51:38
Bin 1-MAIN; System 2-SYSTEM2

Page

9

Matrices (cont.)

```

-39 -1.2104D+00 1.7253D+00 -2.2595D+00
40 -4.1149D-10 -6.4910D-11 -8.4809D-12
-41 3.8625D-01 -4.6872D-01 4.6966D-01
42 -1.2428D-10 -5.3558D-11 -1.0776D-10
43 -4.7666D-13 -1.5642D-13 -9.3138D-14
44 -5.2453D-10 -2.2287D-10 -4.5158D-10
-45 -1.6240D+00 2.2041D+00 -2.6958D+00
46 -4.8007D-10 -7.5675D-11 -9.8661D-12
-47 4.4062D-01 -4.8612D-01 3.9726D-01
48 -1.4233D-10 -6.1717D-11 -1.2347D-10
49 -5.3311D-13 -1.7423D-13 -1.0667D-13
50 -6.7581D-10 -2.8863D-10 -5.8279D-10
-51 -2.0907D+00 2.6922D+00 -3.0440D+00
52 -5.4874D-10 -8.6440D-11 -1.1268D-11
-53 4.9215D-01 -4.8740D-01 2.9456D-01
54 -1.5995D-10 -6.9657D-11 -1.3850D-10
55 -6.0212D-13 -1.8884D-13 -1.2209D-13
56 -8.4446D-10 -3.6223D-10 -7.2871D-10
57 -2.6074D+00 3.1738D+00 -3.2773D+00
58 -6.1730D-10 -9.7228D-11 -1.2683D-11
-59 5.4086D-01 -4.7335D-01 1.6884D-01
60 -1.7705D-10 -7.7368D-11 -1.5286D-10
61 -6.8185D-13 -2.0569D-13 -1.3234D-13
62 -1.0300D-09 -4.4341D-10 -8.8864D-10
-63 -3.1714D+00 3.6341D+00 -3.3767D+00
64 -6.8578D-10 -1.0803D-10 -1.4084D-11
-65 5.8676D-01 -4.4493D-01 2.8108D-02
66 -1.9364D-10 -8.4803D-11 -1.6650D-10
67 -7.5209D-13 -2.1596D-13 -1.4278D-13
68 -1.2319D-09 -5.3190D-10 -1.0619D-09
-69 -3.7800D+00 4.0592D+00 -3.3313D+00
70 -7.5428D-10 -1.1880D-10 -1.5495D-11
-71 6.2988D-01 -4.0323D-01 -1.1919D-01 *
72 -2.0963D-10 -9.1918D-11 -1.7941D-10
73 -8.1068D-13 -2.2922D-13 -1.4984D-13
74 -1.4494D-09 -6.2732D-10 -1.2476D-09
-75 -4.4303D+00 4.4365D+00 -3.1389D+00
76 -8.2265D-10 -1.2955D-10 -1.6896D-11
-77 6.7025D-01 -3.4950D-01 -2.6454D-01

```

78 -2.2490D-10 -9.8688D-11 -1.9156D-10
 79 -8.5933D-13 -2.4055D-13 -1.5825D-13
 80 -1.6818D-09 -7.2933D-10 -1.4451D-09
 -81 -5.1196D+00 4.7547D+00 -2.8056D+00
 82 -8.9094D-10 -1.4031D-10 -1.8297D-11
 -83 7.0791D-01 -2.8511D-01 -3.9975D-01
 84 -2.3923D-10 -1.0507D-10 -2.0297D-10

1

SDRC I-DEAS VI: System_Dynamics_Analysis
 02-OCT-92 11:51:39
 Bin 1-MAIN; System 2-SYSTEM2

Page 10

Matrices (cont.)

85 -8.8122D-13 -2.4691D-13 -1.6758D-13
 86 -1.9280D-09 -8.3752D-10 -1.6537D-09
 -87 -5.8452D+00 5.0037D+00 -2.3453D+00
 88 -9.5923D-10 -1.5103D-10 -1.9718D-11
 -89 7.4289D-01 -2.1155D-01 -5.1728D-01
 90 -2.5257D-10 -1.1109D-10 -2.1363D-10
 91 -8.8016D-13 -2.5458D-13 -1.7827D-13
 92 -2.1871D-09 -9.5157D-10 -1.8725D-09
 -93 -6.6045D+00 5.1753D+00 -1.7791D+00
 94 -1.0278D-09 -1.6177D-10 -2.1138D-11
 -95 7.7523D-01 -1.3040D-01 -6.1058D-01
 96 -2.6504D-10 -1.1676D-10 -2.2358D-10
 97 -8.7914D-13 -2.6294D-13 -1.8796D-13
 98 -2.4583D-09 -1.0711D-09 -2.1010D-09
 -99 -7.3948D+00 5.2626D+00 -1.1340D+00
 100 -1.0966D-09 -1.7253D-10 -2.2616D-11
 -101 8.0500D-01 -4.3305D-02 -6.7443D-01
 102 -2.7654D-10 -1.2201D-10 -2.3278D-10
 103 -8.8763D-13 -2.7283D-13 -1.9930D-13
 104 -2.7404D-09 -1.1957D-09 -2.3382D-09
 -105 -8.2137D+00 5.2605D+00 -4.4127D-01
 106 -1.1651D-09 -1.8329D-10 -2.4074D-11
 -107 8.3224D-01 4.8049D-02 -7.0514D-01
 108 -2.8715D-10 -1.2684D-10 -2.4122D-10
 109 -8.9727D-13 -2.8306D-13 -2.0673D-13
 110 -3.0327D-09 -1.3249D-09 -2.5835D-09
 -111 -9.0585D+00 5.1656D+00 2.6464D-01
 112 -1.2324D-09 -1.9389D-10 -2.5500D-11
 -113 8.5702D-01 1.4196D-01 -7.0071D-01
 114 -2.9678D-10 -1.3125D-10 -2.4893D-10
 115 -9.3590D-13 -2.8992D-13 -2.1458D-13
 116 -3.3342D-09 -1.4582D-09 -2.8362D-09
 -117 -9.9269D+00 4.9763D+00 9.4838D-01
 118 -1.3002D-09 -2.0401D-10 -2.6769D-11
 -119 8.7941D-01 2.3673D-01 -6.6091D-01
 120 -3.0515D-10 -1.3524D-10 -2.5595D-10
 121 -9.7858D-13 -2.9884D-13 -2.1933D-13
 122 -3.6432D-09 -1.5954D-09 -3.0955D-09
 -123 -1.0817D+01 4.6924D+00 1.5752D+00
 124 -1.3679D-09 -2.1421D-10 -2.8230D-11
 -125 8.9950D-01 3.3074D-01 -5.8728D-01
 126 -3.1231D-10 -1.3885D-10 -2.6231D-10
 127 -1.0482D-12 -3.0574D-13 -2.2417D-13
 128 -3.9590D-09 -1.7360D-09 -3.3609D-09
 -129 -1.1725D+01 4.3156D+00 2.1128D+00
 130 -1.4361D-09 -2.2881D-10 -3.2553D-11

1

SDRC I-DEAS VI: System_Dynamics_Analysis
 A16

Page 11

02-OCT-92 11:51:39
Bin 1-MAIN; System 2-SYSTEM2

Matrices (cont.)

-131	9.1736D-01	4.2240D-01	-4.8303D-01
132	-3.1878D-10	-1.4217D-10	-2.6808D-10
133	-1.1156D-12	-3.1062D-13	-2.2815D-13
134	-4.2809D-09	-1.8798D-09	-3.6318D-09
-135	-1.2651D+01	3.8489D+00	2.5326D+00
136	-1.5164D-09	-2.4180D-10	-3.5725D-11
-137	9.3308D-01	5.1028D-01	-3.5282D-01
138	-3.2482D-10	-1.4524D-10	-2.7325D-10
139	-1.1792D-12	-3.2088D-13	-2.3311D-13
140	-4.6086D-09	-2.0265D-09	-3.9076D-09
-141	-1.3591D+01	3.2967D+00	2.8117D+00
142	-1.5992D-09	-2.5313D-10	-3.7588D-11
-143	9.4678D-01	5.9303D-01	-2.0256D-01
144	-3.3047D-10	-1.4805D-10	-2.7785D-10
145	-1.2225D-12	-3.3040D-13	-2.3698D-13
146	-4.9419D-09	-2.1759D-09	-4.1876D-09
-147	-1.4543D+01	2.6649D+00	2.9333D+00
148	-1.6752D-09	-2.6607D-10	-4.0546D-11
-149	9.5855D-01	6.6952D-01	-3.9015D-02
150	-3.3572D-10	-1.5058D-10	-2.8187D-10
151	-1.2620D-12	-3.3649D-13	-2.4271D-13
152	-5.2801D-09	-2.3277D-09	-4.4714D-09
-153	-1.5507D+01	1.9601D+00	2.8878D+00
154	-1.7493D-09	-2.8037D-10	-4.4188D-11
-155	9.6852D-01	7.3877D-01	1.3052D-01
156	-3.4060D-10	-1.5283D-10	-2.8532D-10
157	-1.2840D-12	-3.4589D-13	-2.4677D-13
158	-5.6232D-09	-2.4816D-09	-4.7583D-09
159	-1.6480D+01	1.1900D+00	2.6727D+00
160	-1.8214D-09	-2.9455D-10	-4.7583D-11
-161	9.7680D-01	8.0004D-01	2.9867D-01
162	-3.4515D-10	-1.5479D-10	-2.8821D-10
163	-1.3128D-12	-3.4671D-13	-2.4897D-13
164	-5.9705D-09	-2.6374D-09	-5.0479D-09
-165	-1.7460D+01	3.6282D-01	2.2932D+00
166	-1.8866D-09	-3.0518D-10	-4.8928D-11
-167	9.8353D-01	8.5282D-01	4.5838D-01
168	-3.4904D-10	-1.5642D-10	-2.9058D-10
169	-1.3234D-12	-3.5014D-13	-2.5098D-13
170	-6.3215D-09	-2.7946D-09	-5.3396D-09
-171	-1.8447D+01	-5.1275D-01	1.7609D+00
172	-1.9492D-09	-3.1451D-10	-4.9089D-11
-173	9.8885D-01	8.9685D-01	6.0334D-01
174	-3.5224D-10	-1.5773D-10	-2.9247D-10
175	-1.3318D-12	-3.5452D-13	-2.5325D-13
176	-6.6751D-09	-2.9529D-09	-5.6329D-09

1

SDRC I-DEAS VI: System Dynamics Analysis
02-OCT-92 11:51:40
Bin 1-MAIN; System 2-SYSTEM2

Page 12

Matrices (cont.)

-177	-1.9438D+01	-1.4280D+00	1.0932D+00
178	-2.0182D-09	-3.2417D-10	-4.9405D-11
-179	9.9290D-01	9.3216D-01	7.2843D-01
180	-3.5450D-10	-1.5869D-10	-2.9389D-10
181	-1.3735D-12	-3.5590D-13	-2.5372D-13
182	-7.0306D-09	-3.1120D-09	-5.9274D-09


```

-183 -2.0432D+01 -2.3743D+00 3.1187D-01
184 -2.0932D-09 -3.3424D-10 -4.9652D-11
-185 9.9585D-01 9.5907D-01 8.3001D-01
186 -3.5587D-10 -1.5933D-10 -2.9489D-10
187 -1.3891D-12 -3.5870D-13 -2.5522D-13
188 -7.3870D-09 -3.2716D-09 -6.2228D-09
-189 -2.1429D+01 -3.3435D+00 -5.5844D-01
190 -2.1653D-09 -3.4597D-10 -5.1501D-11
-191 9.9785D-01 9.7818D-01 9.0632D-01
192 -3.5662D-10 -1.5971D-10 -2.9554D-10
193 -1.3621D-12 -3.5360D-13 -2.5319D-13
194 -7.7439D-09 -3.4314D-09 -6.5186D-09
-195 -2.2427D+01 -4.3284D+00 -1.4924D+00
196 -2.2292D-09 -3.5785D-10 -5.4132D-11
-197 9.9909D-01 9.9043D-01 9.5765D-01
198 -3.5686D-10 -1.5989D-10 -2.9592D-10
199 -1.3266D-12 -3.4222D-13 -2.4728D-13
200 -8.1008D-09 -3.5914D-09 -6.8146D-09
-201 -2.3427D+01 -5.3225D+00 -2.4663D+00
202 -2.2855D-09 -3.6976D-10 -5.8622D-11
-203 9.9973D-01 9.9706D-01 9.8661D-01
204 -3.5696D-10 -1.5997D-10 -2.9610D-10
205 -1.3261D-12 -3.4172D-13 -2.4402D-13
206 -8.4578D-09 -3.7514D-09 -7.1108D-09
-207 -2.4427D+01 -6.3211D+00 -3.4599D+00
208 -2.3389D-09 -3.8047D-10 -6.2508D-11
-209 9.9997D-01 9.9962D-01 9.9822D-01
210 -3.5697D-10 -1.5999D-10 -2.9617D-10
211 -1.3285D-12 -3.3829D-13 -2.4294D-13
212 -8.8148D-09 -3.9114D-09 -7.4070D-09
-213 -2.5427D+01 -7.3210D+00 -4.4594D+00
214 -2.3655D-09 -3.8524D-10 -6.3850D-11
-215 1.0000D+00 1.0000D+00 1.0000D+00
216 -3.5699D-10 -1.6000D-10 -2.9618D-10

```

Modal Mass Matrix

1

SDRC I-DEAS VI: System Dynamics_Analysis
02-OCT-92 11:51:41
Bin 1-MAIN; System 2-SYSTEM2

Page 13

Matrices (cont.)

```

Col 1
Row
1 2.0697D-01
2 1.7159D-02
3 6.3665D-03

```

Modal Stiffness Matrix

```

Col 1
Row
1 1.4564D+01
2 4.7417D+01
3 1.3793D+02

```

Appendix D

Matlab Variables

Mass matrix from FEA

m =

$$\begin{bmatrix} 0.2070 & 0 & 0 \\ 0 & 0.0172 & 0 \\ 0 & 0 & 0.0064 \end{bmatrix}$$

Damping ratio used for simulation

dratio =

$$\begin{bmatrix} 0.0100 & 0 & 0 \\ 0 & 0.0100 & 0 \\ 0 & 0 & 0.0100 \end{bmatrix}$$

Calculated damping ratio used in FEA

damp =

$$\begin{bmatrix} 0.0347 & 0 & 0 \\ 0 & 0.0180 & 0 \\ 0 & 0 & 0.0187 \end{bmatrix}$$

Stiffness matrix from FEA

k =

$$\begin{bmatrix} 14.5640 & 0 & 0 \\ 0 & 47.4170 & 0 \\ 0 & 0 & 137.9300 \end{bmatrix}$$

State Space Matrix [A]

am = 1.0e+004 *

$$\begin{bmatrix} 0 & 0 & 0 & 0.0001 & 0 & 0 \\ 0 & 0 & 0 & 0 & 0.0001 & 0 \\ 0 & 0 & 0 & 0 & 0 & 0.0001 \\ -0.0070 & 0 & 0 & 0.00 & 0 & 0 \\ 0 & -0.2763 & 0 & 0 & -0.0001 & 0 \\ 0 & 0 & -2.1665 & 0 & 0 & -0.0003 \end{bmatrix}$$

State Space Matrix [B]

bm =

$$\begin{bmatrix} 0 & 0 & 0 \\ 0 & 0 & 0 \\ 0 & 0 & 0 \end{bmatrix}$$

$$\begin{bmatrix} 0.0003 & 0.0006 & 0.0008 \\ -0.0066 & 0.0010 & 0.0085 \\ 0.0068 & -0.0130 & 0.0166 \end{bmatrix}$$

State Space Matrix [C]

cm = 1.0e+004 *

$$\begin{bmatrix} 0.0001 & 0.0001 & 0.0001 & 0 & 0 & 0 \\ 0 & 0 & 0 & 0.0001 & 0.0001 & 0.0001 \\ -0.0025 & -0.0007 & -0.0004 & 0 & 0 & 0 \\ 0 & 0 & 0 & -0.0025 & -0.0007 & -0.0004 \\ 0.1789 & 2.0231 & 9.6613 & 0.0004 & 0.0008 & 0.0013 \end{bmatrix}$$

State Space Matrix [D]

dm =

$$\begin{bmatrix} 0 & 0 & 0 \\ 0 & 0 & 0 \\ 0 & 0 & 0 \\ 0 & 0 & 0 \\ 0.0113 & 0.0342 & -0.1553 \end{bmatrix}$$

Applied moment vector from piezo film to beam

tg3 =

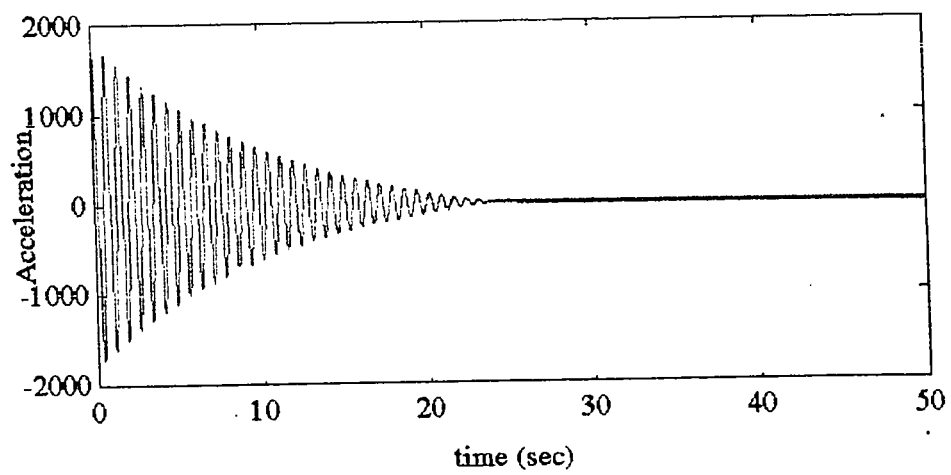
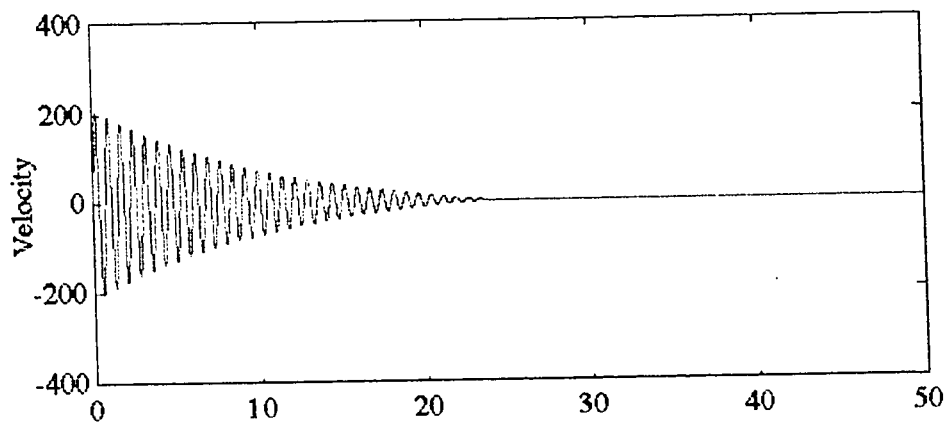
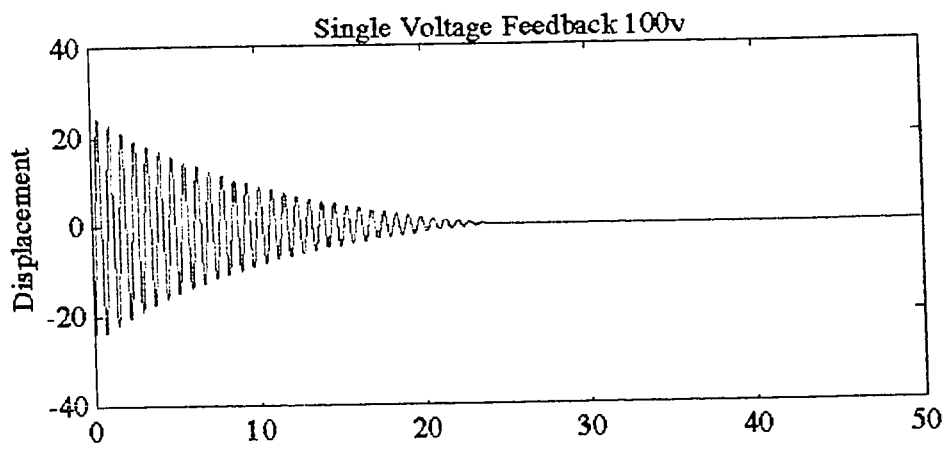
$$\begin{bmatrix} 4.0923 & 9.9667 & 11.8616 \\ -8.4642 & 1.2633 & 10.8151 \\ 3.2404 & -6.1590 & 7.8591 \end{bmatrix}$$

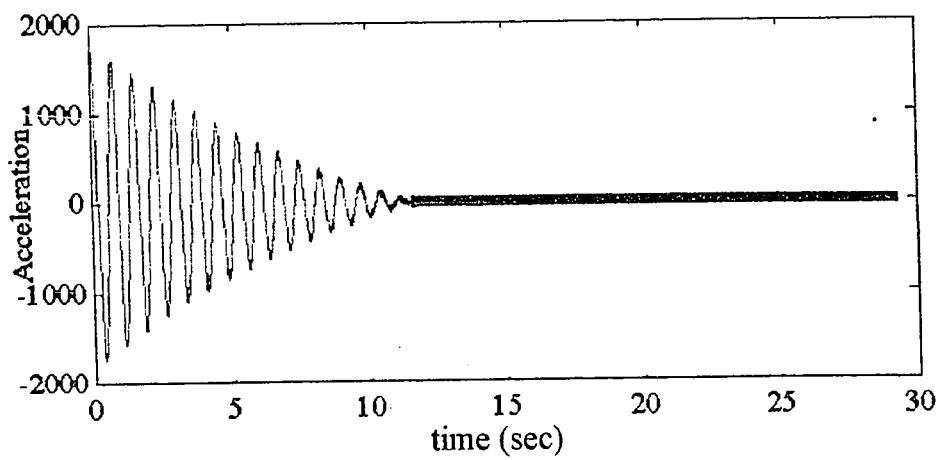
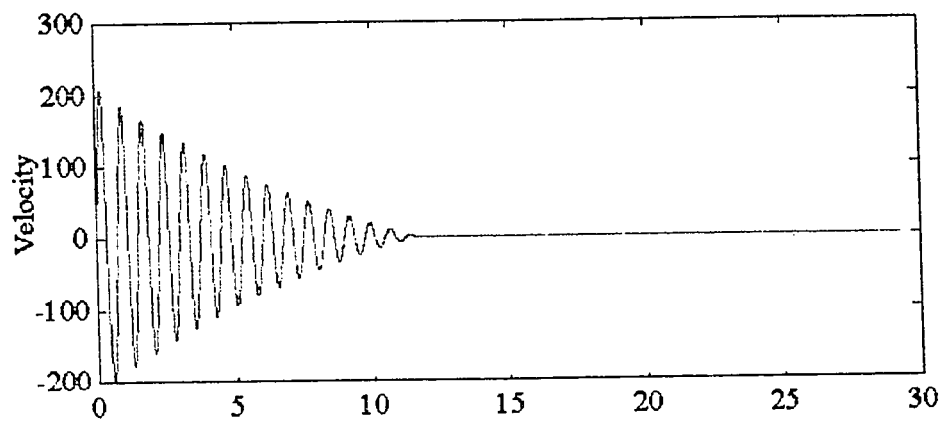
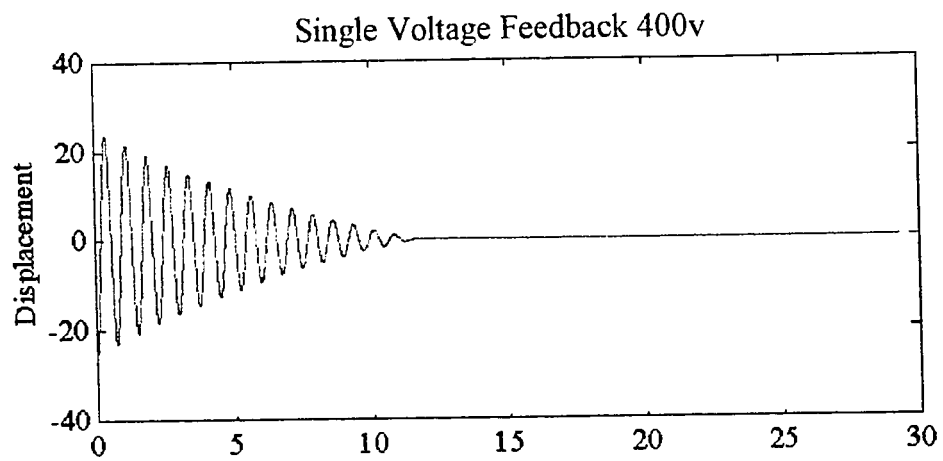
Voltage to applied moment constant

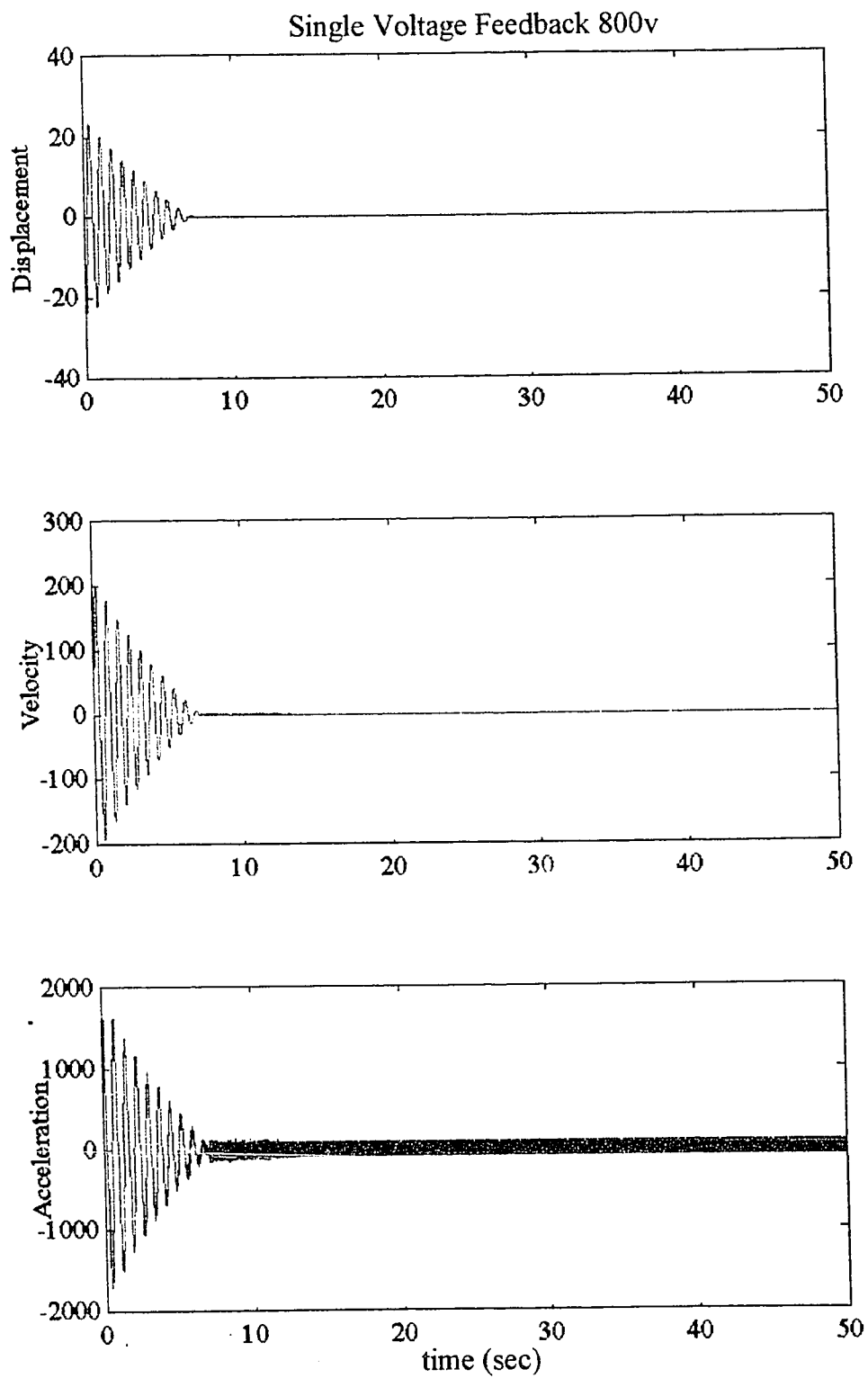
const = 1.3417e-005

Appendix E

Bang Bang Control Plots







Appendix F

Observability and Controllability

Controllability Matrix

M

=

1.0D+07 *

Columns	1 thru	8					
0.0000	0.0000	0.0000	0.0000	0.0000	0.0000	0.0000	0.0000
0.0000	0.0000	0.0000	0.0000	0.0000	0.0000	0.0000	0.0000
0.0000	0.0000	0.0000	0.0000	0.0000	0.0000	0.0000	0.0000
0.0000	0.0000	0.0000	0.0000	0.0000	0.0000	0.0000	0.0000
0.0000	0.0000	0.0000	0.0000	0.0000	0.0000	0.0000	0.0000
0.0000	0.0000	0.0000	0.0000	0.0000	0.0000	0.0000	0.0000
0.0000	0.0000	0.0000	0.0000	0.0000	0.0000	0.0000	0.0000

Columns	9 thru	16					
0.0000	0.0000	0.0000	0.0000	0.0000	0.0000	0.0000	0.0000
0.0000	0.0000	0.0000	0.0000	0.0000	0.0000	0.0000	0.0000
0.0000	0.0000	0.0000	0.0000	0.0000	0.0000	0.0000	0.0000
0.0000	0.0000	0.0000	0.0000	0.0000	0.0000	0.0000	0.0000
0.0000	0.0000	0.0000	0.0000	0.0000	0.0000	0.0000	0.0000
0.0000	0.0000	0.0000	0.0000	0.0000	0.0000	0.0000	0.0000
0.0000	0.0000	0.0000	0.0000	0.0000	0.0000	0.0000	0.0000

Columns	17 thru	24					
0.0000	0.0000	0.0000	0.0000	0.0000	0.0000	0.0000	0.0000
0.0000	0.0000	0.0000	0.0000	0.0000	0.0000	0.0000	0.0000
0.0000	0.0000	0.0000	0.0000	0.0000	0.0000	0.0000	0.0000
0.0000	0.0000	0.0000	0.0000	0.0000	0.0000	0.0000	0.0000
0.0000	0.0000	0.0000	0.0000	0.0000	0.0000	0.0000	0.0000
0.0000	0.0000	0.0000	0.0000	0.0000	0.0000	0.0000	0.0000
0.0000	0.0000	0.0000	0.0000	0.0000	0.0000	0.0000	0.0000

Columns	25 thru	32					
0.0000	0.0000	0.0000	0.0000	0.0000	0.0000	0.0000	0.0000
0.0000	0.0000	0.0000	0.0000	0.0000	0.0000	0.0000	0.0000
0.0000	0.0000	0.0000	0.0000	0.0000	0.0000	0.0000	0.0000
0.0000	0.0000	0.0000	0.0000	0.0000	0.0000	0.0000	0.0000
0.0000	0.0000	0.0000	0.0000	0.0000	0.0000	0.0000	0.0000
0.0000	0.0000	0.0000	0.0000	0.0000	0.0000	0.0000	0.0000
0.0000	0.0000	0.0000	-0.0001	0.0001	0.0000	0.0000	0.0001

Columns	33 thru	40					
0.0000	0.0000	0.0000	0.0000	0.0000	0.0000	0.0000	0.0000
0.0000	0.0000	0.0000	0.0000	0.0000	0.0000	0.0000	0.0000
0.0000	0.0000	0.0000	-0.0001	0.0001	0.0000	0.0000	0.0001
0.0000	0.0000	0.0000	0.0000	0.0000	0.0000	0.0000	0.0000
0.0000	0.0000	0.0000	0.0000	0.0000	0.0000	0.0000	0.0000
0.0000	-0.0003	0.0003	0.0000	0.0000	0.0005	-0.0005	0.0006
0.0000	0.0278	-0.0278	-0.0666	0.0666	0.0282	-0.0282	0.0945

Columns	41 thru	48					
0.0000	0.0000	0.0000	0.0000	0.0000	0.0000	0.0000	0.0000
0.0000	-0.0003	0.0003	0.0000	0.0000	0.0005	-0.0005	0.0006
0.0000	0.0278	-0.0278	-0.0666	0.0666	0.0282	-0.0282	0.0945
0.0000	0.0000	0.0000	0.0000	0.0000	0.0000	0.0000	0.0000
0.0000	0.0047	-0.0047	-0.0005	0.0005	-0.0077	0.0077	-0.0096
0.0000	-1.2431	1.2431	2.9758	-2.9758	-1.2604	1.2604	-4.2202

RM

=

RANK(M)

6.

O

=

Output Controllability Matrix Two Accelerometers

1.0D+12 *

Columns	1 thru	8					
0.0000	0.0000	0.0000	0.0000	0.0000	0.0000	0.0000	0.0000
0.0000	0.0000	0.0000	0.0000	0.0000	0.0000	0.0000	0.0000

Columns	9 thru	16
---------	--------	----

0.0000	0.0000	0.0000	0.0000	0.0000	0.0000	0.0000	0.0000
0.0000	0.0000	0.0000	0.0000	0.0000	0.0000	0.0000	0.0000

Columns	17 thru	24					
0.0000	0.0000	0.0000	0.0000	0.0000	0.0000	0.0000	0.0000
0.0000	0.0000	0.0000	0.0000	0.0000	0.0000	0.0000	0.0000

Columns	25 thru	32					
0.0000	0.0000	0.0000	0.0000	0.0000	0.0000	0.0000	0.0000
0.0000	0.0000	0.0000	0.0000	0.0000	0.0000	0.0000	0.0000

Columns	33 thru	34
0.0020	1.4245	
0.0007	0.5419	

RO = RANK(O)

2.

L = Observability Matrix (Two Accelerometers)

1.0D+10 *

0.0000	0.0000	0.0000	0.0000	0.0000	0.0000
0.0000	0.0000	0.0000	0.0000	0.0000	0.0000
0.0000	0.0000	0.0000	0.0000	0.0000	0.0000
0.0000	0.0000	0.0000	0.0000	0.0000	0.0000
0.0000	0.0000	0.0000	0.0000	0.0000	0.0000
0.0000	0.0000	0.0000	0.0000	0.0000	0.0000
0.0000	0.0000	0.0000	0.0000	0.0000	0.0000
0.0000	0.0000	-0.0001	0.0000	0.0000	0.0000
0.0000	0.0000	-0.0001	0.0000	0.0000	0.0000
0.0000	-0.0056	-0.2051	0.0000	0.0000	-0.0003
0.0000	0.0040	-0.0818	0.0000	0.0000	-0.0001
0.0000	0.0601	6.0356	0.0000	-0.0055	-0.2010
0.0000	-0.0425	2.4076	0.0000	0.0039	-0.0802

RL = RANK(L)

6.

C1 =

-25.4300 -7.3200 -4.4600 0.0000 0.0000 0.0000

O1 = Output Controllability Matrix (One Accelerometer)

1.0D+06 *

Columns	1 thru	8					
0.0000	0.0000	0.0000	0.0000	0.0000	0.0000	0.0000	0.0000

Columns	9 thru	16					
0.0000	0.0000	0.0000	0.0000	0.0000	0.0000	0.0000	0.0000

Columns	17 thru	24					
0.0000	0.0000	0.0000	0.0000	0.0000	0.0000	0.0000	0.0000

Columns	25 thru	32					
0.0000	0.0001	-0.0001	-0.0001	0.0001	0.0001	-0.0001	0.0002

Columns	33 thru	40					
0.0000	-0.0016	0.0016	0.0041	-0.0041	-0.0019	0.0019	-0.0060

Columns	41 thru	48					
0.0000	-1.2199	1.2199	2.9691	-2.9691	-1.2934	1.2934	-4.2572

RO1 = RANK(O1)

1.

L1 = Observability Matrix (One Accelerometer)

1.0D+10 *

0.0000	0.0000	0.0000	0.0000	0.0000	0.0000
0.0000	0.0000	0.0000	0.0000	0.0000	0.0000
0.0000	0.0000	0.0000	0.0000	0.0000	0.0000
0.0000	0.0000	-0.0001	0.0000	0.0000	0.0000
0.0000	-0.0056	-0.2051	0.0000	0.0000	-0.0003
0.0000	0.0601	6.0356	0.0000	-0.0055	-0.2010

RL1 = RANK(L1)

6.

Appendix G

Optimal Control Simulations

q1 =

1	0	0	0	0	0
0	1	0	0	0	0
0	0	1	0	0	0
0	0	0	10	0	0
0	0	0	0	10	0
0	0	0	0	0	10

q2 =

1	0	0	0	0	0
0	1	0	0	0	0
0	0	1	0	0	0
0	0	0	50	0	0
0	0	0	0	50	0
0	0	0	0	0	50

q3 =

1	0	0	0	0	0
0	1	0	0	0	0
0	0	1	0	0	0
0	0	0	100	0	0
0	0	0	0	100	0
0	0	0	0	0	100

q4 =

1	0	0	0	0	0
0	1	0	0	0	0
0	0	1	0	0	0
0	0	0	500	0	0
0	0	0	0	500	0
0	0	0	0	0	500

q5 =

1	0	0	0	0	0
0	1	0	0	0	0
0	0	1	0	0	0
0	0	0	1000	0	0
0	0	0	0	1000	0
0	0	0	0	0	1000

q6 =

1	0	0	0	0	0
0	1	0	0	0	0
0	0	1	0	0	0
0	0	0	10000	0	0
0	0	0	0	10000	0
0	0	0	0	0	10000

q7 =

1	0	0	0	0	0
0	1	0	0	0	0
0	0	1	0	0	0
0	0	0	1000000	0	0

```

      0      0      0      0 1000000      0
      0      0      0      0      0 1000000
q8 =

```

```

      1      0      0      0      0      0
      0      1      0      0      0      0
      0      0      1      0      0      0
      0      0      0 80000      0      0
      0      0      0      0 80000      0
      0      0      0      0      0 80000
r1 =

```

```

      1  0  0
      0  1  0
      0  0  1
r2 =

```

```

      100  0  0
      0 100  0
      0  0 100
r3 =

```

```

      1000      0      0
      0      1000      0
      0      0      1000
r4 =

```

```

      100000      0      0
      0      100000      0
      0      0      100000
r5 =

```

```

      5  0  0
      0  5  0
      0  0  5
r6 =

```

```

      5.0000      0      0
      0  6.5000      0
      0      0  9.0000
r7 =

```

```

      2.0000      0      0
      0  3.5000      0
      0      0  5.0000
r8 =

```

```

      1  0  0
      0  2  0
      0  0  3
Chosen K and Lp
k6 =

```

```

0.1025 -0.1623 -2.4592 11.5680 -40.4510 16.3685

```

-0.0041	0.8053	0.4171	21.6714	4.6445	-23.9316
-0.0844	-0.1739	1.9029	18.6270	28.7139	22.0547

lp6 =

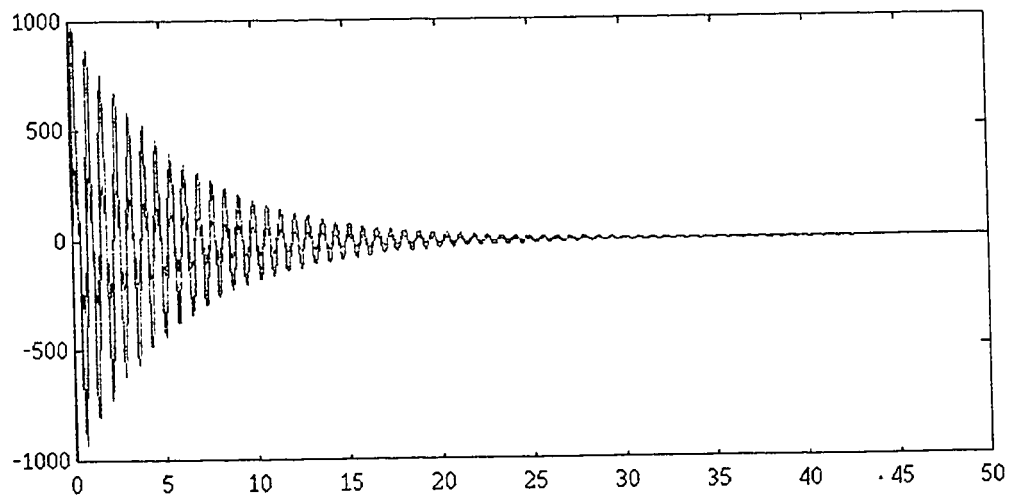
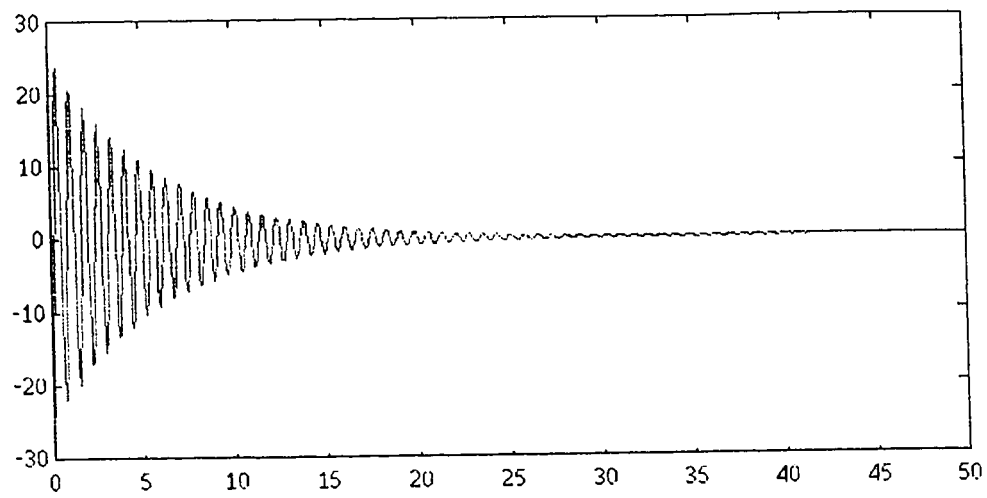
1.0e-004 *

0.1755	0.2546	0.0815	-0.0028	-0.0211	0.0507
--------	--------	--------	---------	---------	--------

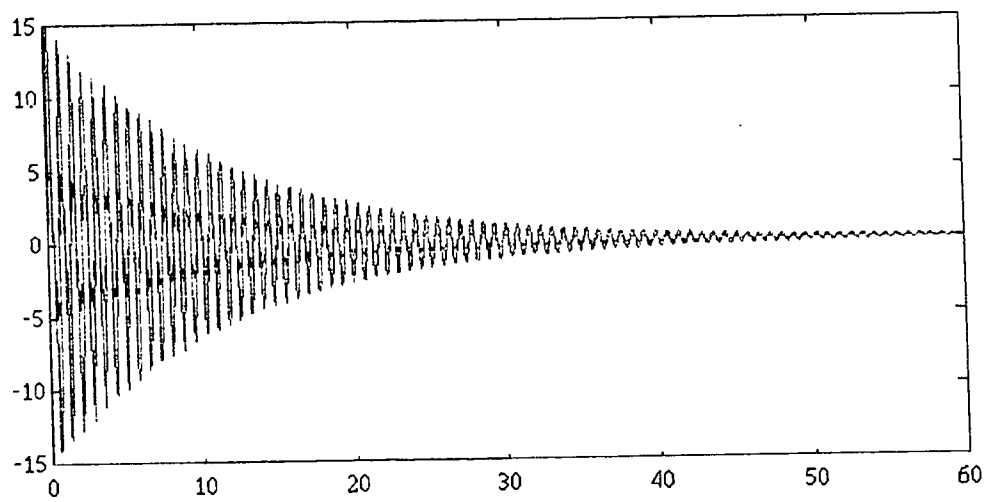
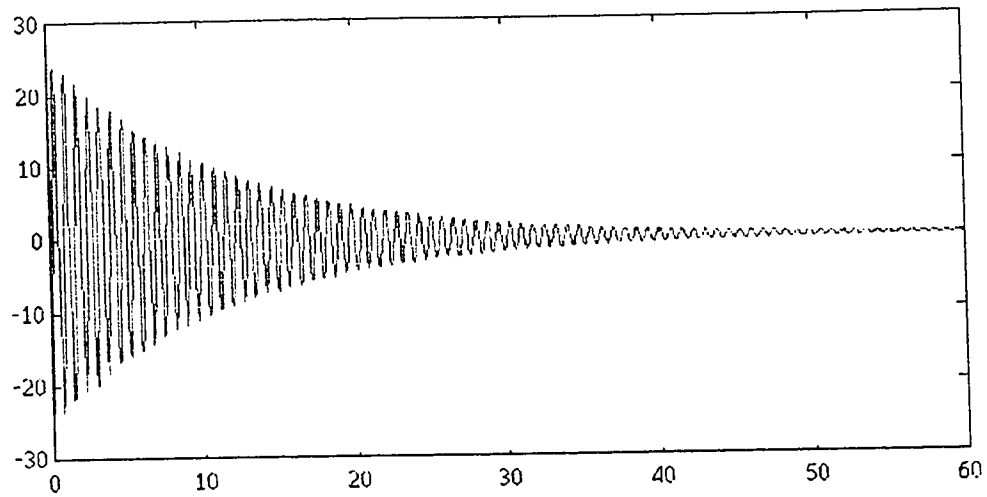
4/27/93

run 2

Weighting matrix = q8. r1



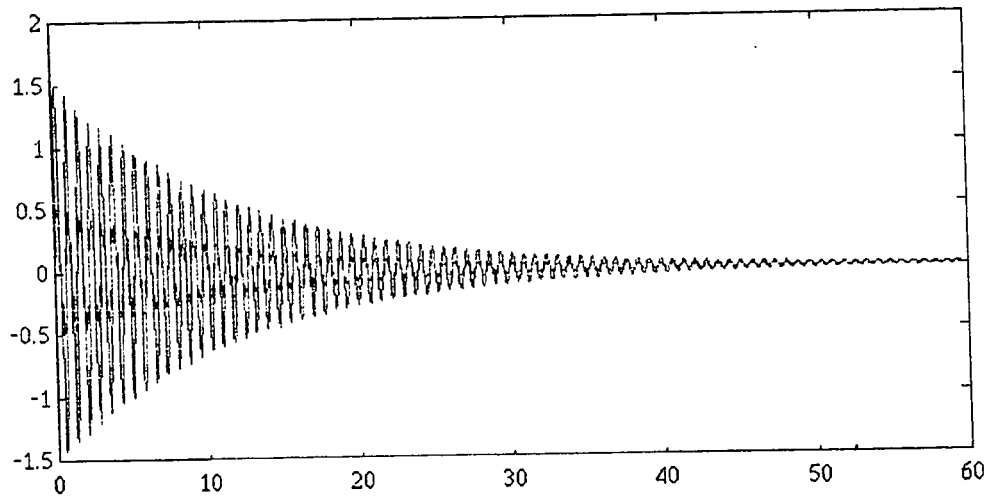
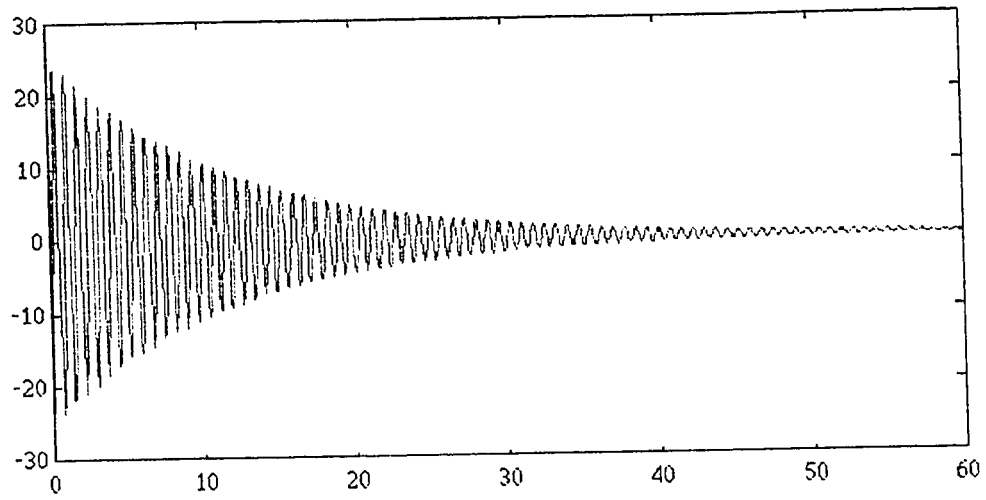
4/27/93run 4
Weighting matrix = q8. r2



4/27/93

run 3

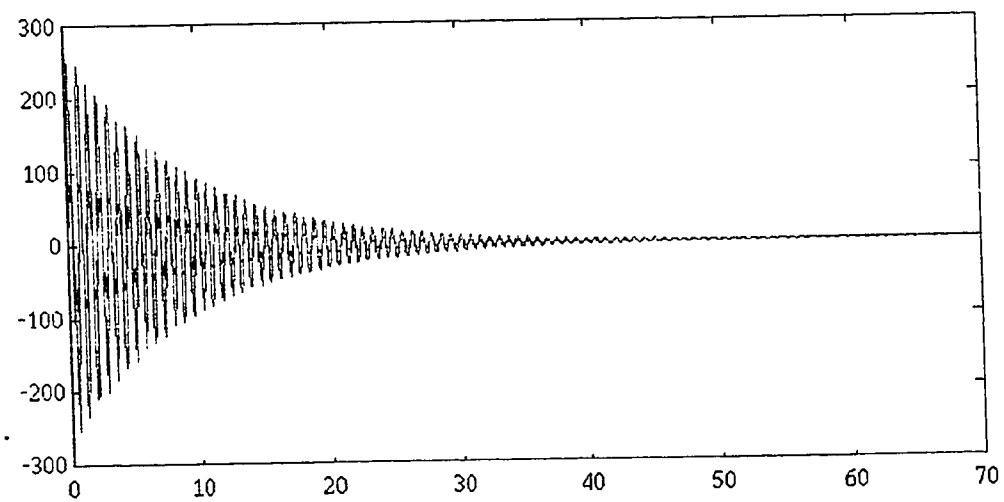
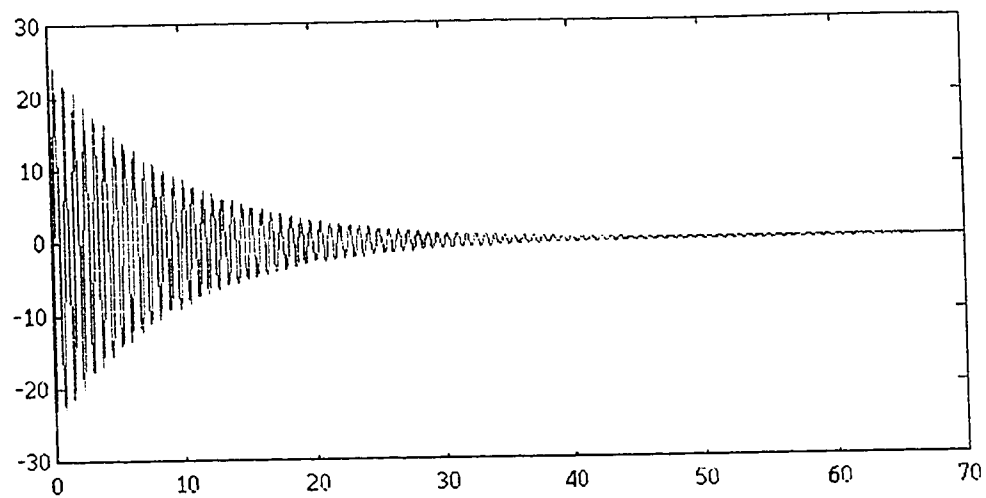
Weighting matrix = q8. r3



4/27/93

run 5

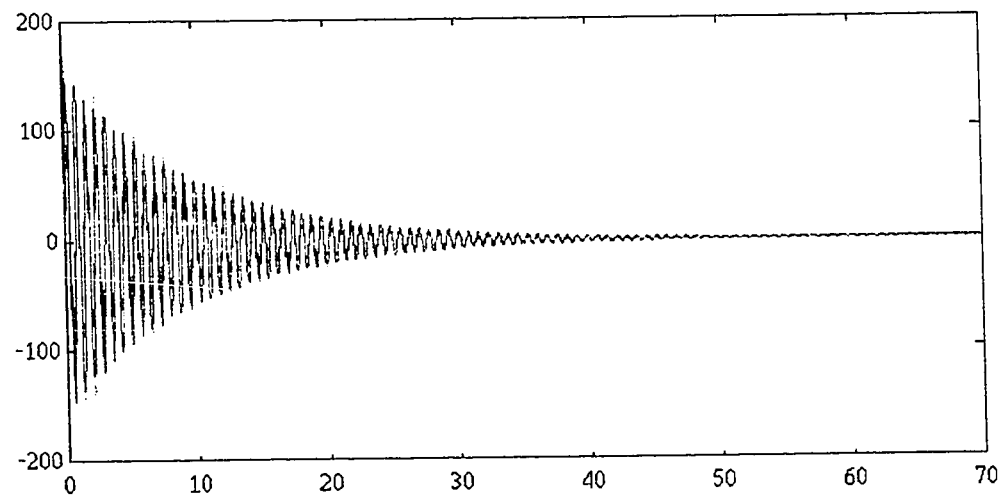
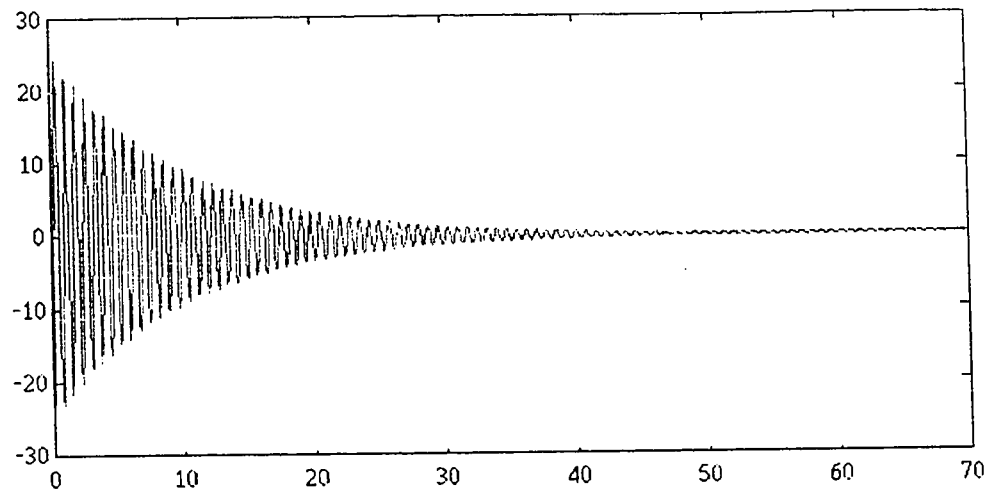
Weighting matrix = q8, r5



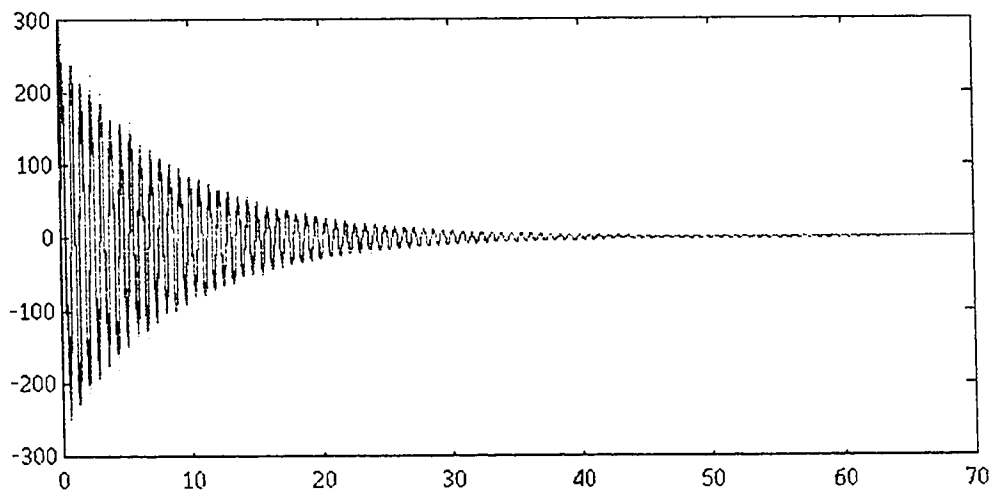
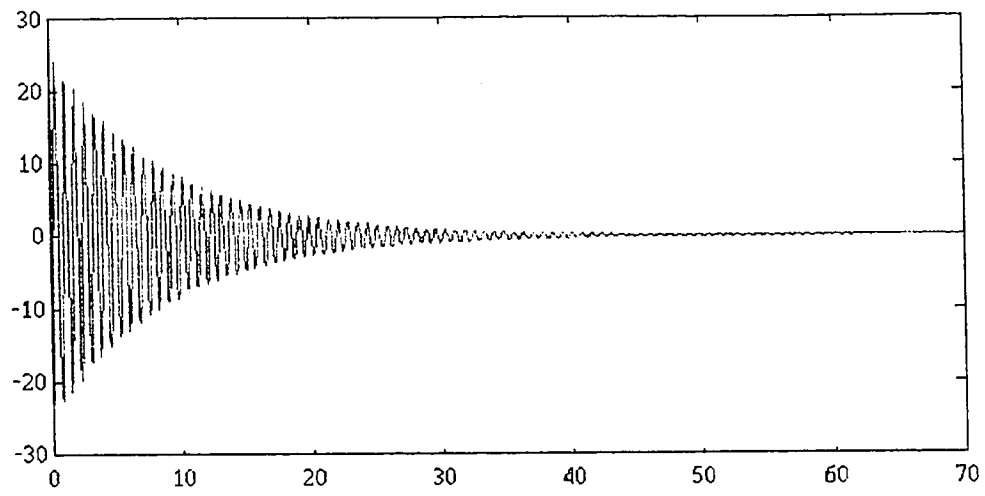
4/27/93

run 6

Weighting matrix = q8. r6



q8.r7



q8.r8

